SECOND ORDER NONLINEAR OPTICAL ACTIVITY OF AMINO ACIDS, GUANIDINES AND PYRIDINIUM SALTS OF INORGANIC ANIONS

Abstract

The present work is committed to organic nonlinear optical materials (NLO materials) and their prospective applications. The literary part consists of the theoretical background of organic NLO materials. Properties of organic and inorganic compounds as NLO materials are compared and the reason why most commercial NLO products are inorganic compounds despite the numerous and better NLO properties of organic molecules over inorganic molecules is justified. Characteristics of good NLO crystals such as phase matchability, wide optical transparency second order nonlinear susceptibility, thermal and chemical stability, availability of large single crystals and environmental stability, high second harmonic generation (SHG) efficiency, high mechanical strength and high laser damage resistance are discussed in detail. Second order nonlinear optical phenomena for instance SHG, optical mixing and optical parametric oscillation are considered. Attention is paid to amino acid based compounds and quanidine compounds as organic NLO materials.

In the experimental part, pyridinium salts of inorganic anions were synthesized and the structures of the products were identified with the help of ^{1}H NMR spectroscopy and X-ray crystallography. The inorganic acids used during the synthesis are HBF_4, H_3PO_4, HNO_3 and H_2SO_4. Synthesis with H_2SO_4 was carried out twice in 1:1 and 1:2 molar ratios with the pyridine compounds.

The SHG efficiencies of the synthesized compounds were investigated using the Kurtz and Perry powder method. Compounds **26, 28, 30, 32, 35, 39, 44, 46** and **50** showed some NLO activity by displaying some SHG efficiencies with intensities about 1-5% that of urea reference.

Preface

This master`s thesis is based on work carried out during the 2017-2018 academic year at the Department of Chemistry, Faculty of Mathematics and Science, University of Jyväskylä under the supervision of Prof. Jari Konu and support from the Ph.D student Esa Kukkonen.

Basic knowledge about the topic was gotten from available materials in the University Library in addition to self-studying. The literature cited in this work was acquired through the use of Reaxys and Scifinder search systems. Reaction schemes were drawn using the Chem draw program and the molecular packing diagrams build up using the Mercury program.

I desire to immensely express my sincere appreciation to my teachers and supervisor for their incredible contribution to this work and most especially to my development and growth as a scientist. This work would have been hardly made possible without their support.

In a special way, I am grateful to my parents Raymond Ayeah and Perpetua Mbuh and friends for their constant support and encouragement to me throughout my studies.

Contents

List of Abbreviations

SHG – Second harmonic generation

NLO materials - Nonlinear optical materials

PNA- Para-nitroaniline

POM- 3-methyl-4-nitropyridine oxide

KDP- Potassium dihydrogen phosphate

EDCN- 1,1-ethylenedicarbonitrile

HOMO- Highest occupied molecular orbital

LUMO-Lowest unoccupied molecular orbital

2A4PNN2- Amino-4-picolinium-nitrophenolate nitrophenol

LA4NPM- L-Argininium-4-nitro phenolate monohydrate

GMNB- Guanidinium meta-nitrobenzoate

LITERATURE PART

1 Introduction

Nonlinear optical materials (NLO materials) are materials that interact with light to produce a nonlinear response.[1] This nonlinear optical response can be frequency mixing processes such as second harmonic generation (SHG) which is a situation that arises when the input wave generates a wave whose frequency is twice the optical frequency in the medium. This implies the frequency of the output wave is twice the frequency of the input wave. NLO materials can be classified into two main groups: organic NLO materials and inorganic NLO materials. Organic materials often have stronger nonlinear optical properties than inorganic materials due the molecular units bearing
highly delocalized electrons in the π- π orbitals, additional electron donor and electron acceptor groups on opposite sides of the molecules. The main advantage of organic materials over inorganic materials as nonlinear optical materials is the ability to alter the molecular structure in order to maximize the nonlinear optical properties. Organic crystals have weak intermolecular bonding interactions. Considering these weak intermolecular bonding interactions, the molecules in organic crystals function independently of each other and only their resultant orientations within the crystal lattice contribute significantly to the macroscopic optical properties of the organic crystal. In inorganic nonlinear optical materials, lattice vibrations play a dominant role in enhancing the nonlinear optical properties but in organic crystals, the nonlinear optical properties are determined largely by the electron polarizability in the π-bonding orbitals. In table 1, some common properties of organic and inorganic compounds as NLO active materials are compared. Despite the better NLO properties of organic molecules over inorganic molecules, a majority of the commercial NLO products are inorganic materials, mainly due to the stability factors with organic molecules.

Amines are common donor groups with predominantly p-character with an available electron pair on the p-orbital. Nitro (NO_2) and nitrile are common acceptor groups with more s-character orbital bonding. Primary focus on this literature review will be on chiral organic material having these NLO properties. Organic materials with p-electrons have been identified to have nonlinear optical applications but organic materials having π-electron conjugated systems provide a larger optical nonlinearity and even faster optical response. Typical examples of organic materials with p-electrons and π-electron

conjugated systems are shown in figure 1. The NLO activity of chiral organic compounds is further discussed followed by detailed examination of pyridine salts of inorganic acids as future NLO active materials.

(i) One ring system
(benzene analogue)

(ii) Two ring system
(stilbene analogue)
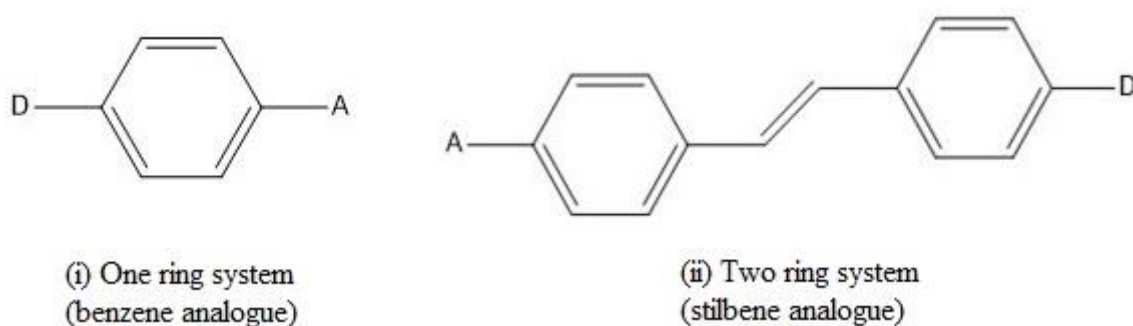
Figure 1. Typical organic materials for second order nonlinear optical effects. These are substituted molecules with π -electron ring systems. Donor groups are represented as (D) and acceptor groups represented as (A). (i) one ring system (benzene derivatives), (ii) two ring system (stilbenes derivatives).

2 Comparison of the properties of organic and inorganic compounds as NLO materials

NLO active materials can be classified into two main classes which are ionic crystals, mainly inorganic compounds, and covalent crystals, mainly organic compounds.[53] Organic compounds are highly soluble in a large range of organic solvents and are not thermally stable at temperatures above their melting points. Inorganic compounds are very soluble in water and highly polar solvents. They are stable even at temperatures above their melting points. The sensitivity of organic compounds to ionic strength and pH of solvents is quite low and their crystal structures consist of covalently bonded molecules. The crystal structure of inorganic compounds consists of molecules held together by ionic bonds. Under favourable growth conditions, crystals of inorganic compounds typically grow much larger in size compared to those of organic compounds. A comparison of the properties of organic and inorganic compounds as NLO materials is summarized in Table 1.

Table 1. Comparison of the properties of organic and inorganic compounds as NLO materials

Property	Organic compounds	Inorganic compounds
Solubility	High solubility in a large variety of organic solvents	High solubility in water and other highly polar solvents
Thermal stability	Mostly, organic compounds are thermally stable only up to their melting temperature. This implies less thermal stability	Very high thermal stability even after their melting points
Sensitivity to ionic strength and pH of solvents	Low sensitivity	High sensitivity
Chemical structure of the crystals	Crystal structure consist of molecules that are covalently bonded to each other	Crystal structure consist of molecules that are held together by ionic bonds
Size of the crystals	Using the common methods known for growing crystals, the sizes of the crystals obtain usually range from 0.1-10mm^3	Most inorganic compounds do not have any limited size for crystal growth. They can grow as large as possible under favourable conditions.
Mechanical strength	Averagely, organic compounds have good mechanical strength	Inorganic molecules exhibit excellent mechanical strength
Quality of X-ray diffraction	Good	Extremely good

3 Characteristics of a good NLO crystal

The major problem faced with NLO crystalline materials is the lack of the ability to be processed, adaptability and the ability to grow large sized crystals.[3] Most NLO materials are prepared by evaporating a solution having stoichiometric amounts of the components. Usually, there is a high possibility that no reaction occurs, and the crystals obtained in solution may just be one or more of the initial starting material. Hence, accurate identification of the crystal is a crucial and delicate factor that must be carried out appropriately. Using the poling process during which a strong electric field is applied to position dipolar organic chromophores within a polymer matrix close its glass transition temperature, NLO activities can be obtained in polymeric films.[3] Though this is possible, the obtained NLO material still lack long term stability and reproducibility. The strong electric field applied during its preparation can cause the crystal to breakdown. As basic data, the linear optical data from the principal refractive indices and their dispersion must be determined with very high precision.[6] The data needed to qualify the material as an NLO material depends on the effect being measured. Most of the cases consider the effect of SHG on the material. Selection of outstanding NLO materials is based on factors such as phase matchability, , ease of synthesis with low production cost, second order nonlinear susceptibility, thermal and chemical stability, wide optical transparency, availability of large single crystals and environmental stability, architectural flexibility for molecular design, ability to tune the surface morphology, high SHG efficiency, high mechanical strength, ultrafast response and high laser damage resistance. These requirements are difficult to be all fulfilled by a single crystal. It is only when most of these requirements are fulfilled that one can say exactly based on the data obtained that a given material is an NLO material or not.

3.1 Phase matching

The dependency of the SHG on particle size is used as a parameter to determine the phase matchability of a given NLO material. The phase matching ability of the material can be confirmed from the continuous increase in the SHG signal up to a saturation point with an increase in the size of the particle.[33] An increase in the SHG nonlinearity due to

an increase in the size of the particle and saturation up to a maximum value is known as type-1 phase matching. Phase matching refers to a group of techniques for obtaining effective nonlinear interactions in a medium. This means making sure that an appropriate phase relation between the interacting waves for optimum nonlinear frequency conversion is sustained along the direction of propagation. These interactions may be parametric processes such as frequency doubling, sum and difference of frequency generation, parametric amplification and oscillation and four wave mixing.[5] Amplitude contributions generated from different locations to the product wave can only be in phase at the end of the nonlinear crystal if phase matching is performed. Phase has to be maintained between the interacting waves for efficient conversion in optical SHG and other nonlinear optical processes. One method to achieve this is by using the birefringent and dispersive properties of the crystal. A birefringent crystal is one with different refractive indices for different polarization of light. This method makes use of the ordinary refractive index of the harmonic wave which is the same as the extraordinary refractive index of the fundamental wave in a particular cone of directions about the optical axis. The two waves travel through the crystal in these directions with the same speed. It is difficult to obtain phase matching in isotropic crystals (crystals in which physical properties do not depend on the crystal orientation). This is due to the scattering of the refractive index between the fundamental and the second harmonic wavelengths. However, it is possible to have a wave vector mismatch in anisotropic crystal equal to zero by simply choosing a suitable direction of propagation of the waves. An effective nonlinear interaction is obtained when some phase mismatch is close to zero. Generally, dispersion usually leads to a non-zero phase mismatch. Figure 2 below illustrates phase mismatch for second harmonic generation.
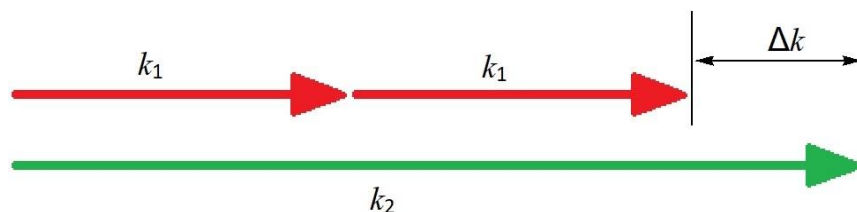
Figure 2. Phase mismatch for second harmonic generation.[5]

The wave number for the second harmonic is more than double that of the fundamental wave as a result of chromatic dispersion. Phase matching can be achieved through birefringence or quasi-phase matching.[5] Birefringence of a nonlinear optical material is

the difference in the refractive indices of the material at certain particular wavelengths. Its size directly affects the phase matching wavelength range. With birefringence, a different polarization in the crystal is chosen. With quasi-phase matching, the amplitude of the field is allowed to grow over a single coherence length, the relative interactive field phases manipulated so that the desired amplitude increases when propagating over the next coherent length before the field starts to reduce.[6] This is achieved by inverting the nonlinear susceptibility sign after each coherence length or by introducing sections having linear propagation after each coherence length of nonlinear interactions to rearrange the relative phases.

3.2 Second order nonlinear susceptibility

Generally, only laser light has sufficient intensity to alter the optical properties of a nonlinear optical material system.[4] Laser beam has a wide range of beneficial characteristics because of its good coherence, high density, high speed responsivity, parallel processing ability, diverse wavelength and frequency. These characteristics are necessary to realize large capacity information and processing, high density recording and storage. However, the alignment of the constituent molecules in the crystal during crystal growth process can be such that the nonlinear optical properties of the molecule is enhanced.[5] Nonlinear optical susceptibilities generally depend on the frequency of the applied field. They can be considered constant under the assumption that the medium response to the applied optical field instantaneously. As a consequence, such materials cannot create second order nonlinear interactions. Hence, both centrosymmetric and non-centrosymmetric materials can exhibit second order nonlinear susceptibility.

3.3 Wide optical transparency

Wide optical transparency remains a good property for nonlinear optical materials. Generally, in a material, the transparency range is limited by the band edge absorption at high frequency and by two photon absorptions at twice the Reststrahlen frequency at low frequencies.[4] This is particularly important because of the fact that growing high quality optical crystals is a difficult task. Intensity dependent losses have recently been

identified as very significant factors in the transparency properties of a crystal. Two photon absorptions may even become the dominant loss mechanism at the short wavelength end of a material´s transparency range and the frequency range that is usually transparent to low intensity radiation.

3.4 Adequate resistance to optical damage by intense optical irradiation

Resistance to laser damage by an NLO active material is a very important characteristic. The laser damage threshold depends on the laser parameters for example energy, pulse duration, wavelength, longitudinal and transverse mode structure, beam size and its location.[6] The input laser intensity may damage the crystal, and this limits the maximum nonlinear conversion efficiency. This may arise because of a number of different processes in the material such as thermal heating, self-focusing, surface preparation, dielectric breakdown, stimulated Brillouin scattering and even induced absorption due to multiphoton absorption. The most common of the crystal damages is thermal heating. This causes the material to break down as a result of a proportionate rise in temperature thereby damaging the material. Deposited energy is also a frequent damage mechanism in metals and highly absorbing materials.[9] Phase matching reduces surface damage in nonlinear optical materials. Surface preparation is very important because damage occurs much more readily along surface scratches. The damage intensity restricts the energy handling capabilities of the optically nonlinear crystal. Hence the damage threshold should be used to prescribe the maximum possible power for a particular crystal. The schematic diagram to illustrate the laser damaged threshold measurements setup is shown in Figure 3.
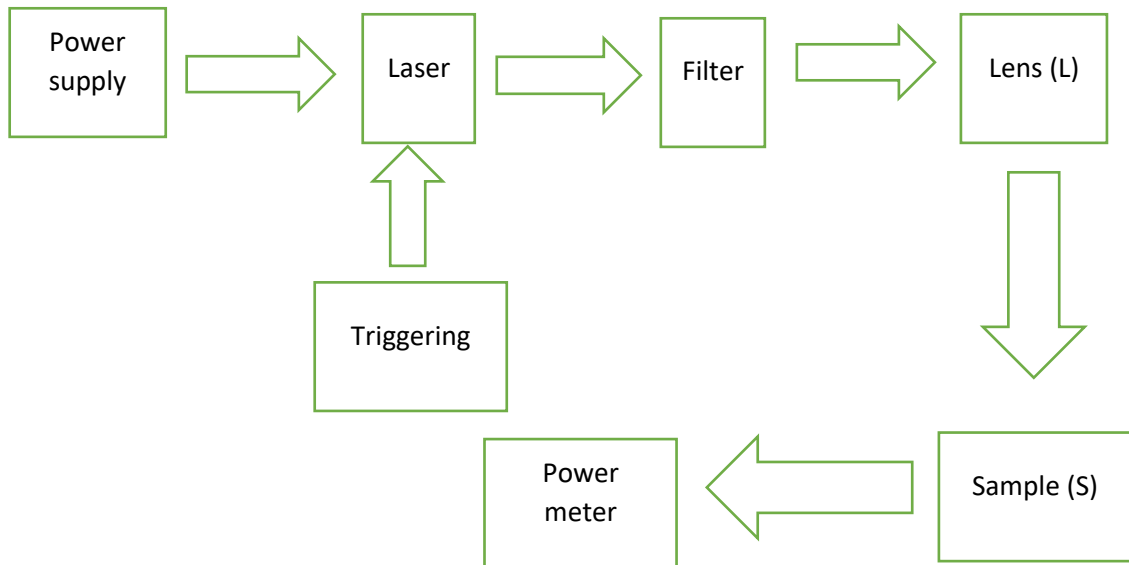
Figure 3. Schematic representation of the laser damage threshold measurement setup.

In such a setup, the sample S is mounted on a translator which easily brings different parts of the sample for accurate exposure.[10] The different parts of the crystal are irradiated by the laser beam at different pulse energies to determine single shot damage threshold. This is very necessary to avoid the cumulative effects that results from multiple exposures. The damage onset can be determined by observing the scattering of the laser beam passing through the damage volume.

3.5 Easy growth of large single high-quality crystals

Large and good enough high-quality crystal growth appears to be the biggest challenge for NLO materials. Considering a suitable size that the NLO material must possess, it is necessary that all three dimensions of the crystal should be a minimum of 5mm.[28] As for high quality, the peak generated by the rocking curve measurements around Bragg reflection should have a full width at half-maximum less than 100 arcseconds or below 50 arcsecond for a better quality crystal. Many methods such as top-seeded solution growth, Czochralski, Bridgman and floating zone though better suited for inorganic materials exist for good quality crystal growth but there is no specific method that can be used to grow crystals for all materials. To grow single crystals with the required dimension is usually a difficult task due the effects of the organic solvents on the growth of the crystal. Most often, crystals grown from organic solvents ranges from needle

shape to prismatic crystals depending on certain factors such as polarity, solubility, chemical nature and the evaporation rate of the solvents.[17] This is mainly due to the interaction of the molecules of the solvent on the surface of the growing crystal. The solvent`s chemical nature determines the quality of the grown crystal in a majority of cases. Therefore, suitable solvents have to be selected for the crystal growth of a particular material based on the solubility of its solute throughout the entire temperature range of crystallization. Apart from growing the crystal, it also needs to be cut, polished and indexed before measuring the NLO properties.

Chemical stability of the NLO material is also an important property to be considered. A good NLO material must be air and moisture stable.[17] Its synthesis must not require any toxic reagents.

4 Second order nonlinear optical phenomena

Materials respond in a nonlinear manner to the applied electric field. Subjecting a nonlinear optical material to electromagnetic radiation causes the molecules of the material to be polarized. Nonlinear optical interactions in solids and the resulting nonlinear coupling of electromagnetic waves lead to second order nonlinear optical processes such as second harmonic generation, optical mixing and optical parametric oscillation.[24]

4.1 Second harmonic generation (SHG)

SHG is a phenomenon in which nonlinear materials generate light with a frequency that doubles that of the input beam.[25] This occurs as the frequency of two photons mix to generate a third photon with frequency double that of the initial photons. This is illustrated in figure 8 below. The characteristics of the wave produced such as monochromacity are the same as that of the fundamental wave. Both waves are emitted in the same direction. The electronic origin of optical nonlinearities in the electric dipole approximation suggest that only the valence electrons contribute to second order nonlinear susceptibility[27]. The asymmetry of the electron clouds and the direction of the

electronic wave functions determine the magnitude of the nonlinear coefficient. This explains why noncentrosymmetric crystals exhibit good SHG. SHG is the most commonly and frequently affect that is investigated in NLO materials. During this process, photons having identical frequency interact with a nonlinear material and successfully combine to generate new photons whose energy and frequency doubles that of the initial photons. Usually, the results obtained are compared to that of other known compounds like potassium dihydrogen phosphate (KDP). A preliminary check for the SHG of a crystalline species can be carried out by a microcrystalline powder test known as the Kurtz-Perry technique. Surfaces and interfaces are used to study SHG since media with inversion symmetry cannot generate second harmonic light.[26] SHG discriminates against signals from the bulk and label them as surface specific techniques. Below is a diagram of SHG process.
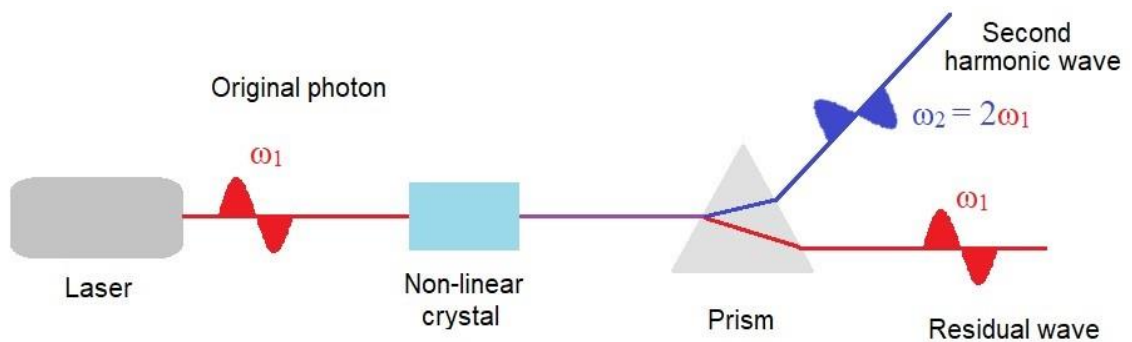
Figure 4. Diagram of a second harmonic generation process.[4]

4.2 Optical mixing

Optical mixing is a nonlinear optical phenomenon that occur at a single photon level with single photon stimulated four wave mixing. It is the generation of new frequencies based on nonlinear phenomena. During the process, two pump photons whether degenerate or nondegenerate are destroyed and a pair of signal and idler photons are stimulated by the seeded single photons.[7] A very important aspect of this process is that one of the correlated generated photons is in the similar mode as the seeded photons. This occurs as a result of single photon level waves injected into the nonlinear medium alongside strong pump wave(s). With the use of proper optical arrangements as illustrated in Figure 5, one can have sufficiently intense output at any one of the

generated frequencies. If the two pump photons sum up thereby generating a new wave, the process is called frequency-up conversion but if the frequency of the second photon is subtracted from that of the first, the process is called frequency- down conversion.[14] KDP crystal can be used for the frequency-up conversion and LiNbO$_3$ or quartz can be used for frequency-down conversion processes.
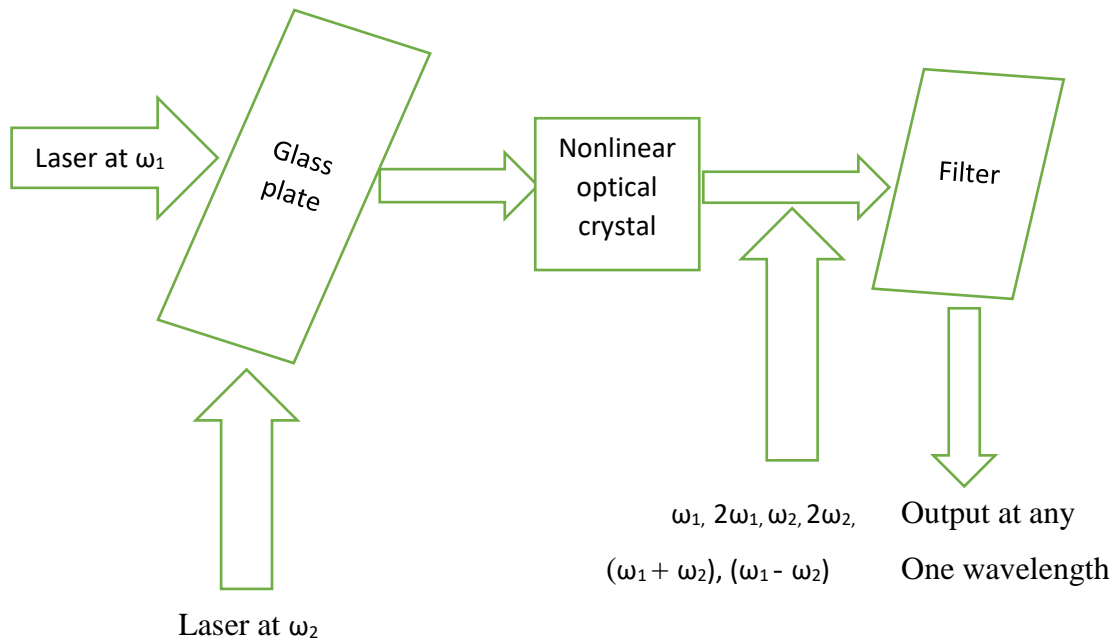
Figure 5. Schematic set up for generating a new frequency by optical mixing.[7]

4.3 Optical parametric oscillation

Optical parametric oscillation is the generation of a signal and idler wave using a parametric amplifier in a resonator without an input signal.[18] A parametric oscillator that oscillates at optical frequencies is called a parametric optical oscillator. Using second order nonlinear optical interactions, an optical parametric oscillator changes an input laser wave called the pump wave into two output waves with lower frequencies. The frequency sum of these two waves is equal to that of the input wave frequency. These two output waves are called signal wave that is the output wave with the higher frequency and the idler wave. The pump, signal wave and the idler overlap in a nonlinear optical material. These three waves interact leading to parametric amplification and a

corresponding deamplification of the pump wave[15]. If the idler wave is sent out alongside the pump beam, then the process is known as difference frequency generation. This process is even more efficient than the optical parametric oscillation. Based on the proposed novel interaction configuration, second order nonlinear optical materials in a waveguide can be used to obtain transversely pumped counter propagating optical parametric oscillation and amplification[8]. The output frequency can be tuned through a large range by simply changing the incident angle of the pump beam.[16] No cavity is needed in the proposed configuration to establish the oscillation. Practically, in any second nonlinear medium, the suggested transverse pumping geometry is a flexible geometry. Efficient degenerate parametric oscillation that is same frequency for the signal and idler for a considerable wavelength range of the pump wave can be effectuated using this geometry. The output frequency can be adjusted over a large range by regulating the incident angle of the pump beam. Figure 6 below illustrate the phenomenon of optical parametric oscillation exhibited by nonlinear optical materials.
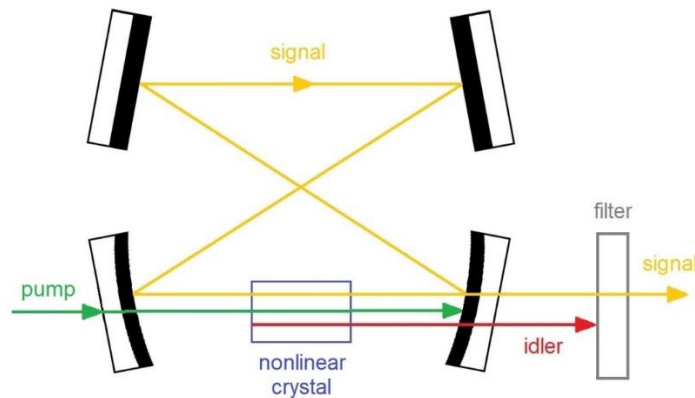
Figure 6. Apparatus for optical parametric oscillation exhibited by nonlinear optical materials[8].

5 Factors influencing NLO activity in a material

A good number of factors influence the NLO activity in a given material. Some of those factors include molecular structure, conjugated π- electron system, effects of substitution, electronic properties of the donor-acceptor groups, different counter anion

effect, intermolecular interactions and molecular packing.[20] The structural states of molecules exhibiting NLO activity is also an important factor to be considered.

(i) Higher state   (ii) Ground state   (iii) First excited state
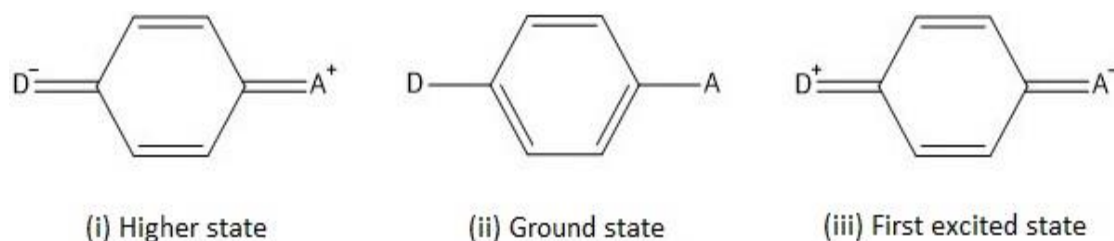
Figure 7. Structural states of molecules for nonlinear optics. (i) is a higher state -a condition during which there is the transfer of an electron from the acceptor to the donor (a very unusual situation), (ii) is the neutral state, (iii) is the first excited state – a condition in which there is the transfer of an electron from the donor to the acceptor.

Applying an electromagnetic radiation to molecules with donor and acceptor groups results in asymmetric electronic response of the polarization unlike symmetric electronic response for centrosymmetric molecules[22]. If the benzene ring (in figure 2) is replaced with a thiophene ring, this will lead to a remarkable increase in the second order molecular polarizabilities. Systems having two or more rings often show higher molecular second order polarizabilities. In such cases, the nonlinearity of such systems may decrease due to the fact that nonlinearity per unit volume becomes smaller as the molecules require more space. This shift the absorption wavelengths towards longer wavelengths. Large π-electron systems that can easily be moved upon application of electric fields and strong donor -acceptor substitutions are needed for high optical molecular second order nonlinearities.

5.1 Effects of substituents

Substitution in a nonlinear optical molecule greatly affects the NLO properties of the molecule. For example, consider the diamino (1), dithio (2) and thioamino (3) derivatives shown in Figure 8.
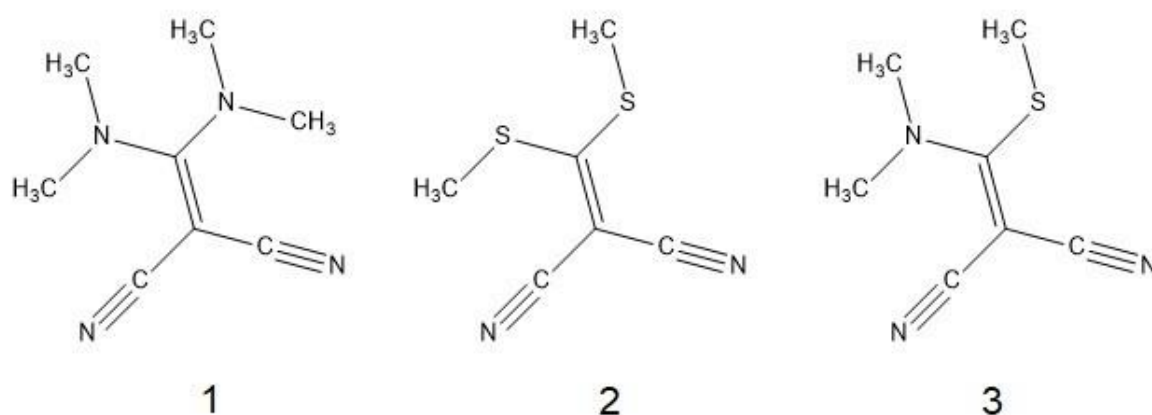
Figure 8. Diamino (1), dithio (2), thioamino (3) derivatives of EDCN (1,1-ethylenedicarbonitrile).

Compounds **1** and **2** are symmetric molecules but substituting one of the dimethylamino with methylthio results in the asymmetric molecule 3. The diamino 1 and the dithio 2 derivatives crystallized in the centrosymmetric structures while the aminothio derivative (3) crystallize in the noncentrosymmetric structure with interesting NLO properties. The thioamino (3) with the noncentrosymmetric structure has a higher dipole moment (thrice that of (1) and double that of (2)) compared to the centrosymmetric structures diamino (1) and dithio (2) as shown in figure 9.
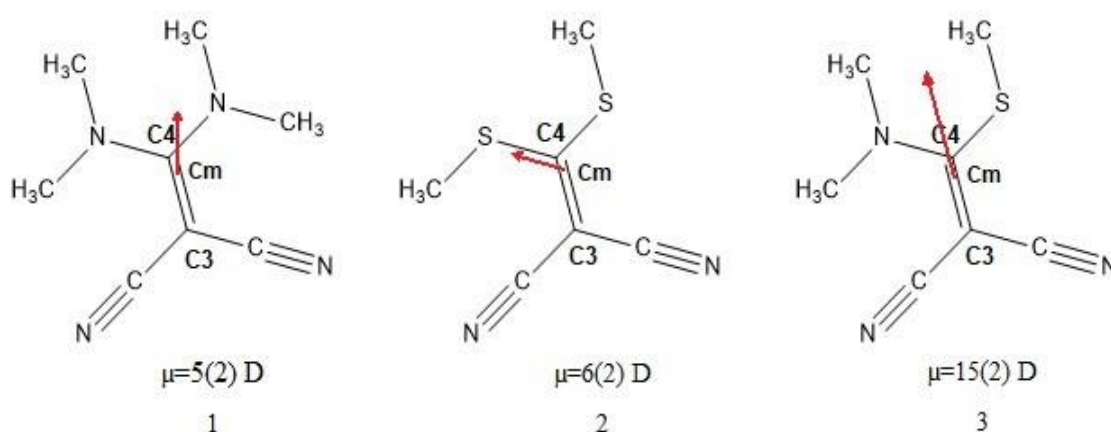
Figure 9. Molecular diagrams illustrating the dipole moment vectors of the diamino (**1**), dithio (2), thioamino (3) derivatives of EDCN calculated from charge density. The centre of mass of the molecule is represented by Cm.[9]

The optimization of the dipole moment in 3 may be as a result of two factors:

- The two electron donating groups are asymmetrically substituted.
- Decrease of the noncentrosymmetric crystal field within the thioamine derivative (3) molecule results in an increased charge separation which consequently increases the dipole moment in the crystal.

Looking along the C_3-C_4 bond of the 1,1- ethylenedicarbonitrile moiety, the three derivative show different conformations. The diamine derivative (1) has a pseudo two fold symmetry, the dithio derivative (2) and the thioamine derivative (3) show a syn-antimetylthio conformation. The variations in the dipole moment and molecular conformations as a result of substitution greatly affects the NLO properties of the molecule.

5.2 Intermolecular effects

Intermolecular interactions can greatly affect the hyperpolarizability in NLO interactions. Intermolecular π- π interactions play a very significant role towards the determination of the second order nonlinear optical response of some molecule. For example, consider the para-nitroaniline (PNA) (**4**) and 3-methyl-4-nitropyridine oxide (POM) (**5**) chromophores , Figure 10.

4   **5**
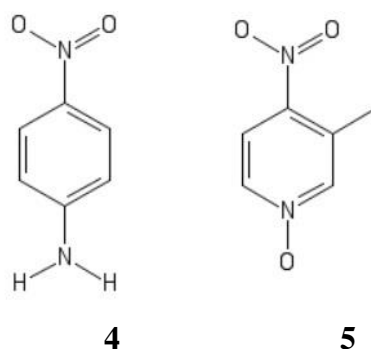
Figure 10. Chromophores of PNA (**4)** and POM (**5**).

The difference in the NLO response of PNA and POM chromophore clusters can be accounted for in terms of the difference in their intermolecular interactions. The intermolecular interactions in PNA clusters are basically electrostatic (dipole-dipole) in

nature and presides over the other contributing interactions both at long and short interplanar distances.[31] The intermolecular interactions shift their energies without mixing the resulting excited states. Consequently, at various interplanar distances, the hyperpolarizability response is greatly influenced by the location of the lowest energy charge- transfer transition.

With the POM clusters, intermolecular interactions are dominated by the delocalization or intermolecular charge-transfer interactions which operate only at short distances. POM excited states strongly mix at short intermolecular distances. When intermolecular distances are relatively large, an additional contribution to the hyperpolarizability is observed as each molecule behaves independently of the surrounding one.

This therefore shows that the intermolecular chromophore-chromophore interactions may greatly affect the macroscopic second order susceptibilities of NLO materials which are molecular based. The NLO response of the material depends to a larger extent not only on the molecular geometries but significantly on a variety of characteristics that constitute the material. However, the NLO response is strongly influenced at chromophore-chromophore equilibrium distance by the relative molecular orientations.

5.3 Effects of structural order on second order polarizability

5.3.1 Effects of substituents on second order polarizability

Optical nonlinearity can be strengthened considerably by strong donor-acceptor substituents. In the para-position. For example, in the para-position of benzene, increasing the strength of the donor and acceptor groups results in an increase in the optical nonlinearity of the system. The order of strength of the most common donor and acceptor groups are as follows:

Donor groups $N(CH_3)_2 > NH_2 > OCH_3 > OH$

Acceptor group $NO > NO_2 > CHO > CN$

Multiple substituents of the same functional group on the ring typically has very little significance if second order polarization needs to be maximized. Substitution of a hydrogen atom in unsaturated molecules has typically two effects, the induce effect and the mesomeric effect. The inductive effect is basically an electronic effect which occurs

as a result of the σ-bonds polarization in a molecule. In the induce effect, due to the difference in the electronegativities of the atoms at both ends of the bond, the bonded electrons are pulled towards the more electronegative atom thereby creating a bond polarization. Charge screening of the σ-bonding molecular framework causes this effect to be short range.[21] This effect is observed in both saturated and unsaturated molecules. Conjugated systems especially the aromatic systems display the mesomeric effect. The resultant flow of the electron charge density either towards or away from the substituted atom on the ring is due to the charge delocalization and mobility of the π-electron system. Hence, the mesomeric effect affects mostly the strength of the π-electron charge transfer. The mesomeric dipole moment of a system is the difference in dipole moment between the conjugated molecule and the corresponding saturated molecule bearing the same substituents. This helps to classify substituent groups into donor (D(+)) and acceptor (A(-)) functional groups. This classification is based on whether charge is drawn into or out of the conjugated system. The mesomeric dipole moment scales roughly with the size of the conjugated molecules.[22]

5.3.2 Effects of conjugation length of the molecule on second order polarizability

Most often, the length of the π-conjugated molecular system increases the magnitude of the second order polarizability of the organic molecule. This can be achieved in two ways, either by π-conjugated elongation through fused rings or by π-conjugated elongation by alternating single and double bonds. Fused ring systems usually have short absorption wavelengths with higher second order polarizability compared to the those with elongation by alternating single and double bonds. Figure 11 illustrates the structures of some para-substituted conjugated organic systems.
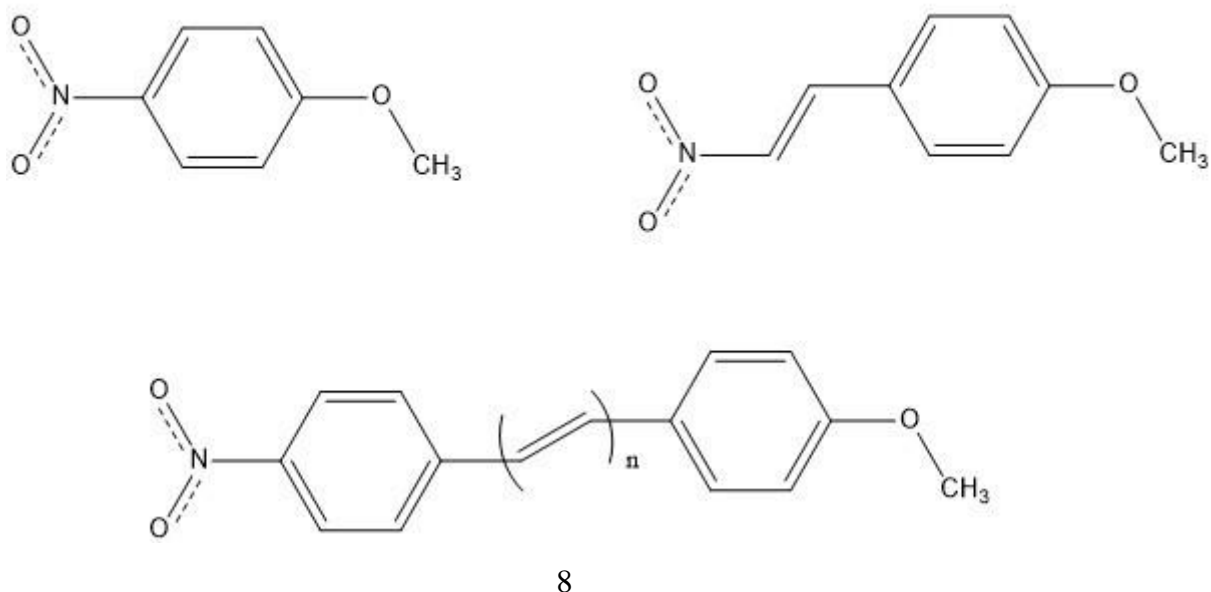
Figure 11. Structures of some para-substituted conjugated organic systems.

The magnitude of the second order polarization increases three times as the length of the conjugated π-electron system of the molecule based on the number of alternating single and double bonds. This is because the conjugated π-electron moiety paves the way for the electronic charge to be redistributed throughout the entire conjugation length under the influence of an external electric field. An increase in second order polarizability as a result of an increase in conjugation leads to an increase in molecular volume and loss of transparency. For polyphenyl molecules, there is a big loss in nonlinear optical susceptibilities which is proportional to the number of molecules per unit cell. This makes molecules with n>3 not suitable for microscopic samples as shown in Figure 12.

9
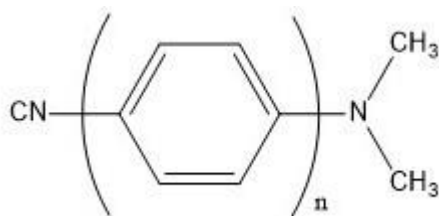
Figure 12. molecular representation of molecules with n>3.

5.3.3 Effects of planarity of the molecule on second order polarizability

Another important aspect besides considering the donor/acceptor groups and conjugated length of the system is the planarity of the molecules. The shape of any molecule depends largely on the atoms that constitute the molecule and the electrons of the central metal atom. Planarity is exceptionally important for two or multi-ring systems. The mobility of the electrons and the magnitude of the π-electron system are affected by the planarity of the molecular system. For example, in biphenyl ring systems, the effect of twist angles between rings drastically reduces the charge transfer contribution. Considering the two nonlinear optical molecules in Figure 13 introducing the OH-group into the molecule forces the molecule into planarity leading to an increase in second order polarizability.[22]

11
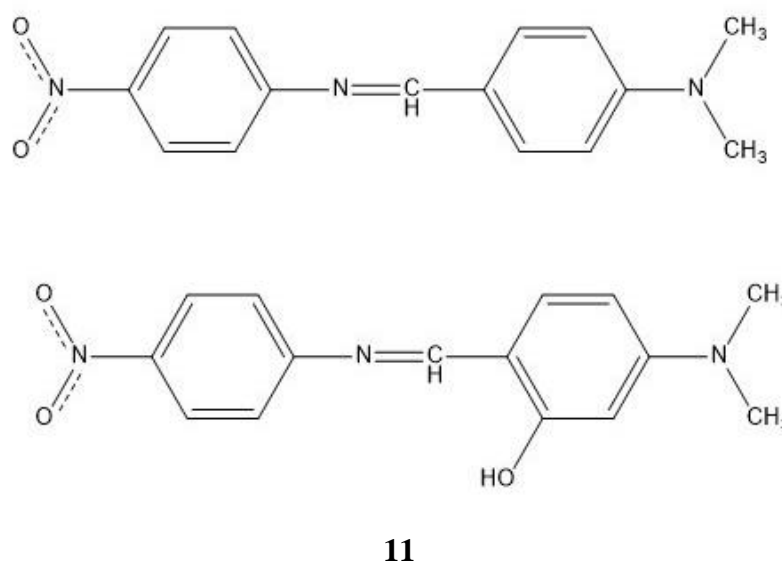
Figure 13. Increase in the second order polarizability of a molecule due to an increase in planarity.

Hence, optimizing structures for highly efficient nonlinear optical effects, the influence of substitution on the molecule, conjugation length of the molecule and the planarity of the molecule on second order polarizability are all extremely important aspects to be considered.

5.4 Molecular packing

Second order nonlinear optical properties of a material are closely related to the nature of molecular packing in the material.[23] The way the π-conjugated chromophores are aligned to each other greatly influenced the microscopic second order susceptibility of the NLO material. Most often, a greater percentage of nonchiral organic chromophores crystalized in centrosymmetric form and show no macroscopic second order optical nonlinearity. To have highly efficient and ideal second order NLO crystalline materials, the noncentrosymmetric packing of the chromophores in the crystalline lattice play a very important role because noncentrosymmetric space group is one of the main requirements that enhance the SHG in an NLO material. Hence noncentrosymmetric crystal packing greatly influence the NLO properties of the material. This can be achieved through strong coulombic interactions as it is the case in the crystallization of ionic salts which strongly enhance the second order susceptibility of the NLO material. In the case of donor- π-acceptor organic ionic materials, the main origin of the nonlinear properties is the cation while the counter anion adjusts the crystal packing by coulombic interactions. Combining the cation and the anion in a suitable way in the crystal lattice will lead to high and efficient second order optical nonlinearity in the NLO material.

5.5 Effects of particle size

In order to be able to evaluate and understand the importance of the measured SHG intensity, the effect of particle size needs to be considered. The frequency conversion process generates at the surface of particles. If the particle size is big, the electromagnetic field will be retarded and due to this retardation effect, a major quadrupolar contribution will be observed.[35] Destructive interference of the polarization of the molecules may cause the second harmonic generation not to be detected if the size of the particle is so small relative to the optical coherent length. Good and efficient SHG activity is observed with particles in the micrometre or sub micrometre size range. Interferences of all the second harmonic waves generated at the entire particle surface results in the shape of the second harmonic intensity pattern that is determined by the refractive index, the size of the particle and the wavelength of the incident light[35]. For compounds that are not phasematchable, the second harmonic intensity does not

increase in a linear manner with corresponding increase in the size of the particle.[43] For this case, the intensity peaking for the sizes of the particles will be comparable to the average coherence length. If the particle size is big relative to the coherence length, the second harmonic intensity will decrease inversely. However, compounds that are phasematchable show an almost linear increase in the second harmonic intensity with a corresponding increase in the size of the particle up to the average coherence length. At this point, the intensities will become saturated and will no longer depend on the size of the particle. Summarily, SHG of phasematchable compounds depends on the powder particle size and the SHG of non-phasematchable compounds is independent of the powder particle size. Figure 14 below illustrate how SHG of phasematchable and non-phasematchable compounds vary with the size of the particle.
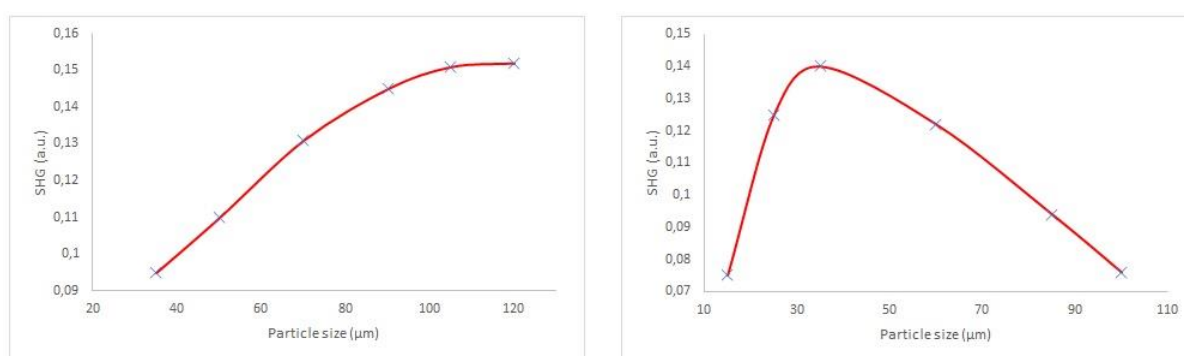
Figure 14. Illustration of the variation of SHG of phasematchable and non-phasematchable compounds with particle size.

For non-phasematchable compounds, varying the particle size causes the SHG to oscillate.[43] The period of oscillation will be doubled the average coherence length. Second harmonic intensity in terms of particle size can be obtained in the forward scattering direction and in terms of scattering angles. With respect to scattering angles, the maximum second harmonic intensity tilts towards larger scattering angles if the size of the particle is small.

6 Kurtz and Perry powder method for SHG measurements

Determination of second order nonlinear susceptibilities is carried out by measuring the SHG efficiencies of single crystals. However, most often, good enough single crystals of the compound to be measured are not obtained. So, the powder method instituted by Kurtz and Perry which is today named after them as the Kurtz and Perry powder technique is used. This is a common method most commonly used to determine if a particular compound possess some SHG properties or not. The schematic representation of   this   technique   is   illustrated   in   Figure   15
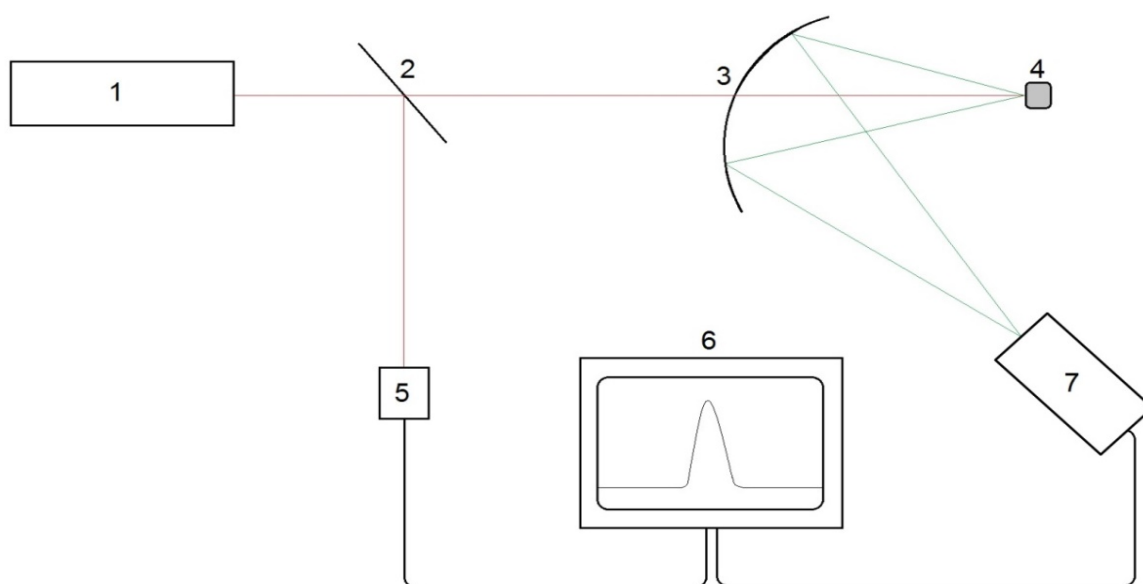
Figure 15. Schematic representation of the Kurtz and Perry powder technique for measuring SHG in NLO materials (1) Laser or radiation source, (2) Beam splitter, (3) Concave mirror, (4) Sample, (5) Optical switch, (6) Oscilloscope, (7) Photomultiplier tube.

During the operation of this technique, the Q-switched laser unfocused beam hits a tiny section (approximately 0.2mm) of the powder sample of the material under investigation. These powder samples are randomly oriented and the spot size of approximately 0.2mm is considered large enough that the incident beam from the laser impinges on particles oriented along all the possible crystal direction.[43]

The fundamental beam is filtered using a series of short wavelengths passing filters. The second harmonic signal is then detected using a photomultiplier. This second harmonic

signal is displayed on an oscilloscope. A beam splitter is placed ahead of the sample to be measured in order to obtain the reference beam. This helps the second harmonic signal that is generated in a reference sample to be observed by displaying the two signals at the same time on a dual-beam scope. This system also allows narrow-pass filters at the second harmonic wavelength to be fitted in between the photomultiplier and the Shoot filters. This is done to help take off spurious signals like signals from multiple photon absorption. In order to be able to achieve efficiency in the second harmonic signal collected at the detector, a parabolic reflector having a small hole which enables the laser beam to pass through is positioned directly in front of the sample powder that is between the laser and the sample.

Kurtz and Perry powder technique provides an idea of the nonlinear efficiencies of materials as it is based on analysing only the SHG output of the powder crystal monolayer.[43] This idea renders this technique very effective and allows the SHG obtained from the sample to be comparable to that obtained from a single particle after averaging in all directions. The SHG field will be sensitive to the polarization of the incident beam of light scattering is negligible.[43] This method can also be used to identify materials with NLO activity (SHG) and phase matching capabilities.

7 Amino acid base compounds as NLO active materials

Among organic compounds as NLO materials, amino acids possess some specific and interesting characteristics or features such as weak Van der Waals forces, molecular chirality and hydrogen bonds. Wide transparency ranges in the UV and Vis regions of the electromagnetic spectrum, absence of strongly conjugated bonds and the molecules being zwitterionic in nature. This zwitterionic nature of organic molecules favours crystal hardness. Amino acids contain chiral carbon atoms which help to direct the crystallization of the NLO material into the noncentrosymmetric space group which is an additional advantage for materials to be NLO active. All these features highly nominate amino acid base compounds to be applied as NLO active materials in NLO applications. Some amino acid compounds which are highly advantageous as NLO active materials due to their interesting NLO properties are discussed in this chapter.

7.1 2-amino-4-picolinium-nitrophenolate nitrophenol (2A4PNN) (12)

The phenolic compound 4-nitrophenol is typically known for its one dimensional donor-π-acceptor system. It contains both the electron donating group (hydroxyl) and the electron accepting group (nitro) which are connected through the benzene aromatic ring. The highest occupied molecular orbital (HOMO) which is also the outermost orbital responsible for donating electrons and for the potential ionization of the compound is mainly localized on the nitrophenolate anion. The lowest unoccupied molecular orbital (LUMO) which is the innermost orbital acting as the electron acceptor and therefore directly relating to the electron affinity of the compound is localized on the entire 2-amino-4-picolinium cation and also on the nitrophenolate anion.[40] This enables the flow of charge from the phenolate anion to the 2-amino-4-picolinium cation via hydrogen bonding. This is a significant characteristic towards obtaining second order NLO activity in the compound. Due to the presence of the phenolic group in 4-nitrophenol, it can form many salts with varying organic and inorganic bases.[39] The 4-nitrophenolate is highly desirable in the synthesis of noncentrosymmetric structures due to its lower dipole moment, higher polarizability and its achiral counter anions. The NLO active compound 12 is prepared according to reaction 1 below.

4-nitrophenol   2-amino-4-picoline

2-amino-4-picolinium nitrophenolate nitrophenol
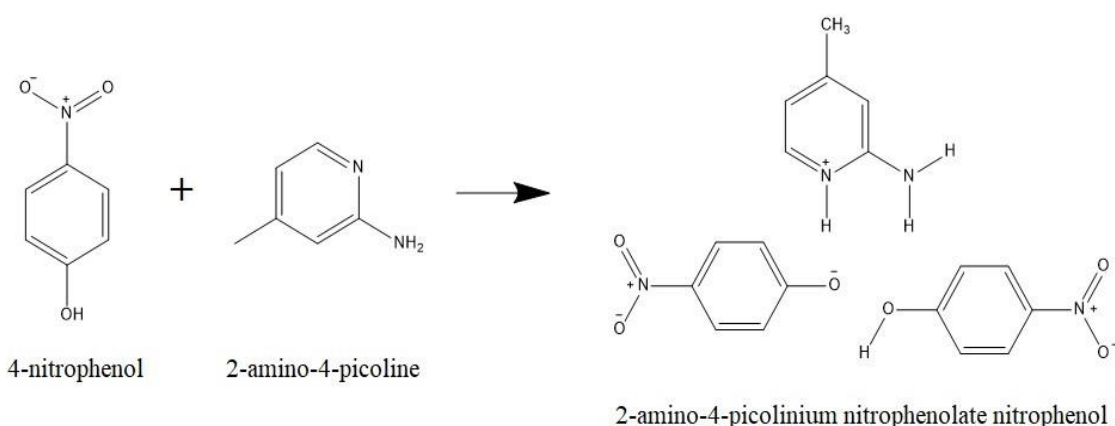
Reaction 1. Chemical reaction of 4-Nitrophenol and 2-Amino-4-picoline to form compound 12.

There is a transfer of the proton of the hydroxyl group of the phenol to the nitrogen atom of the pyridine which is confirmed from the change in the pKa value between the 4-nitrophenol and 2-amino-4-picolinium (protonated pyridine compound).[37]The reaction occurs as a result of the possibility to protonate one out of the two nitrophenol molecules which protonates the ring nitrogen of the picoline molecule. This enhances the asymmetric nature of the compound.[38] The hyper-polarizable neutral 4-nitrophenol, 4-nitrophenolate anion and 2-amino-4-picoline in the molecular structure are linked together via strong and directional hydrogen bonds which enables it to form noncentrosymmetric crystals in the Pna2$_1$ space group. Molecular packing diagram shown in Figure 16 below.
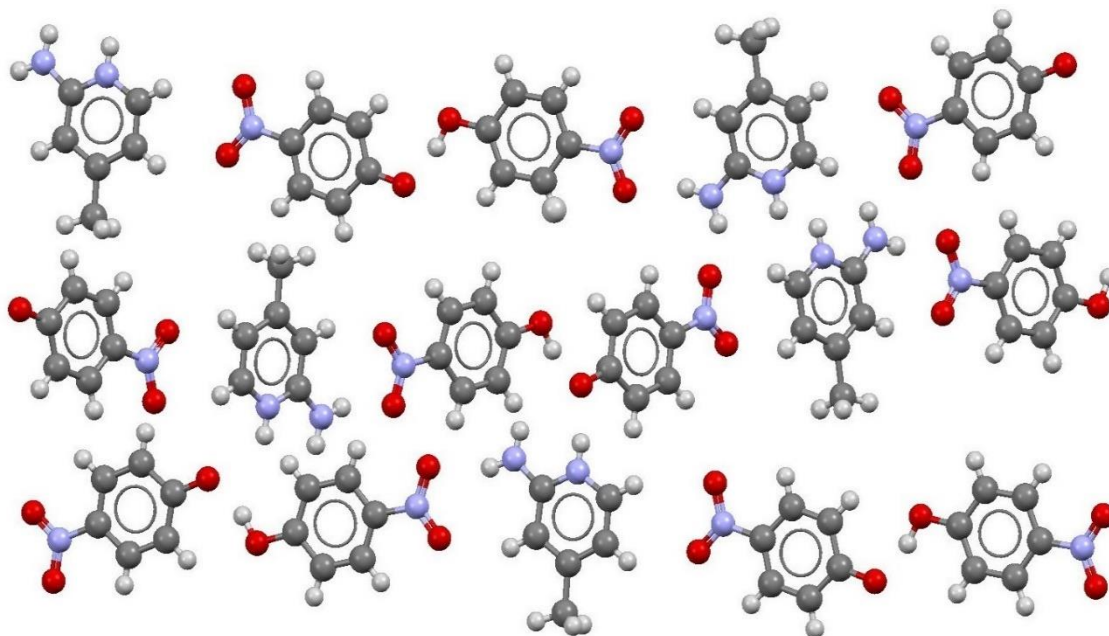
Figure 16. Molecular packing diagram for 2A4PNN.

This is a very important factor to be able to generate second harmonic signal from the crystal. 2A4PNN shows intramolecular herringbone structure in which 4-nitrophenolate anion and 4-nitrophenol are linked by hydrogen bonds. The picolinium cation and the nitrophenolate anion are both formed from proton transfer during which the phenoxide anion accepts the neutral 4- nitrophenol as a third molecule via hydrogen bonds. 2A4PNN possesses a donor-π-acceptor groups on either ends of the π-conjugated path thereby making it a suitable NLO material. Both the phenoxide anion and the picolinium cation are kept together in the structure by ionic attraction and hydrogen bonding interactions. 2A4PNN is soluble in ethanol which makes it easier to obtain large enough

size single crystals as it provides a moderate solubility temperature gradient for the compound. These crystals are obtained either by slow cooling or by slow solution evaporation technique. 2A4PNN possesses a SHG efficiency of 1.95 times compared to that of urea. The SHG efficiency of 2A4PNN depends on the particle size as illustrated in Figure 17 below.
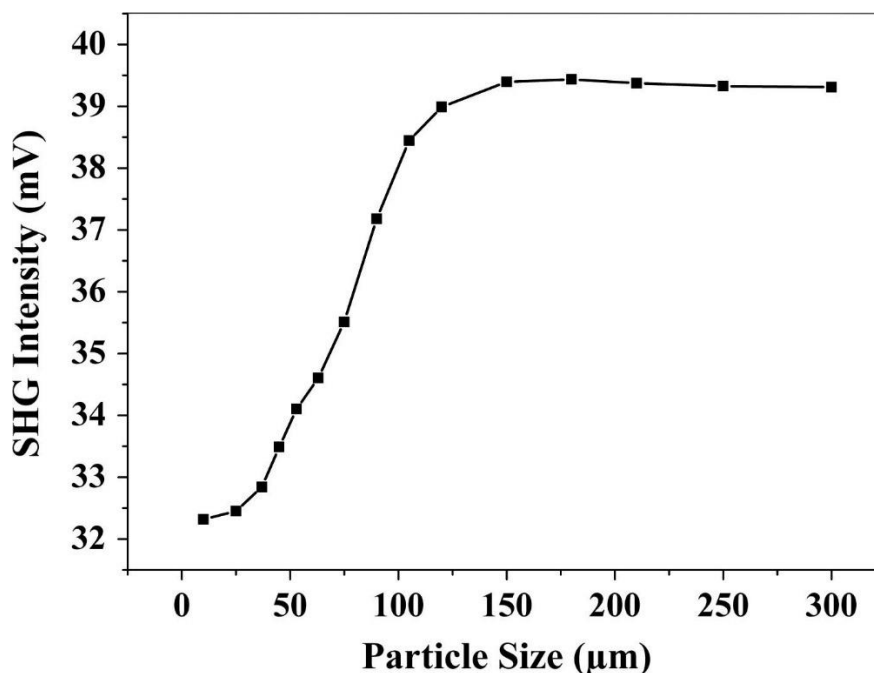
Figure 17. Illustrates the relationship between particle size and SHG intensity of 2A4PNN.[37]

This shows that 2A4PNN is a phase-matchable compound (see chapter 6). From the figure, the SHG intensity of 2A4PNN increases linearly with the increase size of the particle until the average coherence length is reached. A further increase in the size of the particle does not result to a corresponding increase in the SHG intensity after this point.[37] This is due to the second harmonic wave and the fundamental waves being equal. 2A4PNN has a laser damage threshold of $3.6 GW/cm^2$ with weak anisotropy thermal expansion which is a very good characteristic to grow and process its crystals. This value for the laser-induced damage makes it advantageous to be employed as an NLO material. 2A4PNN is a polar molecule and has a molecular dipole moment of 21.18 Debye, polarizability value of 18.56×10^{-24} esu and first order hyperpolarizability value of 11.16×10^{-30} esu which give strong bases for the origin and existence of NLO activity in this compound.[37]

7.2 L-Argininium-4-nitro phenolate monohydrate (LA4NPM) (13)

4-nitrophenol derivatives are quite interesting and promising molecules for NLO applications due to the fact that they are one-dimensional donor-π-acceptor system with the phenolic -OH group facilitating its formation of salts with both organic and inorganic bases.[39] LA4NPM is prepared by reacting equimolar amounts of 4-nitrophenol and L-arginine in deionized water. Reaction 2 is a schematic representation of the reaction that occurs between 4-nitrophenol and L-arginine to form the titled compound.
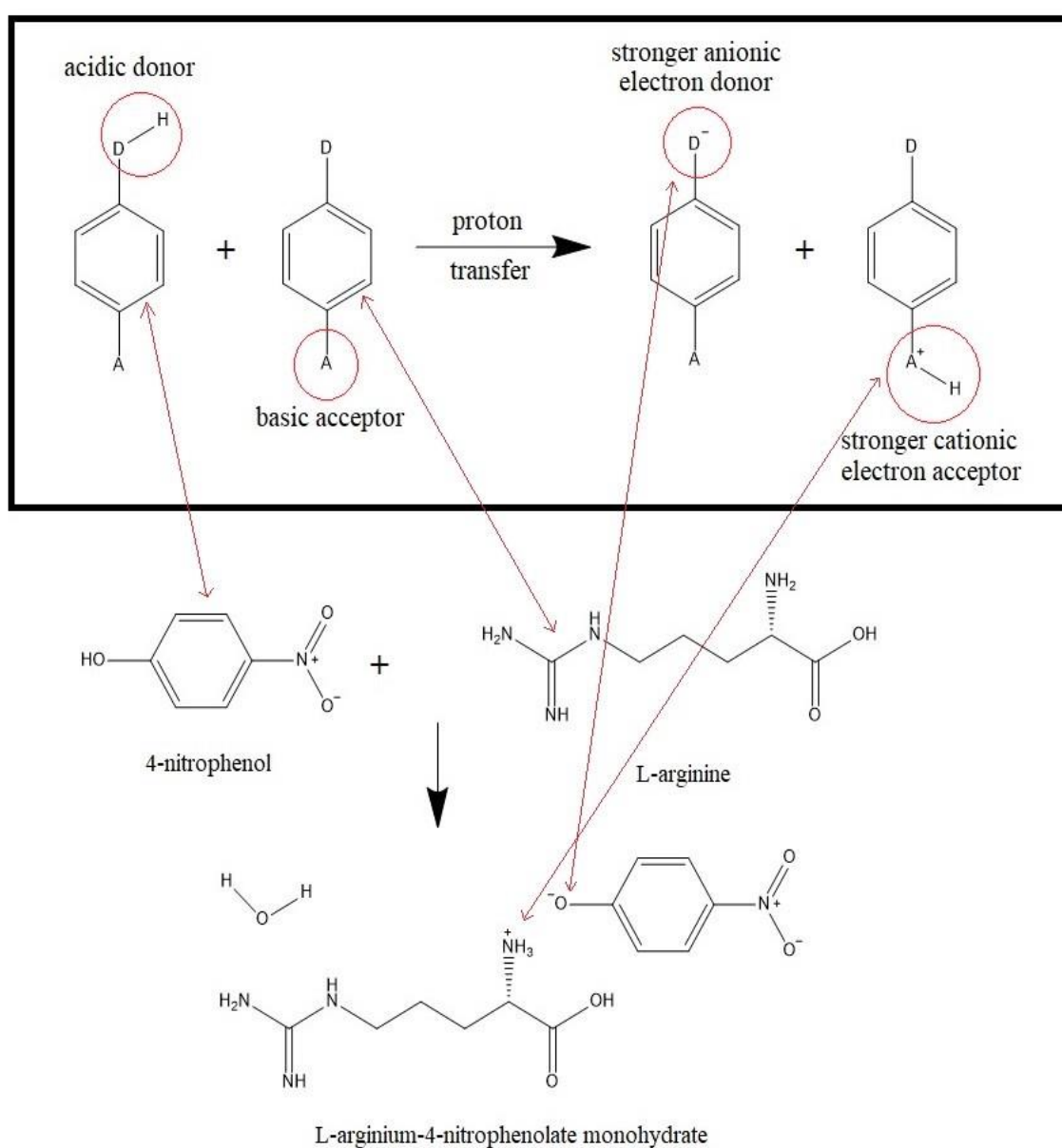
Reaction 2. Schematic representation of the chemical reaction for the formation of L-arginium-4-nitrophenolate monohydrate.

During this reaction, there is the protonation of the amino group of L-arginine by 4-nitrophenol to form the L-argininium cation and the 4-nitrophenolate anion. As a result, the phenolate conjugate base O$^-$ has a better electron donating character and therefore an increase molecular hyperpolarizability compared to the phenolic OH[38]. Similarly, the L-argininium conjugate acid NH_3^+ has an increase molecular hyperpolarizability compared to the NH_2. LA4NPM has first-order polarizability value of 4.20×10^{-29}esu. This high first-order polarization value for LA4NPM is as a result of planar molecular structure, favourable conditions for the conjugation of electrons and charge transfer for the molecule. The diagram for the LA4NPM single crystal is illustrated in Figure 18.
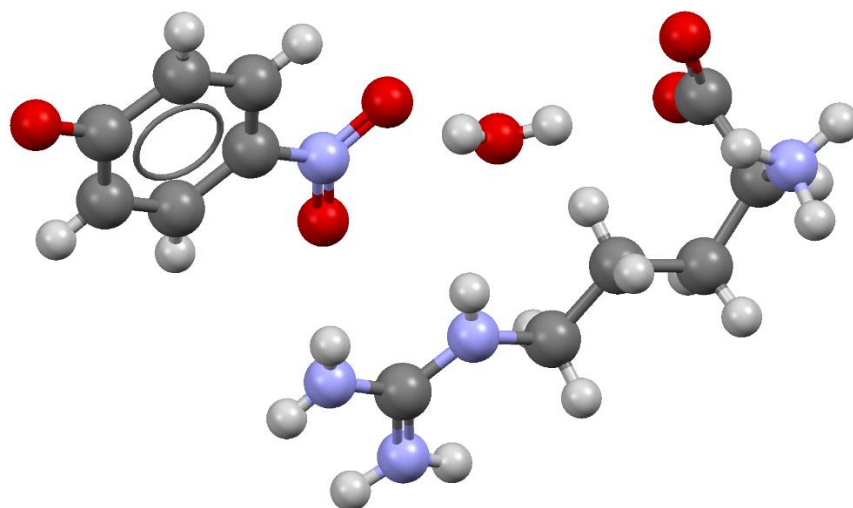
Figure 18. Structure of a molecule of LA4NPM.

However, this increase in the molecular hyperpolarizability is only possible if the proton transfer takes place between separate organic NLO chromophores resulting in noncentrosymmetric organic salts in which one is a base and the other an acid. This idea to increase the hyperpolarizabilities of molecular chromophores by proton transfer was first put in place by Evans and co-workers.[38] The amino group present in cation of L-argininium forms strong intermolecular hydrogen bonds with the oxygen atoms of adjacent phenolate anion (N−H⋯O) which stabilizes the molecule. These intermolecular hydrogen bonds play a significant role towards obtaining the molecule in a noncentrosymmetric structure.[39] Figure 19 below shows the molecular packing diagram for LA4NPM.
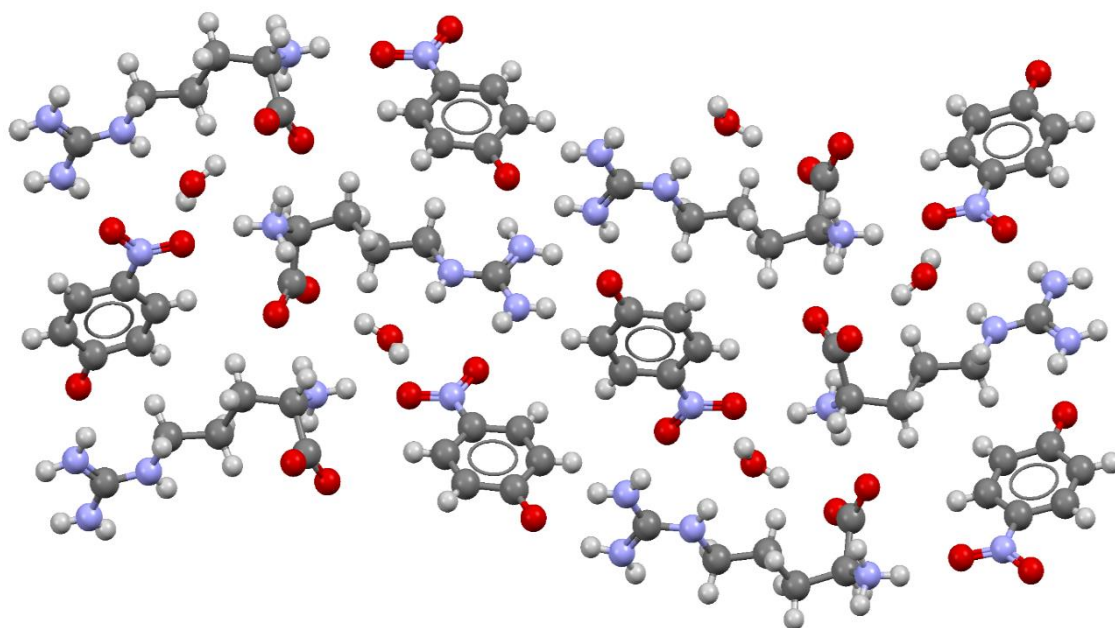
Figure 19. Molecular packing diagram for LA4NPM.

Also, there is an intramolecular N−H···O hydrogen bonding with the phenolic O atom. In the molecule, the carbonyl group undergo π- π* transitions which also enhances the NLO properties in the compound. LA4NPM exhibits a very high SHG efficiency with a signal output of 312mV compared to that of KDP which has an output of only 9mV. This strongly nominates LA4NPM as a potential material in SHG applications.

7.3 L-Arginine maleate dihydrate (14)

L-arginine is actually one of the well-known basic amino acids that has gained more popularity in the developing world of nonlinear optics. Maleic acid also is one of the most popular basic dicarboxylic acid that has attracted more attention in the field of potential application in nonlinear optics as a result of its large π-conjugation system. Compound 14 has a molecular formula of $C_6H_{15}N_4O_2^{+}.C_4H_3O_4^{-}.2H_2O$. This chemical compound is synthesized by reacting equimolar amounts of L-arginine and maleic acid. compound 14 crystals are obtained by the liquid diffusion method. Reaction 3 below illustrates the chemical reaction that takes place between L-arginine and maleic acid to form compound 14
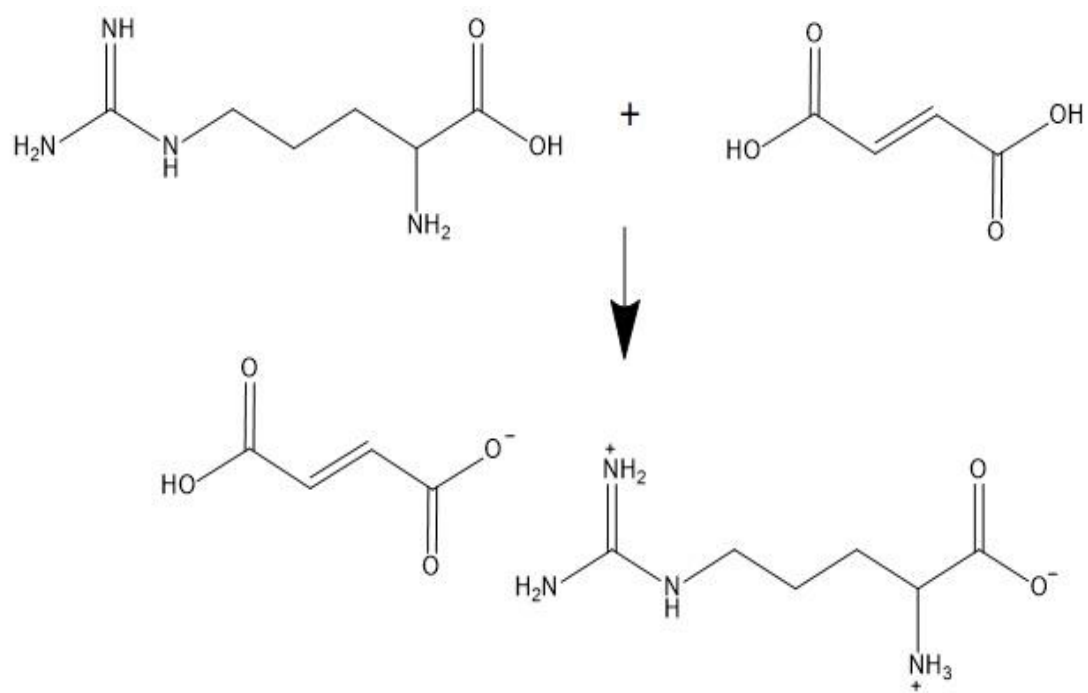
Reaction 3. Schematic representation of the chemical reaction for the formation of L-Arginine maleate dihydrate.

Compound 14 consist of positively charged zwitterionic arginine molecules and semi-maleate anions with intramolecular symmetric O−H−O hydrogen bonds. Amino acid molecules build up into layers in which interactions between the layers incorporate the semi-maleate anions in to the complex. Figure 20 presents the molecular packing for compound 14.
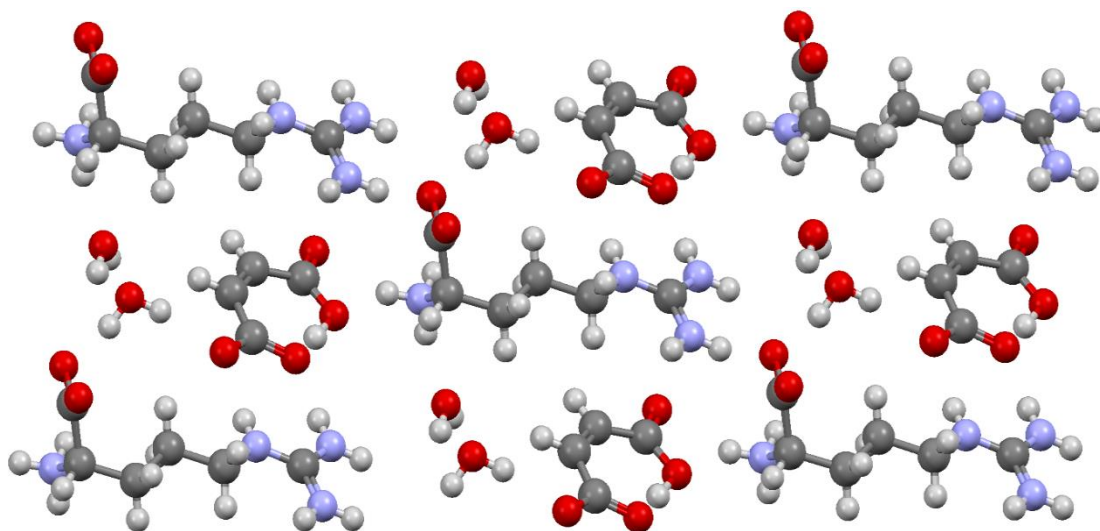
Figure 20. Molecular packing for L-arginine maleate.

Compound 14 crystals is noncentrosymmetric and belong to the triclinic space group.[46] It is a phase matchable compound which is advantageous in materials with NLO activity. Compound **14** has a density of 1.419 gm/cm^3 with an optical absorption and transmission spectra in the region of 190 nm to 1100 nm of the electromagnetic spectrum. It has a lower cut-off wavelength at 238 nm without any absorption in the visible and the near infrared regions of the electromagnetic spectrum. This is a typical characteristic of amino acids that they do absorb radiation all through the entire visible region of the electromagnetic spectrum.[45] The lack of absorption (good transmittance) in every part of the visible and the infrared regions of the electromagnetic spectrum is an additional advantage for the second harmonic generation activity in the compound. This nominates it as a suitable material for SHG applications.[46]

Compound 14 has a melting point of about 90°C without any phase transition occurring before melting.[47] Decomposition of the material starts at a temperature of 107°C with a loss of the water molecule, then at temperatures between 301°C and 538°C, ammonia is removed. The actual decomposition of the compound continues up to temperatures about 700°C. This high decomposition temperature reveals the better thermal stability of the material which is one of the characteristics that good NLO materials should have (see chapter 4). During all these stages of decomposition, the compound is highly volatile. L-arginine maleate dihydrate has a second harmonic efficiency of 1.5 times that of KDP.[47] This compound exhibits a continuous increase in the SHG efficiency with an increase in the size of the particle which confirms the phase matching ability of the compound.[47] This shows that the SHG efficiency of L-arginine maleate depends strongly on the size of the particle. The dependence of the SHG efficiency of L-arginine on the size of the particle is illustrated in Figure 20. Hence, growing large size and good quality crystals of Compound 14 may result in very interesting SHG results. Materials that are phase matchable are easily grown into large size single crystals for NLO applications.[47]
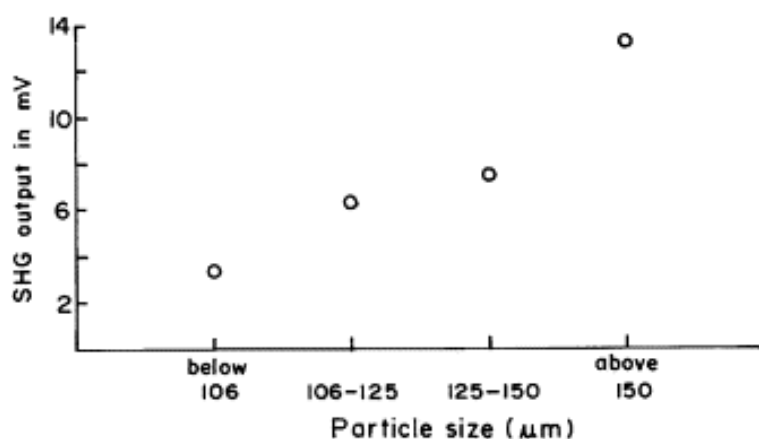
Figure 20. Illustration of the dependency of SHG of Compound 14 on particle size.[47]

All the characteristics outlined so far such as phase matchability, noncentrosymmetric crystal structure, no absorbance (high transmittance) all through the entire visible region of the electromagnetic spectrum, increase in the SHG efficiency due to the increase in the size of the particle and the SHG efficiency of 1.5 times higher than that of the standard KDP material highly points out that Compound 14 stands a better chance as a potential material for NLO applications.

7.4 L-Valinium picrate (15)

With glycine as an exception, amino acids contain chiral carbons, carboxyl groups (-COOH) as a proton donating group and the amino group (-NH$_2$) as the proton accepting group.[41] L-valine is one of the amino acids that have been extensively used to synthesize a variety of salts with different organic acids. Compound 15 with a molecular formula of $C_5H_{12}NO_2^+.C_6H_2N_3O_7^-$ is a promising NLO material with L-valine acting as the electron donor and picric acid acting as the electron acceptor. This makes available the ground state charged asymmetry of the molecule which is very important for the presence of second order nonlinear optical properties of the compound. Compound 15 has a melting point of about 269°C without any initial phase transition, but the compound decomposes totally at a temperature of about 800°C. This is an indication that the compound is highly stable thermally which is a characteristic of a good NLO material as discussed in chapter 3. Hence. Compound 15 can be employed in NLO applications up to this melting point. It has a mechanical stability of about 50 kg.

Equimolar amounts of the amino acid L-valine and picric acid react to form Compound 15 according to reaction 4 below.
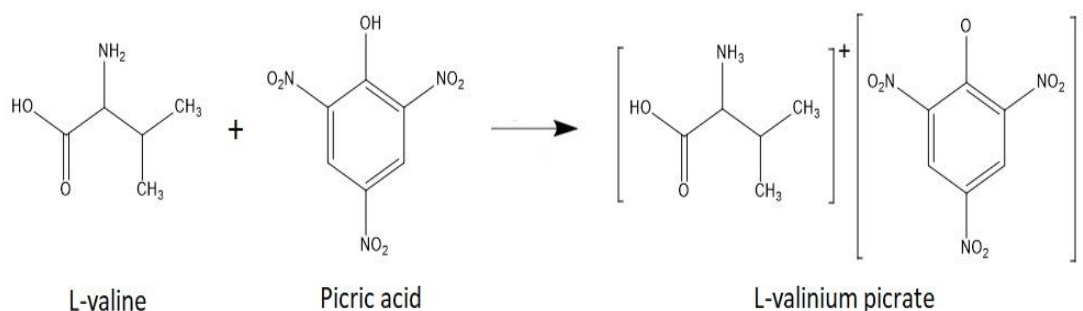
Reaction 4. Formation of compound 15 by the reaction of L-valine and Picric acid.

Crystals of compound 15 can be obtained from a mixture of equal amounts of water and acetone. Compound 15 has a transmittance of about 65% between 500 nm to 100 nm.[41] L-valinium picrate does not absorb appreciably in the visible region of the electromagnetic spectrum as it is the case with other amino acids, but its optical transmission range nominates it as a promising candidate for SHG. Compound 15 single crystal has a band gap energy of about 2.24eV. The molecular representation of the structure of compound 15 is illustrated in Figure 22 below.
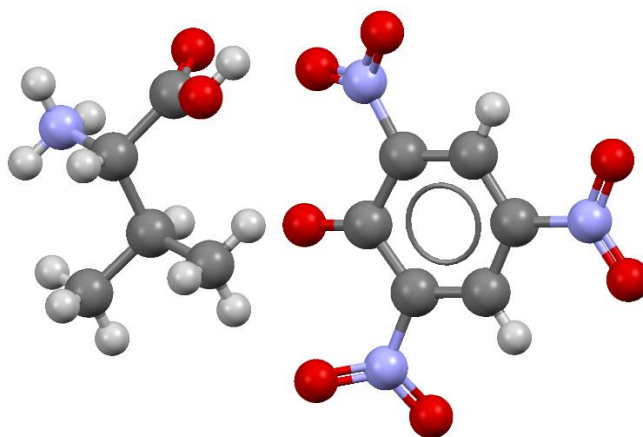
Figure 22. Representation of the molecular structure of compound 15.

The SHG conversion efficiency of compound 15 can be approximated to 60 times compared to that of standard KDP. This high SHG conversion efficiency of compound 15 can be explained based on its molecular structure. There exists intermolecular

hydrogen bonding between the picrate anion and the amino group of L-valinium cation.[42] This is achieved through the N atom of the amino group of valinium cation and the O atom of the picrate anion forming the N−H···O hydrogen bonds. This enhances the first-order hyperpolarizability values of the compound giving rise to NLO activity. The first-order hyperpolarizability value for compound 15 is 9.72×10^{-30} esu which can be approximated to 36 times compared to that of urea. This high first-order polarizability value can be associated with the planar molecular structure of the compound and the better conditions for conjugation of electrons and charge transfer. The valinium residue bears the carboxyl group which even forms stronger hydrogen bonds with the picrate anion.[40] Hence, in L-valinium picrate, there exist two types of hydrogen bonds. The strong N−H···O hydrogen bonds and the O−H···O hydrogen bonds which are even stronger. These intermolecular hydrogen bonds hold the L-valinium cation and the picrate anion together in the molecular structure. The dipole-dipole interactions in the solid state of the molecule may lead to the quasi cancellation of the nonlinearity in the molecule. The carboxy substituents on the other hand can be used to enhance acentric alignment of the chromophores in the solid state structure through the network of hydrogen bonds. A non-zero SHG efficiency in the molecule is ensured by the repeating units along the entire length of the chain.[44] All the above mentioned properties highly nominate compound 15 as a potential NLO active material.

7.5 L-Alaninium maleate (16)

Compound 16 is a salt of a weak carboxylic acid (maleic acid with the molecular formula $C_4H_4O_4$) and the amino acid L-alanine having molecular formula CH_3CHNH_2COOH. The chemical reaction between L-alanine and maleic acid to form L-Alaninium maleate ($C_3H_8NO_2^+C_4H_3O_4^-$) occurs according reaction 5
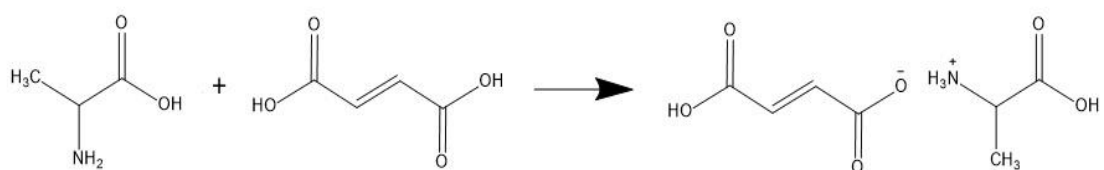
Reaction 5. Schematic representation of the chemical reaction for the formation of L-Alaninium maleate.

During this reaction, Maleic acid protonates the carboxyl group of alanine molecule to form the titled compound. Crystals of L-Alaninium maleate can be obtained by the slow evaporation technique. The solubility of L-alaninium maleate increases with an increase in temperature between $25^{o}C$ to $50^{o}C$. L-Alaninium maleate has a melting point of $162.2^{o}C$ with a phase transition occurring at $105^{o}C$. This indicates that the compound is thermally stable which is one of the characteristics advantageous for an NLO material. L-alaninium maleate is rhombic and has a non-centrosymmetric crystal structure which is one of the basic necessary requirements for materials with SHG efficiencies[49]. The structure of a molecule of L-Alaninium maleate is represented in Figure 23.
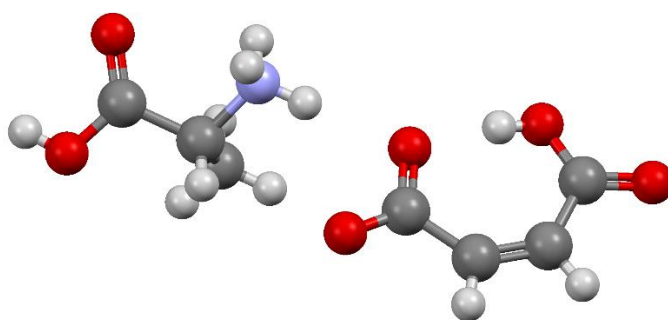
Figure 23. Structure of a molecule of L-Alaninium maleate.

The density of L-Alaninium maleate is $1.39g/cm^3$. L-alaninium maleate shows little or no absorption all through the UV-Vis-NIR regions of the spectrum. This may be a result of electronic transitions between the carboxylic anion ($-COO^-$) and the nitryl cation (NH_3^+). The absence of absorbance in the 320 nm to 1100 nm region implies that L-alaninium maleate can be used as an interesting material for optical window applications. It has a UV cut-off wavelength of 300nm which is appreciably low compared to other applications in the blue region and the SHG laser radiation at 1064 nm.[50] L-alaninium maleate possesses a SHG efficiency of 4.13 times compared to that of KDP. L-alaninium maleate has a major drawback as an NLO active material that can be applied in nonlinear optical applications in that it is really a soft material. This soft characteristic of the molecule can be explained based on the the interaction of the ions that constitute the molecular compound. L-Alanine is a zwitterion and incorporating maleic acid lattice into it leads to ionic vacancies. This defect acts as an obstacle to dislocation motion and the mechanical hardness of the material is greatly reduced. If the maleic acid concentration in the crystal structure are high, the vacancies build up forming larger aggregations.

7.6 L-Prolinium tartrate (17)

L-Proline can be effectively used as a donor residue to introduce chirality into the chromophores of NLO active materials. Proline plays a significant role in the folding of proteins and peptides due to the rigid bonds formed between the amino groups and the carboxyl groups. The stearic effect that arise from the proline side chain aid in determining the stabilities and position of the protein folds.[52] The reason behind organic crystals like proline behaving this way is as a result of their highly conjugated and polarizable molecules which enables the asymmetric π-electron system of the aromatic molecules to induce molecular charge transfer by the movement of electrons between donor and acceptor substituent groups. The molecules are assembled adequately which results in a noncentrosymmetric crystal structure without fading away the second order nonlinear coefficients.[52]

L-Prolinium tartrate has a molecular formula $C_5H_{10}NO_2^+.C_4H_5O_6^-$. This compound is synthesized by reacting equimolar ratios of L-Proline and L-Tartaric acid in double distilled water. L-Prolinium tartrate single crystals can be obtained by the process of slow evaporation. The crystals belong to the monoclinic space group system. The hydrogen tartrate ions form hydrogen bonds that are interconnected through proline molecules. Interaction among the amino acid molecules occur via the formation of weak $C-H\cdots O$ hydrogen bonds. There exist both strong intramolecular and intermolecular hydrogen bonds $N-H\cdots O$ between the NH_2^+ group and the carbonyl oxygen of the tartrate anion. This strong hydrogen bonds existing between the ionic species of L-Prolinium tartrate gives rise to the noncentrosymmetric structure, hence enhancing the molecular hyperpolarizability of the crystal.[53] L-Prolinium tartrate has a first hyperpolarizability value of 7.212×10^{-31} esu which is approximately 10 times compared to that of urea and a ground state dipole moment of 11.79 Debye. Most often, the compounds with a high value of dipole moment also has a high hyperpolarizability value with the corresponding HOMO-LUMO energy gap quite low.[51] The L-Prolinium tartrate crystal is stabilized by the strongest hydrogen bonds $O-H\cdots O$ that interconnects the tartrate anions and the prolinium cations.

L-Prolinium tartrate is a phase matchable compound with a SHG efficiency of 0.3 times compared to that of urea and 95% that of KDP. The SHG efficiency of L-Prolinium tartrate varies with particle size as illustrated in Figure 24
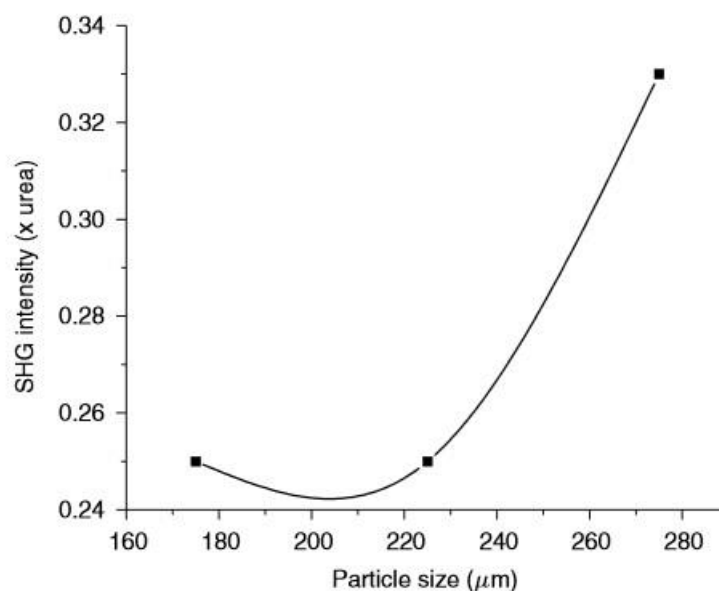
Figure 24. Variation of SHG of L-Prolinium tartrate with particle size.[53]

L-Prolinium tartrate acquires a twisted conformation in the intermolecular charge-transfer state which results in a strong charge-transfer character in the molecule. The twisted conformation acquired by the molecule in the intermolecular charge-transfer state is because of the existence of ground state hydrogen bonding within the molecule.[53] The two main factors responsible for NLO properties in L-Prolinium tartrate is the movement of the π-electron cloud between charged species through ionic hydrogen bonds which makes the molecule highly polarized and the twisted intermolecular charge transfer that occur in the molecule.[52]

All the above mentioned characteristics of L-Prolinium tartrate highly uplifts the molecule as a promising NLO material that can be employed in NLO applications.

7.7 L-Histidine Nitrate (18)

L-Histidine nitrate can be synthesized by the reaction between equimolar ratios of L-Histidine and nitric acid in distilled water as solvent.[49] Crystals of L-Histidine nitrate

can be obtained by slow cooling method due to its high solubility which is dependent on temperature. L-Histidine nitrate is very stable at temperatures up to 234°C without any phase transition taking place. After this temperature, the material stars to melt. This melting temperature of 234°C is a bit lower than that of pure L-Histidine which occurs at 277°C. L-Histidine nitrate starts to break down or decompose at a temperature of 254°C that is a rise in temperature of 20°C from the melting point temperature.[49] This high stability is advantageous for the material to be probably employed in laser applications since laser applications require crystals that can withstand high temperatures. L-Histidine nitrate has a lower cut-off wavelength of 320 nm without any significant absorption throughout the UV region of the electromagnetic spectrum, but it has a transmittance of approximately 50% at wavelengths between 351 nm to 900 nm. This clearly indicates that L-Histidine nitrate possesses good optical transparency which is one of the characteristics for SHG materials. L-Histidine nitrate has a SHG efficiency of 2.5 times compared to that of a standard KDP crystal.

8 Guanidine based compounds as NLO materials

Guanidine, with the molecular formula CH_5N_3, (1) is a simple organic chemical compound (figure 13 below). Guanidine is a colourless solid and soluble in polar solvents. It is a very important compound with many biological, chemical, medical and technical applications especially as its compounds are being used in molecular switches. Its structure is related to those of amides and proteins, but it is unique as it bears three functional amino groups It has a planar configuration as show in Figure 25.
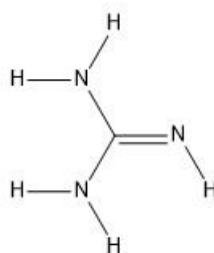

Figure 25. Planar configuration of guanidine molecule.

Its polar configuration makes it a potential hydrogen donor in hydrogen bonds. Guanidine molecule and especially its corresponding monoprotonated cation are very good examples of flat rigid molecules showing extensive π-electron delocalisation. Guanidinium cation is a good example of an octupolar building block (that is exhibiting three-fold rotational symmetry) for the design of molecular NLO materials. The guanidinium cation is a strong Lewis base with a pKa value of 13.5 and can be easily protonated by most organic anions resulting to salts with good crystallinity. This is due to the availability of six potential donor sites for hydrogen bonding interactions. An NLO crystal of guanidinium can be grown by the slow evaporation technique. Guanidinium compounds have physical properties that are potentially interesting for NLO applications. This is because guanidinium is a polarizable acentric two-dimensional cation as shown in its structure below.

$$H_2N \quad \underset{||}{\overset{+}{C}} \quad NH_2$$
$$H_2N$$
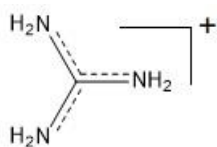
Figure 26. Structure of guanidinium cation.

Looking at the π-π interactions, Guanidine based organic compounds such as guanidinium cinnamate exhibit very good NLO efficiency that can be applied in molecular engineering for tailor made applications.

8.1 Guanidinium Cinnamate (19)

Guanidinium cinnamate with the molecular formula $C_{10}H_{13}N_3O_2$ is a chemical compound made from cinnamic acid ($C_9H_8O_2$) and guanidine. Good quality transparent single crystals of guanidinium cinnamate are obtained by crystallization from an aqueous mixture of cinnamic acid and quinidine in the ratio 1:1 at room temperature. The technique employed is the slow evaporation growth. The packing diagram of guanidinium cinnamate is shown in Figure 27 below.
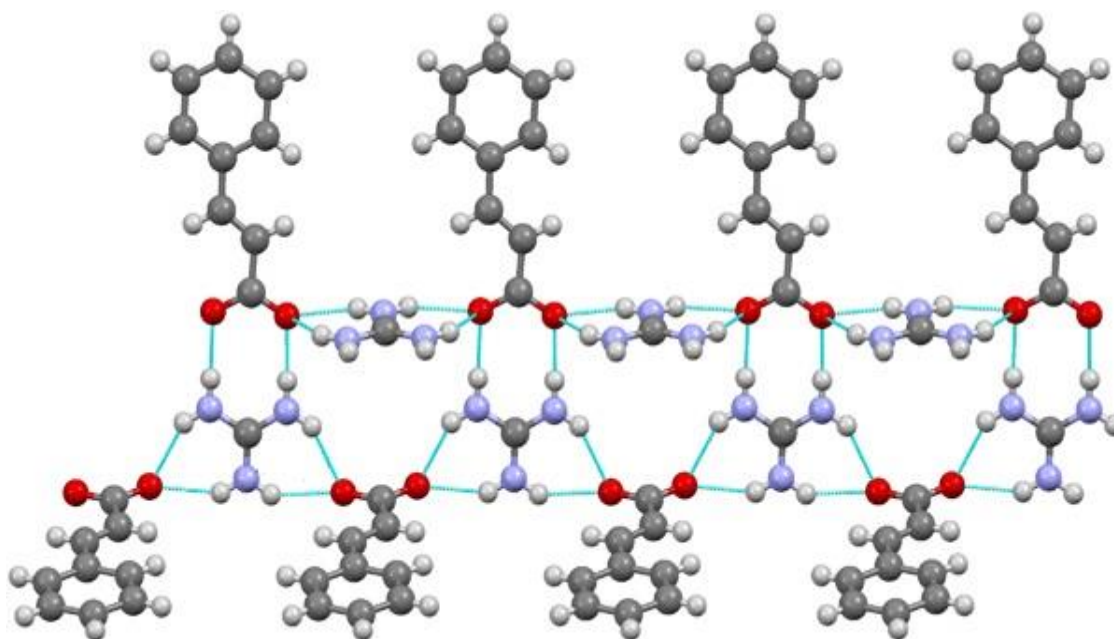
Figure 27. Packing diagram of guanidinium cinnamate viewed down the a-axis.
Dashed lines indicate intermolecular N-H…O hydrogen bonds.[53]

In a given molecule, the interaction of the electromagnetic field generating new fields with different phase, frequency and amplitude to that of the incident field results in the NLO properties of the molecule. The absolute π-conjugation of guanidinium cinnamate brings about the second order NLO properties of the molecule. Guanidinium cinnamate has an electric dipole moment, molecular polarizability, first order hyperpolarizability and second order hyperpolarizability. Its first order hyperpolarizability is 3.8 times greater than that of urea.[28] The molecular polarizability of the molecule offers good second harmonic generation. The electronic delocalization in the molecule is responsible for the NLO activity of the molecule. This makes the molecule a promising candidate to be employed in nonlinear optical applications. The molecule decomposes at temperatures between 251-280°C. The decomposition occurs in two steps. This shows that the compound is thermally stable up to 251°C which is a good characteristic of an NLO material. The NLO properties of guanidinium cinnamate can also be seen possible from the lower band gap values of the frontier orbitals.

8.2 Guanidinium 4-aminobenzoate (20)

Guanidinium 4-aminobenzoate with the molecular formula $C_8H_{12}N_4O_2$ is an NLO organic compound obtained from the reaction between guanidine carbonate and 4-aminobenzoic acid. It is a brown optically transparent solid with the structure as shown in Figure 28 below.
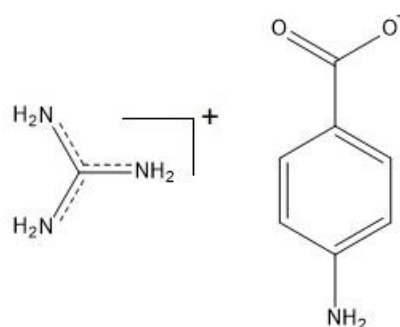

Figure 28. Structure of guanidinium-4-aminobenzoate.

The percentage of transmittance and reflectance of a grown guanidinium-4-aminobenzoate depends on the wavelength. GU4AB has a low transmittance which is attributed to its low reflectance. An increase in wavelength decreases the refractive index which indicates that the crystal absorbs at a low wavelength in the UV region. This variation in the refractive index as a result of change in the wavelength of the incident light beam indicates that some interactions occur between photons and electrons. The SHG of GU4AB is confirmed by using the Kurtz and Perry powder technique in which the laser output from the powder sample is characterized by a bright green emission at a wavelength of 532 nm different from the laser input wavelength of 1064 nm. This actually confirms the SHG of the molecule. The efficiency of the SHG of GU4AB is 2.6 times compared to that of a KDP crystal. A crystal of GU4AB exhibits microhardness anisotropy. The work hardening coefficient (strain hardening) for the crystal is 3.33 which is out of the range of 1-1.6 for hard materials. This indicates that GU4AB is a soft material. Good quality crystals of GU4AB however are easily grown from water-methanol solvent and exhibit good mechanical stability which are excellent characteristics of a good NLO material. These characteristics makes GU4AB a suitable material for applications in photonics. GU4AB crystal can be used in optical switches, optical attenuators and other devices. The packing diagram for GU4AB is shown in Figure 29
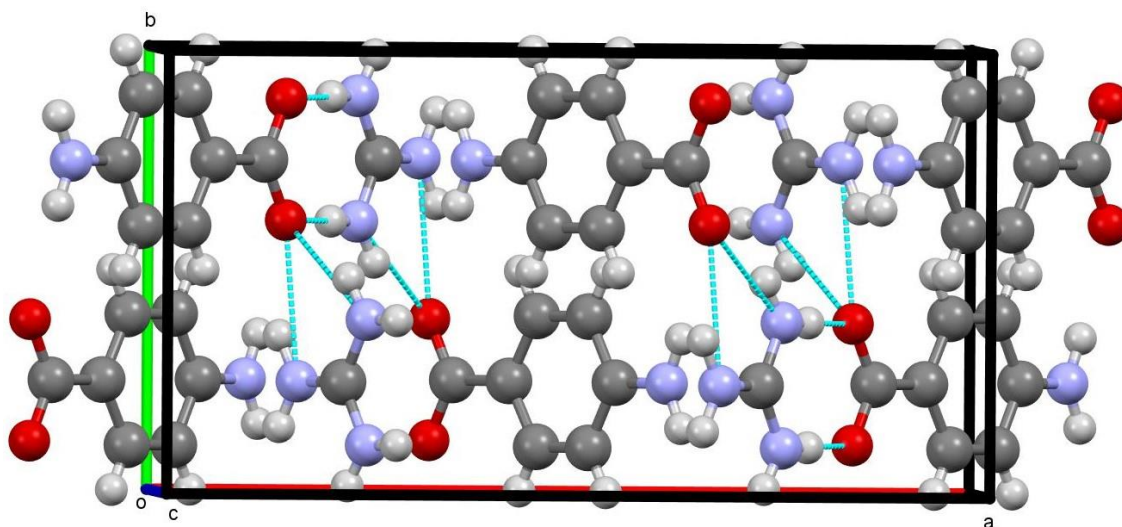
Figure 29. A packing diagram for guanidinium-4-aminobenzoate, viewed down the c axis, with the hydrogen bonds depicted by dashed lines.[54]

8.3 N,N`-Diphenylguanidinium Nitrate (21)

N,N`-Diphenylguanidinium Nitrate (DPGN) is obtained from the equimolar amounts of N,N`-Diphenylguanidine and nitric acid. The reaction scheme is shown in reaction 6
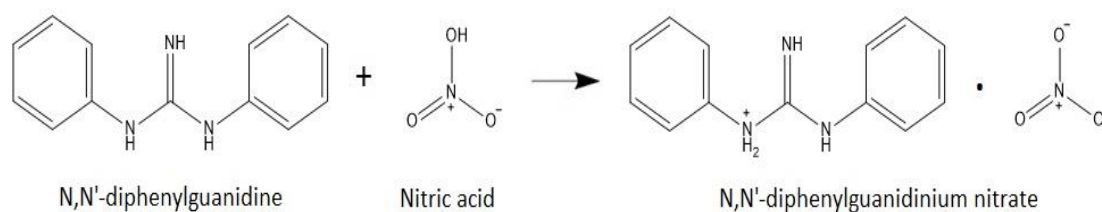
Reaction 6. schematic representation of the reaction of N,N`-Diphenylguanidine with nitric acid to form N,N`-Diphenylguanidinium Nitrate.

DPGN has a transmittance of about 57% and active in the uv-region of the spectrum as illustrted in Figure 30. It has a lower cut-off wavelength of 310 nm.
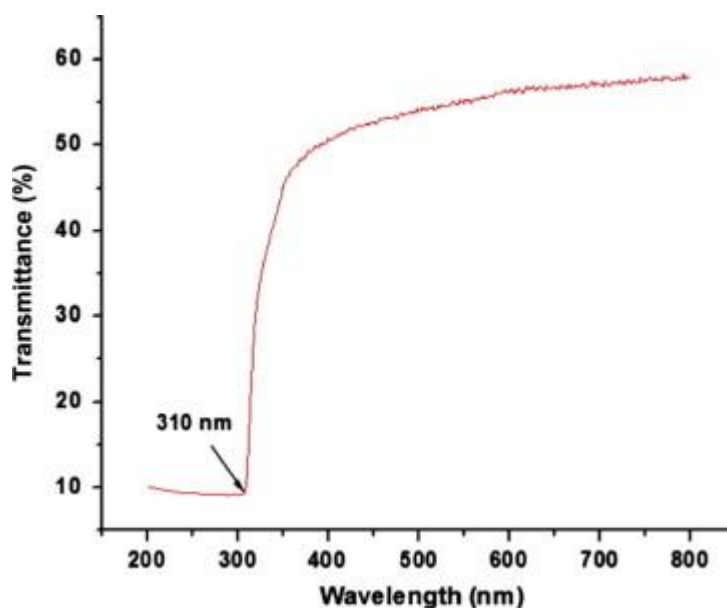
Figure 30. Optical transmittance spectrum of a crystal of DPGN.[29]

These parameters indicate that DPGN is a good potential material for optical applications. Good optical transmission of the second harmonic frequencies is guaranteed by the transmission window of the compound in the visible region. This is confirmed by the wide band gap of the DPGN crystal in this region. DPGN crystal exhibits strong hydrogen bond interactions between the cation and the anion of the molecule. These hydrogen bond interactions lead to SHG activity in the molecule. DPGN molecule is very stable thermally with a thermal stability as high as 196°C. Only above this temperature will the crystal start to decompose at 200 °C.[29] This implies that the DPGN crystal can be employed in NLO applications with temperatures up to 196°C. DPGN crystal thermal stability is a good quality of an NLO material. Another important quality of the DPGN crystal is that it is not moisture sensitive. The effectiveness of the nonlinearity of DPGN crystal is about 0.92 times compared to that of KDP.

All these characteristics of DPGN such as easily grown crystals, good optical transparency throughout the uv-vis region of the spectrum, wide optical band gap, SHG properties paved by the strong hydrogen bond interactions nominate DPGN as a potential material to be applied in photonics, electro optics and SHG devices.

8.4 Guanidinium meta-nitrobenzoate (GMNB) (22)

Guanidinium meta-nitrobenzoate (GMNB) is a nonlinear optical organic compound obtained from the chemical reaction of guanidine carbonate meta-nitrobenzoic acid in a mixed solvent of water and methanol. It belongs to the noncentrosymmetric space group and orthorhombic crystal system. It has a molecular structure as shown in Figure 31.
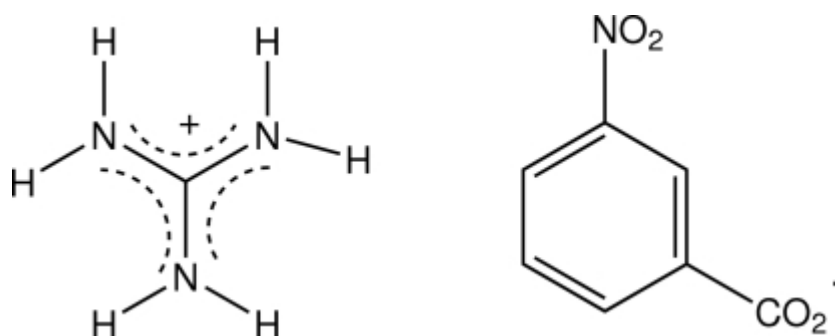

Figure 31. Molecular structure of guanidinium meta-nitrobenzoate.

The configuration of the molecule consisting of the anion and the cation bonded together interionic hydrogen bonds in a crystal of GMNB are shown in Figure 32. The dotted lines represent the inter-ion hydrogen bonds.
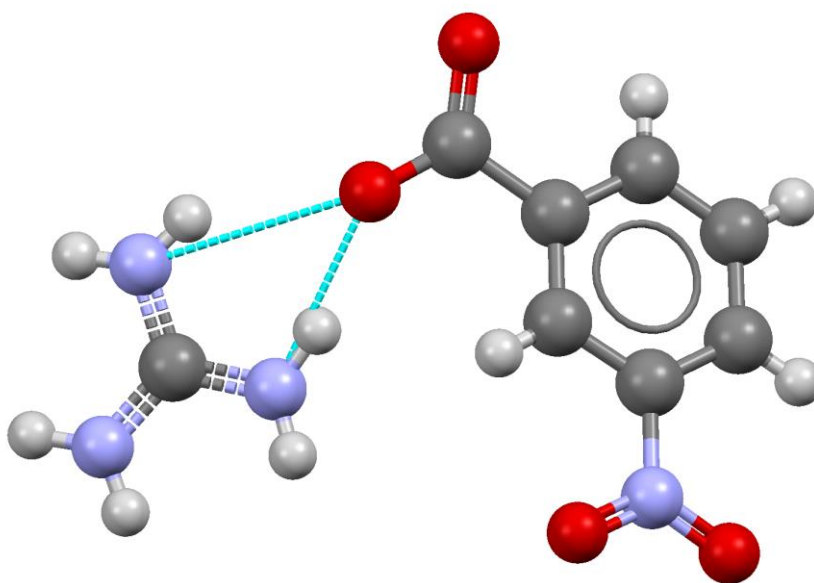
Figure 32. Molecular structure of GMNB with inter-ion hydrogen bonds shown as dotted lines.

The 3-dimensional structure of GMNB as observed along the approximate b cell direction and the non-interactive hydrogen atoms left out is represented in Figure 33.
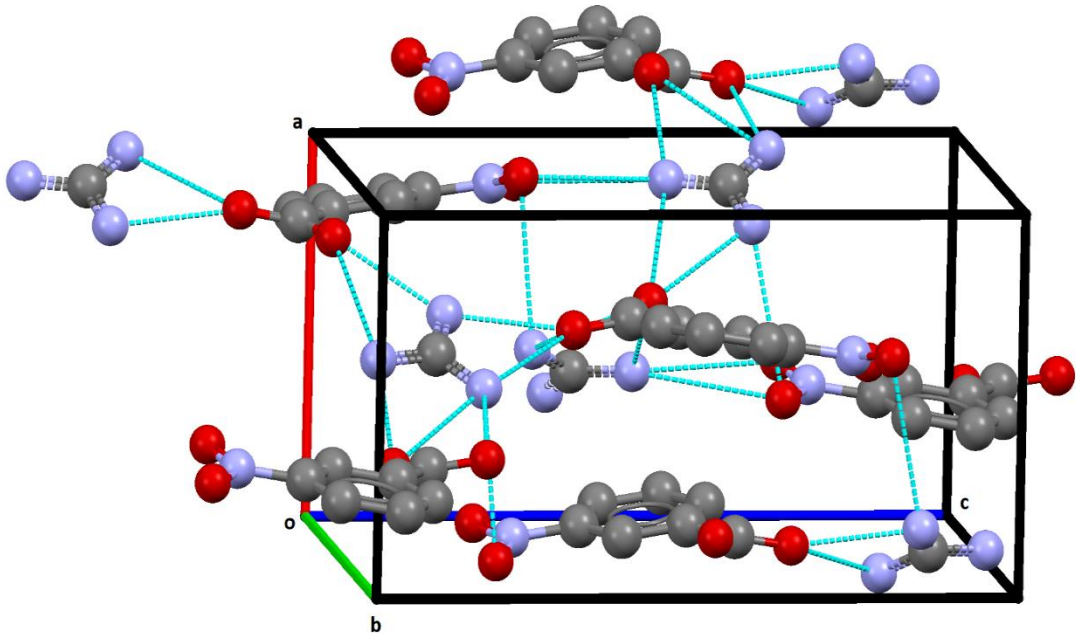
Figure 33. 3-D dimensional structure of GMNB observed along the approximate b cell direction with the non-interactive hydrogen atoms left out.

Good quality single crystals of GMNB has a cut-off wavelength of 255nm with a high transmittance of about 75%. It does not absorb between the wavelengths of 255 nm-800 nm indicating that it is a promising candidate for nonlinear optical applications. GMNB has a laser damaged threshold of 0.58 GW/cm^2 which is almost three times than that of KDP (0.20 GW/cm^2). GMNB crystals are not moisture sensitive and they are thermally stable up to 160°C. GMNB has a maximum number of hardness to be 37 kg/mm^2 at room temperature. GMNB has a SHG efficiency of 1.46 times that of KDP. The SHG nonlinearity of GMNB increases with an increase in particle size and saturates at a maximum value above 250 μm indicating that the GMNB exhibits type-1 phase matching. As a result of this, GMNB can be effectively employed as an efficient candidate for frequency doubler and optical parametric oscillator.

9 Conclusion

Despite the remarkable attainment in the field of nonlinear optics due to the advancements of current NLO materials as both organic and inorganic compounds, organic compounds may still serve as better NLO materials for optical applications. The major advantage of organic compounds over inorganic compounds as NLO materials is their flexibility nature (molecular engineering) though they possess other factors such as low thermal stability as draw backs to their applications in the field of nonlinear optics.

Some guanidine based compounds and amino acid based compounds in particular have received very close attention as they have proven to be beneficial in nonlinear optical applications. Amino acids that are optically active show some interesting peculiar characteristics such as wide optical transparency range in the UV and Vis regions of the electromagnetic spectrum, chiral nature of the molecules, molecular nature being zwitterionic thereby favouring crystal hardness and the presence of donor-acceptor properties leading to large hyperpolarizability. Their polarization behaviour is advantageous to good NLO activity.

Guanidinium based compounds are also good potential NLO active materials as the guanidinium cation acts as an octupolar building block for the design of NLO materials. Guanidinium compounds are highly polarizable which is a property which is a potentially interesting in NLO applications.

For materials to be used in nonlinear optical applications, it is important that they possess certain characteristics such as phase matching, second order nonlinear susceptibility, wide optical transparency, sufficient resistance to optical damage by intense optical irradiation and easy growth of large single high quality crystals. Some potential guanidine based compounds and amino acid based compounds as NLO materials are known in literature and have been discussed in detail above.

EXPERIMENTAL PART

10 Aim of the present work

Nonlinear effects play a very vital role in technology, industrial applications and the future evolution of nonlinear optics. The main purpose of this present work is to improve geometry, clarify the structure-property relationship, examine in detail second order nonlinear behaviour and to create new, improved NLO materials based on ionic/intermolecular interactions. This investigation was conducted by reacting common inorganic acids with pyridine-based compounds having substituents on the carbon para to the nitrogen atom of the pyridine ring. The reason for this was to improve the potential linear organization of cations so that parallel chains would have polar centres lining up. The acids used in this study were tetrafluoroboric acid, sulphuric acid, nitric acid, and phosphoric acid. Pyridine-based compounds were chosen because they are conjugated organic molecules and conjugated organic molecules have a high possibility of possessing nonlinear optical properties due to high second order responses. The π-conjugated system in the pyridine ring with donor and acceptor atoms in the molecule have high tendency of NLO response and further improve the study of these chosen materials. The 3D packing of the pyridine-based compounds was improved by protonation during their reaction with the acids. This made it possible to have the NLO materials from the chosen materials with different structures thereby enhancing the investigation of the structure-property relationship. To further study this structure-property relationship, the chosen materials were reacted with sulphuric acid in a 2:1 molar ratio giving rise to different structures compared to those obtained with the 1:1 ratio reactions. The NLO activity of these chosen materials was confirmed by the second harmonic generation measurements. The structures of the target materials are presented in the results and discussion part of the work.

11 Reagents and methods

The list of reagents used during the synthesis, their purity and supplier is found in table 2 below

Table 2 Reagents and solvents used during the synthesis

Reagent	Purity	Supplier
Tetrafluoroboric acid (HBF$_4$)	8.0 M solution in H$_2$O	Fluka Chemika
Phosphoric acid (H$_3$PO$_4$)	95%	Merck
Nitric acid (HNO$_3$)	65% solution in H$_2$O	Sigma-Aldrich
Sulphuric acid (H$_2$SO$_4$)	95% solution in H$_2$O	Sigma-Aldrich
4-Aminopyridine	98%	Aldrich
4-Methylaminopyridine	98%	Aldrich
4-Mercaptopyridine	95%	Aldrich
4-Hydroxypyridine	95%	Aldrich
Isonicotinic acid	99%	Aldrich
Isonicotine amide	99%	Aldrich
Pyridinethioamide	97%	Aldrich
Methanol	HPLC	J.T Baker
Ethanol	99.5%	Altia
Acetonitrile	HPLC	VWR Chemicals
Pentane	99.5%	Fisher Scientific
Hexane	99%	VWR Chemicals
Tetrahydrofuran (THF)	HPLC	Sigma Aldrich
Dichloromethane (DCM)	100%	VWR Chemicals
Toluene	100%	VWR Chemicals
Diethylether	100%	VWR Chemicals

12 Equipment

The equipment use during this synthetic work are shown in table 3 below

Table 3 Equipment used during the synthesis

Equipment	use
Scale balance	weigh the required masses of the reagents
Vacuum pump ILMVAC Gmbh, TYPE 322004	evaporate the solvent from the reaction mixture
Bruker AV 300 Ultrashield NMR spectrometer	measure the ^{1}H NMR spectra of the target compounds
Olympus SZX16 Microscope	view the crystals formed
X-ray diffractometer Agilent SuperNova Dual Source diffractometer equipped with Atlas CCD area-detector using graphite monochromatized CuKα radiation (λ = 1.54184 Å) and Bruker-Nonius Kappa APEX II CCD diffractometer using monochromated MoKα radiation (λ = 0.71073 Å)	crystal structure determination
125µm sieve	To sieve the samples for NLO measurements
Laser Integra-C, Quantronix femtosecond laser	measure the SHG activity of the target compounds

13 General description of the synthesis

All the reagents and solvents used throughout the synthesis were purchased from commercial sources (Sigma-Aldrich) and used without further purification. The required amounts of the reagents (4-aminopyridine, 4-methylaminopyridine, 4-hydroxypyridine, 4-mercaptopyridine, isonicotinic acid, isonicotinamide and pyridinethioamide) were measured using the scale and dissolved in 30ml of methanol. Those that could not dissolve such as isonicotinic acid were slightly warmed in a water bath. The required amounts of the acids (HBF_4, H_3PO_4, HNO_3 and H_2SO_4) were added and the reaction mixture stirred with a magnetic stir bar at room temperature for at least one hour. The acids protonate the nitrogen of the pyridine ring forming the products with the pyridinium cation and the corresponding anion of the acid. These reactions were carried out in 1:1 molar ratios except for H_2SO_4 that the reactions were also done in 2:1 molar ratios. In the case of H_2SO_4 reactions in the 2:1 molar ratio, there was monoprotonation of two equivalents of pyridines forming the SO_4^{2-} dianion. The reaction mixture was processed by evaporation of the solvent (methanol) under vacuum. The product from most reactions were washed with diethylether and obtained as a powder. Those reactions that produced an oily product were left in the freezer for about 4-5 days after which some become solids and were processed but others remained oily and were difficult to be processed. The yields were obtained by weighing the products on the scale.

Similar reactions were carried out using acetic acid (CH_3COOH) for which protonation occurred only with 4-aminopyridine. The rest of the reactions did not occur probably due to the pKa value of acetic acid which makes it too weak for protonation.

^{1}H NMR spectra (appendix 2) were all measured with the Bruker AV 300 NMR spectrometer using deuterated acetonitrile, methanol or water as NMR solvents. X-ray crystal structure determination and laser measurements were carried out by Prof. Jari Konu and the doctoral student Esa Kukkonen.

^{1}H NMR spectra, crystal structures and crystallographic data for the target compounds are presented in the appendices.

14 Crystallization methods

Crystals from the target compounds were obtained from bulk crystallization and by the solvent layering technique. With the bulk crystallization, the products from the reactions were dissolved in suitable solvents (either methanol or water) in a beaker and allowed to evaporate slowly in a fume cupboard. The beakers were left open or partly covered with paraffin wax depending on the volatility of the solvent used. This method worked well for most of the products.

For the solvent-layering technique, small quantities of samples were dissolved in suitable solvents (denser solvent with high solubility of the sample) in sample tubes. A second less dense solvent in which the sample is less soluble or insoluble was carefully dripped down the sides of the tube with the second solvent forming a separate layer. The tubes were corked with nonperforated corks and left in a quiet cupboard for at least one week. The second solvent slowly diffused into the first solvent forming crystals at the boundary between the two solvents. The solvent-layering technique was quite applicable because the samples were solvent sensitive.
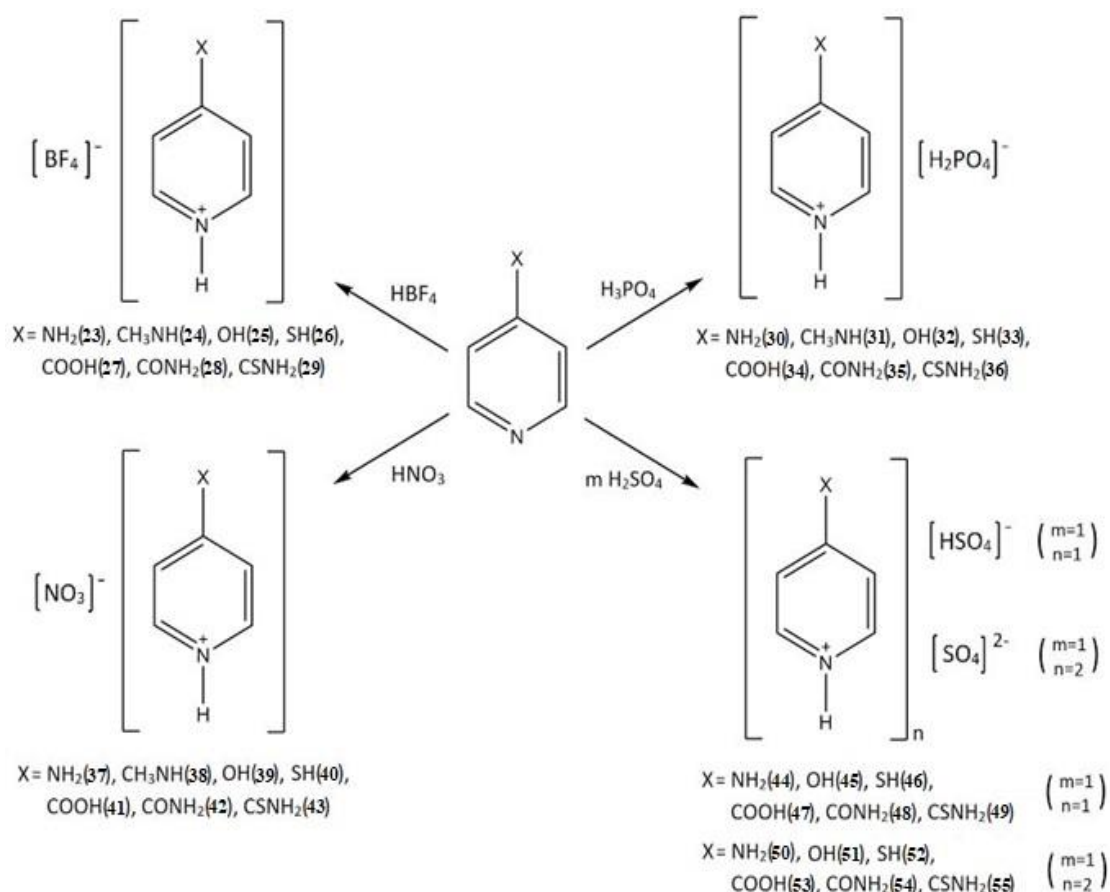
Figure 34. Reaction scheme for the syntheses.

16 Preparation of the NLO samples

The NLO samples were prepared by the sieving technique. The samples from bulk crystallizations were placed in a 125 µm sieve. The sieve was slightly hit with the spatula, and the sample powder that freely passed through the sieve openings were discarded. A spatula was used to crush and press the sample through the sieve openings into a crucible lid resulting into a fine uniform sample powder. The sample powder was then put into the capillary tubes blocked at one end with wax. The sieve provided good enough particle size (see chapter 5 for the effects of particle size on SHG) for the laser measurements. Laser light was passed through the samples in the tubes one at a time and the SHG signals observed.

17 Results and discussion

17.1 Reactions with HBF$_4$

17.1.1 4-Aminopyridine

Compound (4-NH$_2$-C$_5$H$_4$NH$^+$)(BF$_4^-$) (**23**) was prepared by the reaction of HBF$_4$ with 4-aminopyridine in methanol as solvent. The product was obtained as a dry powder after evaporation under vacuum. ^{1}H NMR of the synthesized compound showed a signal from the hydrogen from the protonated nitrogen of the pyridine ring at 10.99ppm. The signal obtained from the protonated hydrogen suggest that the reaction did occur, and the desired and clean product was obtained. All attempts to crystallize the synthesized compound both by bulk crystallization and by solvent diffusion failed as no crystals suitable X-ray crystallographic measurements were obtained.

17.1.2 4-methylaminopyridine

Compound (4-CH$_3$- NH$_2$-C$_5$H$_4$NH$^+$)(BF$_4^-$) (**24**) was prepared by the reaction of HBF$_4$ acid with 4-methyaminopyridine in methanol. The product was obtained as a white dry powder after evaporation under vacuum. ^{1}H NMR spectrum of the synthesized compound was carried out in order to confirm the presence of the protonated hydrogen from the acid. The spectrum showed a signal from the protonated hydrogen of the nitrogen of the pyridine ring at 10.78ppm. This confirmed the protonation of 4-methylaminopyridine by HBF$_4$ leading to the desired product. Crystals of the compound were measured by X-ray diffractometry in order to reveal the crystal structure, space group and the cell parameters. The X-ray diffraction analysis revealed that the compound crystallized in the orthorhombic space group with the space group symbol Pbca and centrosymmetric unit cell . In the crystal structure, the N3···F5 close contact is 2.91Å as shown in Figure 35. In the crystal structure, the anions are regularly aligned in a zig-zag manner between the cation with polarity pointing in opposite directions.
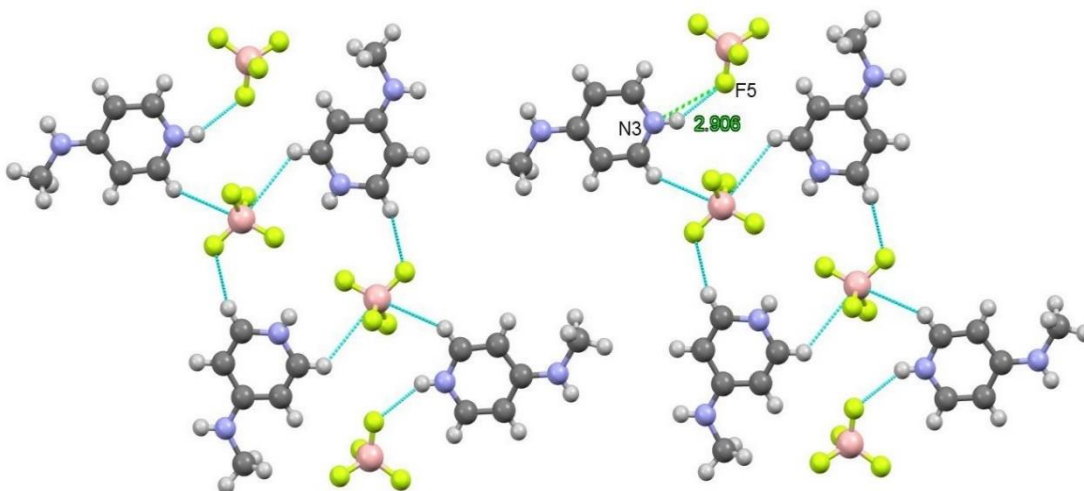
Figure 35. Close contacts between nitrogen atoms of 4-methylaminopyridine and the fluorine atoms of Tetrafluoroboric acid

17.1.3 4-hydroxypyridine

Compound (4-OH-C$_5$H$_4$NH$^+$)(BF$_4^-$) (**25**) was synthesized by the reaction of HBF$_4$ acid with 4-hydroxypyridine in methanol. Evaporation under vacuum yielded the product as a white powder. The ^{1}H NMR spectrum of the compound did not show any signal from the protonated hydrogen. Hence very little information was obtained about the ^{1}H NMR spectrum of the synthesized compound. However, X-ray diffraction analysis revealed a crystal structure of the compound with the nitrogen of the pyridine ring protonated as intended. The X-ray diffraction analysis revealed that the compound crystallized in the orthorhombic space group with the space group symbol P2$_1$/c and centrosymmetric unit cell. In the crystal structure, the O1···F1 close contact is 3.04Å, the N1···F1 close contact is 2.78Å as shown in Figure 36. In the crystal structure, no specific alignment can be observed between anions and cations. Cation pair with polarity in opposite direction form close contacts through the oxygen of the hydroxy group.
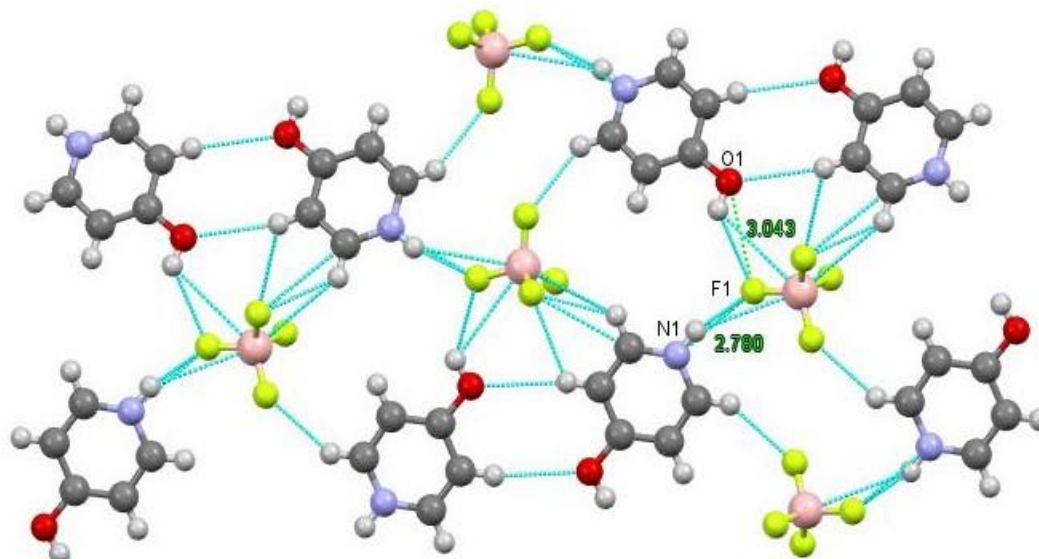
Figure 36. Close contacts between nitrogen and oxygen atoms of 4-hydroxypyridine and fluorine atoms of Tetrafluoroboric acid

17.1.4 4-mercaptopyridine

Compound (4-SH-$C_5H_4NH^+$)(BF_4^-) (**26**) was prepared by the reaction of HBF_4 acid with 4- mercaptopyridine in methanol. Evaporation under vacuum yield a yellowish oily product. ^{1}H NMR spectrum of the compound was complicated but suggests that the compound was not pure. This means that there were other side reactions that occurred alongside the protonation reaction of 4-mercaptopyridine. Recrystallization yielded colourless crystals though the bulk product was yellow. This further confirmed the observation with the ^{1}H NMR spectrum that the product was not pure. X-ray diffraction analysis showed that the reaction did take place as the crystals structure obtained had the nitrogen of the pyridine ring protonated by HBF_4 acid. The X-ray diffraction analysis revealed that the compound crystallized in the monoclinic space group with the space group symbol P2₁/c and centrosymmetric unit cell. Small SHG signal though very low with intensity about 1-5% that of urea reference was obtained from this product implying that the compound was NLO active. In the crystal structure, the S1···S1 close contact is 3.52Å, the N1···F1 close contact is 2.86Å as shown in Figure 37. In the crystal structure, the cations form layers with the anions aligned in a zig-zag manner between

them. The cation pair is linked through the S···S close contact with their polarity in opposite directions.
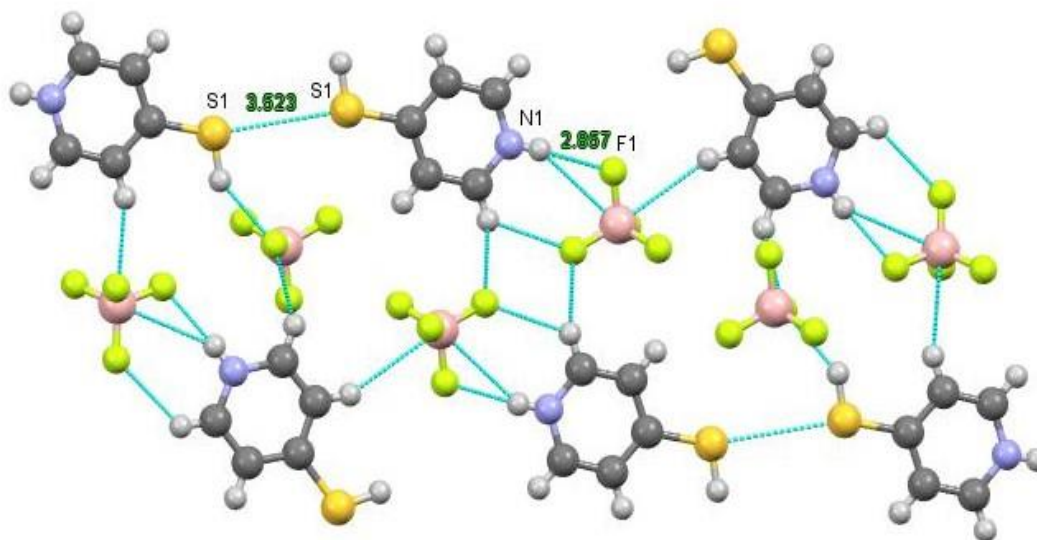

Figure 37. Close contacts between nitrogen and sulphur atoms of 4-mercaptopyridine and fluorine atoms of Tetrafluoroboric acid.

17.1.5 Isonicotinic acid

Compound (4-CO$_2$H--C$_5$H$_4$NH$^+$)(BF$_4^-$) (**27**) was synthesized by the reaction of HBF$_4$ acid with isonicotinic acid in methanol. Evaporation under vacuum yielded the compound as a white powder. ^{1}H NMR spectrum of the compound did not show any signal for the protonated hydrogen, but X-ray diffraction analysis did reveal the crystal structure with the nitrogen of the pyridine protonated. From the X-ray diffraction analysis, the compound crystallized in the monoclinic space group with the space group symbol P2$_1$/c and centrosymmetric unit cell. In the structure, the N1···F4 close contact is 2.83Å, the O1···F1 close contact is 2.68Å, the N1···O2 close contact is 2.88Å as shown in Figure 38. No specific alignment between anions and cations is observed in the crystal structure but the cations have their polarity pointing in opposite directions.
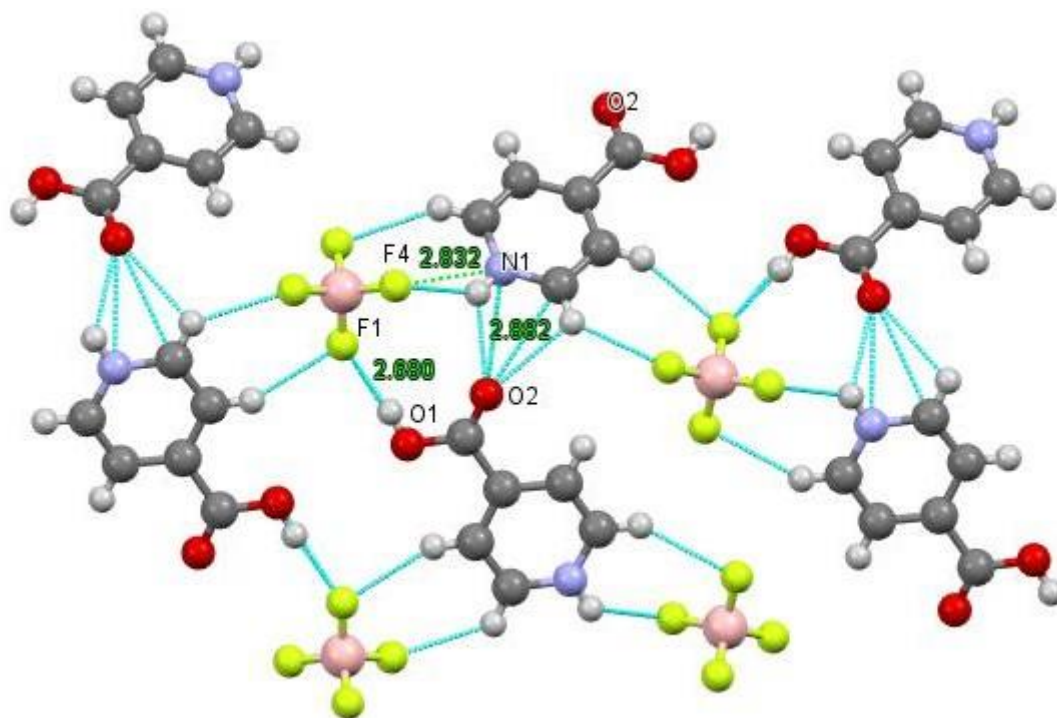
Figure 38. Close contacts between nitrogen and oxygen atoms of isonicotinic acid and fluorine atoms of Tetrafluoroboric acid.

17.1.6 Isonicotinamide

Compound (4-CONH$_2$-C$_5$H$_4$NH$^+$)(BF$_4^-$) (**28**) was prepared by the reaction of HBF$_4$ acid with isonicotinic acid in methanol. The compound was obtained as a white powder after evaporation under vacuum. ^{1}H NMR spectrum of the compound did not show any signal for the protonated hydrogen. X-ray diffractometry showed that the compound crystallized in the monoclinic space group with the space group symbol C1c1 and non-centrosymmetric unit cell. This implies that protonation did take place despite the absence of the NMR signal for the NH proton. Small SHG signal though with very low intensity about 1-5% that of urea reference was obtained from this reaction implying that the compound was NLO active. In the structure, the N1···F4 close contact is 2.85Å, the N1···F1 close contact is 2.79Å, the F2···N2 close contact is 2.99Å and the O1···N2 close contact is 2.95Å as shown in Figure 39. In the crystal structure, layers of cations and anions are linearly aligned with the cation polarity pointing in one direction. This further improves the NLO properties of the compound.
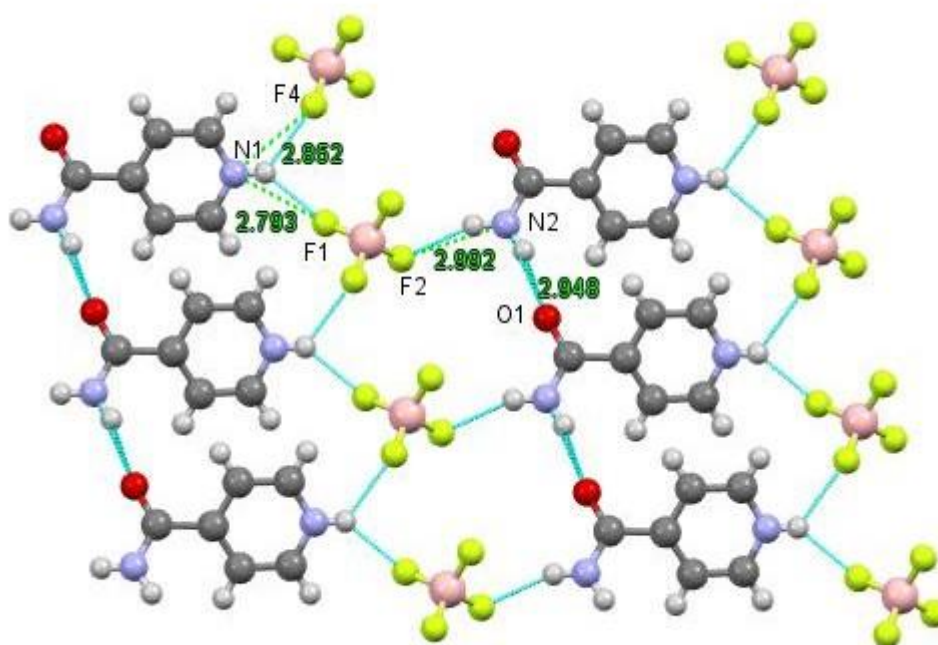
Figure 39. Close contacts between nitrogen and oxygen atoms of isonicotinamide and fluorine atoms of Tetrafluoroboric acid.

17.1.7 4-pyridinethioamide

Compound (4-CSNH$_2$-C$_5$H$_4$NH$^+$)(BF$_4^-$)(**29**) was synthesized by the reaction between HBF$_4$ acid and 4-pyridinethioamide in methanol. Evaporation of the solvent under vacuum yielded the compound as an orange powder. ^{1}H NMR spectrum of the compound was measured but the signal of the NH proton was not obtained. X-ray diffractometry showed that the compound crystallized in the monoclinic space group with the space group symbol P2$_1$/c and centrosymmetric unit cell. In the crystal structure, the F1···N1 close contact is 2.82Å, the N1···F3 close contact is 2.87Å, the F2···N2 close contact is 2.88Å and the S1···N2 close contact is 3.42Å as shown in Figure 40. The crystal structure has cation pairs which are linked together through sulphur atom and the amide nitrogen. No specific alignment between the cations and the anions is observed in the crystal.
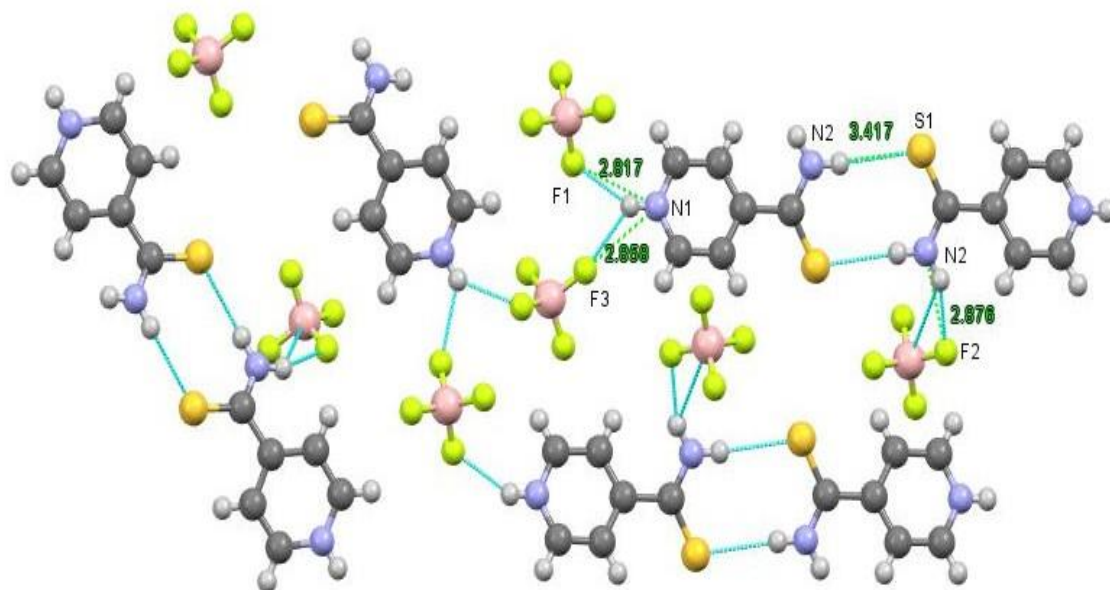
Figure 40. Close contacts between nitrogen and sulphur atoms of 4-pyridinethioamide and fluorine atoms of Tetrafluoroboric acid.

The close contacts for the pyridinium salts of the BF_4^- anion are summarized in table 4.

Table 4. Selected close contacts for the Tetrafluoroboric acid reactions

Compound formula	Bonded atoms	Bond lengths
$(4\text{-}CH_3\text{-}NH_2\text{-}C_5H_4NH^+)(BF_4^-)$	N3-H3	0.82Å
	N3…F5	2.91Å
$(4\text{-}OH\text{-}C_5H_4NH^+)(BF_4^-)$	O1…F1	3.04Å
	N1…F1	2.78Å
$(4\text{-}SH\text{-}C_5H_4NH^+)(BF_4^-)$	S1…S1	3.52Å
	N1…F1	2.86Å
$(4\text{-}CO_2H\text{--}C_5H_4NH^+)(BF_4^-)$	N1…F4	2.83Å
	O1…F1	2.68Å
	N1…O2	2.88Å
$(4\text{-}CONH_2\text{-}C_5H_4NH^+)(BF_4^-)$	N1…F4	2.85Å
	N1…F1	2.79Å
	F2…N2	2.99Å
	O1…N2	2.95Å
$(4\text{-}CSNH_2\text{-}C_5H_4NH^+)(BF_4^-)$	F1…N1	2.82Å
	N1…F3	2.87Å
	F2…N2	2.88Å
	S1…N2	3.42Å

17.2 Reactions with H_3PO_4

17.2.1 4-Aminopyridine

Compound $(4\text{-}NH_2\text{-}C_5H_4NH^+)(H_2PO_4^-)$ (**30**) was prepared by the reaction of 4-aminopyridine with H_3PO_4 acid in methanol. The compound was obtained as a white powder after evaporation under vacuum. This reaction was repeated with 4-aminopyridine in excess and water as solvent. The product was again obtained as a white powder after evaporation under vacuum. No signal for the protonated hydrogen was

obtained in the ^{1}H NMR spectrum of both products. X-ray diffractometry revealed that the two products were the same with the same crystalline structure which was in the triclinic space group with a space group symbol P-1 and a centrosymmetric unit cell. There were water molecules incorporated into the structure. The product from the reaction with excess 4-aminopyridine showed some NLO activity with Laser measurements as small SHG signal was obtained though the signal was weak (1-5% that of urea reference). In the crystal structure, the N1···O002 close contact is 2.77Å, the O002···N2 close contact is 2.98Å, the O2···N2 close contact is 2.95Å, the O1···O2 close contact is 2.68Å and the O3···O4 close contact is 2.67Å as shown in Figure 41. In the crystal structure, the cations regularly align themselves with water molecules between them forming layers which are separated by linearly aligned anions. Though the cations in one layer have their polarity pointing in one direction, those in the next layer have their polarity pointing in the opposite direction.
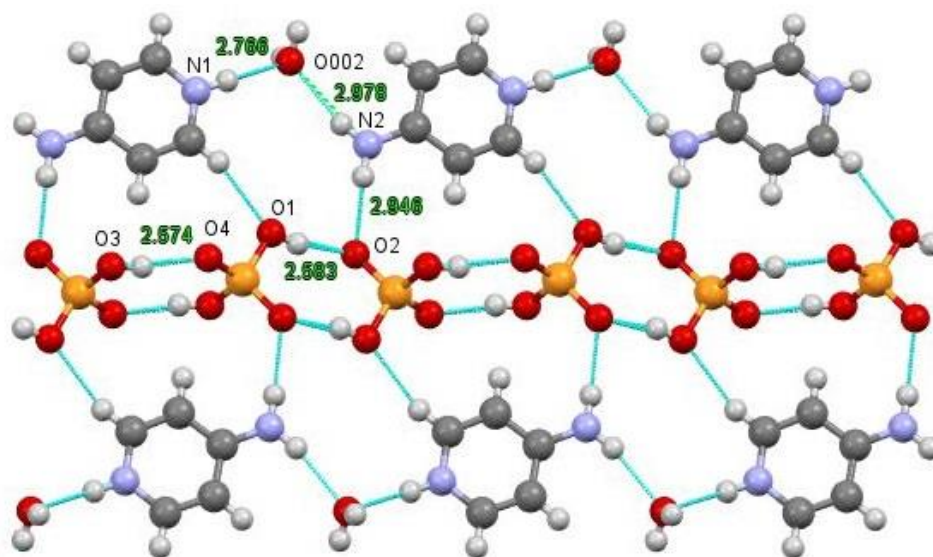

Figure 41. Close contacts between nitrogen atoms of aminopyridine, oxygen atoms of phosphuric acid and water.

17.2.2 4-methylaminopyridine

Compound (4-CH$_3$-NH$_2$-C$_5$H$_4$NH$^+$)(H$_2$PO$_4^-$) (**31**) was synthesized by the reaction of 4-methylaminopyridine with H$_3$PO$_4$ acid in methanol. Evaporation of the solvent under vacuum resulted in an oily compound which was difficult to be processed. No further information was obtained from this compound.

17.2.3 4-hydroxypyridine

Compound (4-OH-C$_5$H$_4$NH$^+$)(H$_2$PO$_4^-$) (**32**) was prepared by the reaction of 4-hydroxypyridine with H$_3$PO$_4$ acid in methanol. Evaporation under vacuum yielded the product as a white powder. ^{1}H NMR spectrum of the compound did not show any signal for the protonated hydrogen. X-ray diffractometry revealed the structure of the compound in the orthorhombic space group with a space group symbol Pbca and centrosymmetric unit cell. Small SHG signal though with very low intensity about 1-5% that of urea reference was obtained from this reaction implying that the compound was NLO active. In the crystal structure, the N1···O5 close contact is 2.66Å, O1···O2 close contact is 2.55Å, O2···O3 close contact is 2.60Å as shown in Figure 42. In the crystal structure, the cations and the anions are linearly arranged into layers with the cations having their polarity pointing in opposite directions.
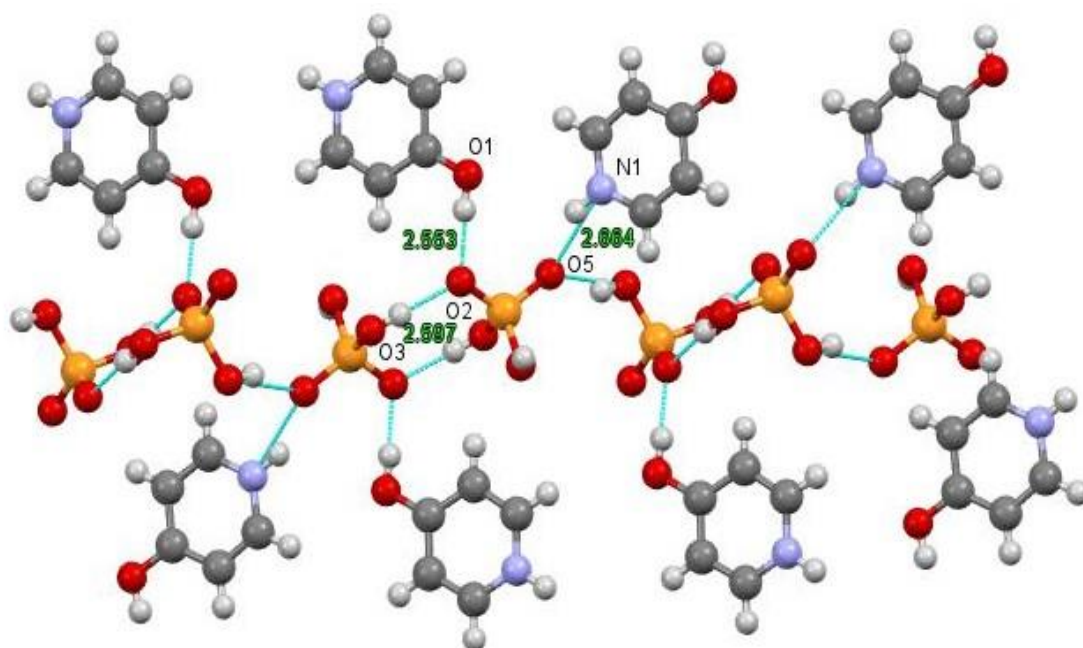

Figure 42. Close contacts between nitrogen and oxygen atoms of the 4-hydroxypyridine and oxygen atoms of phosphoric acid.

17.2.4 4-mercaptopyridine

Compound (4-SH-C$_5$H$_4$NH$^+$)(H$_2$PO$_4^-$) (**33**) was prepared by the reaction of 4-mercaptopyridine with H$_3$PO$_4$ acid in methanol. Evaporation of the solvent under vacuum resulted in an oily compound which was difficult to be processed. No further information was obtained from this compound.

17.2.5 Isonicotinic acid

Compound (4-CO$_2$H-C$_5$H$_4$NH$^+$)(H$_2$PO$_4^-$) (**34**) was synthesized by the reaction of isonicotinic acid with H$_3$PO$_4$ acid in methanol. The compound was obtained as a white powder after evaporation under vacuum. No signal was obtained for the protonated hydrogen in the ^{1}H NMR spectrum of the compound. X-ray diffractometry revealed the structure of the compound in the monoclinic space group with a space group symbol C2/c and centrosymmetric unit cell. In the crystal structure, the N1···O6 close contact is 2.67Å, O1···O4 close contact is 2.57Å, O2···O3 close contact is 2.49Å and O5···O6 close contact is 2.57Å as shown in Figure 43. In the crystal structure, the anions and the cations are linearly arranged with both oxygen atoms of isonicotinamide forming contacts with the anion.
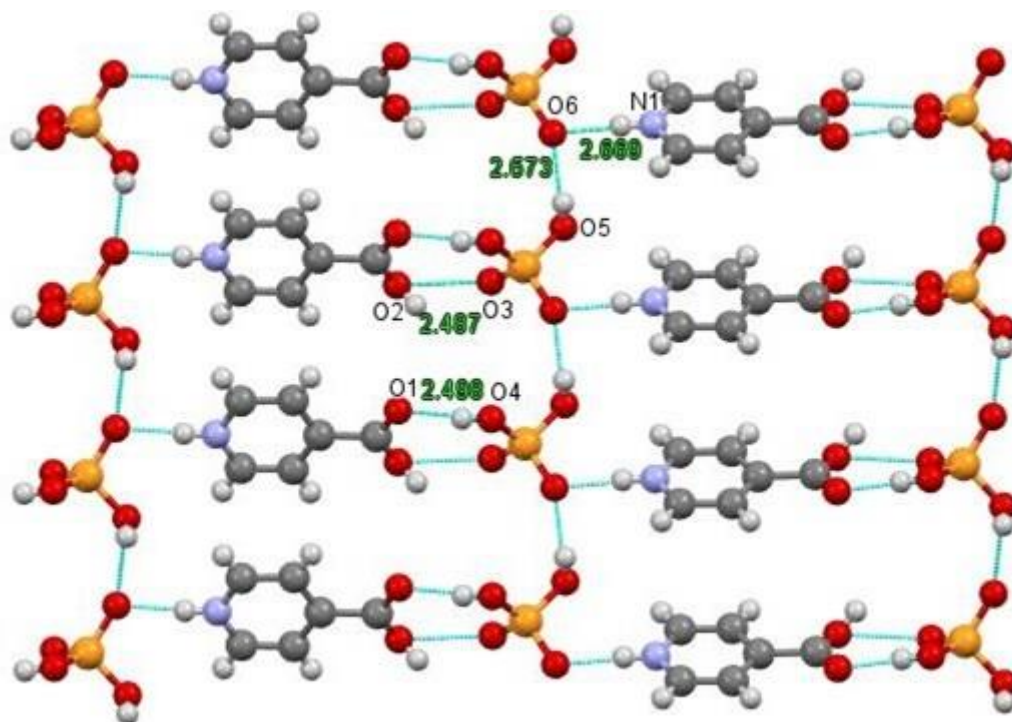
Figure 43. Close contacts between nitrogen and oxygen atoms of isonicotinic acid oxygen atoms of phosphoric acid.

17.2.6 Isonicotinamide

Compound (4-CONH$_2$-C$_5$H$_4$NH$^+$)(H$_2$PO$_4^-$) (**35**) was prepared by the reaction of isonicotinamide with H$_3$PO$_4$ acid in methanol. The compound was obtained as a white powder after evaporation under vacuum. The ^{1}H NMR spectrum of the compound did not show any signal for the protonated hydrogen. X-ray diffractometry revealed the structure of the compound in the monoclinic space group with the space group symbol C1c1 and non-centrosymmetric unit cell. Small SHG signal though with very low intensity about 1-5% that of urea reference was obtained from this reaction implying that the compound was NLO active. In the crystal structure, the N1···O2 close contact is 2.64Å, N2···O1 close contact is 2.91Å, N2···O5 close contact is 2.91Å and O4···O5 close contact is 2.61Å as shown in Figure 44. In the crystal structure, the cations and the anions are linearly arranged in layers with the cation polarity pointing in the same direction. This further enhances the NLO activity of the compound.
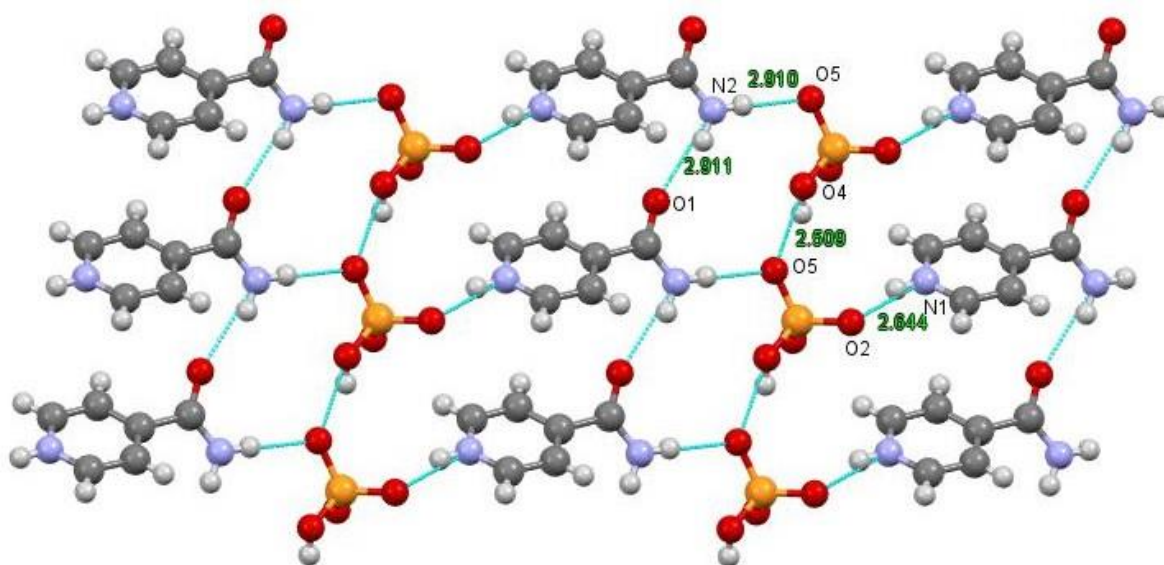
Figure 44. Close contacts between nitrogen and oxygen atoms of isonicotinamide and oxygen atoms of phosphoric acid.

17.2.7 Pyridinethioamide

Compound (4-CSNH$_2$-C$_5$H$_4$NH$^+$)(H$_2$PO$_4^-$) (**36**) was synthesized by the reaction of pyridinethioamide with H$_3$PO$_4$ acid in methanol. Evaporation of the solvent was done under vacuum and the compound obtained as an orange powder. No signal for the protonated hydrogen was obtained from the ^{1}H NMR spectrum of the compound. X-ray diffractometry analysis revealed the structure of the compound in the monoclinic space group with a space group symbol C2/c and centrosymmetric unit cell. In the crystal structure, the N1···O4 close contact 2.68Å, N2···S1 close contact is 3.52Å, O1···O6 close contact is 2.67Å, O3···O6 close contact is 2.01Å and O4···O5 close contact is 2.69Å as illustrated in Figure 45. In the crystal structure, cations form pairs through the sulphur atoms and the amide nitrogen. The cation pairs and anions are linearly arranged in layers with the cations having their polarity in opposite directions.
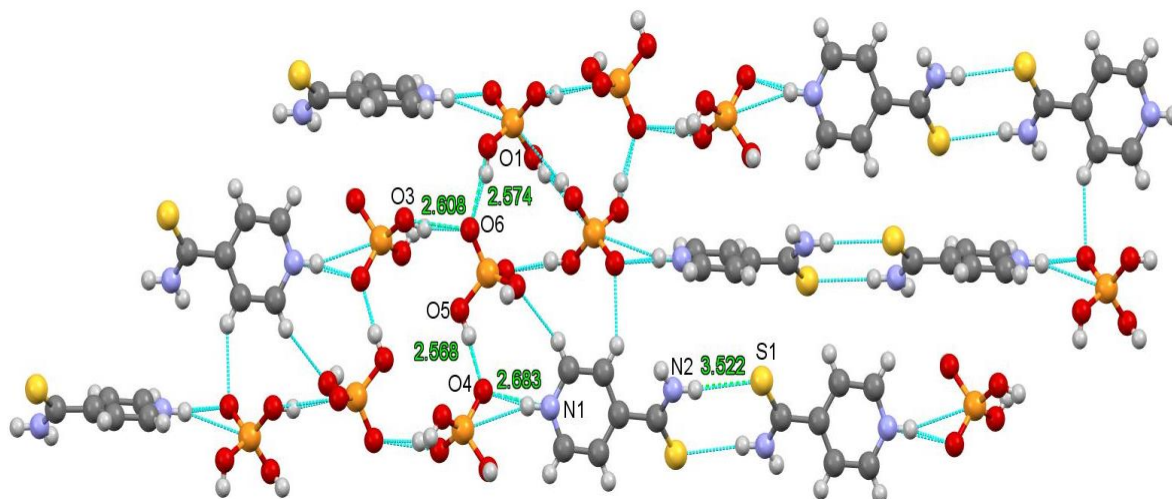
Figure 45. Close contacts between nitrogen atoms of 4.pyridinethioamide and oxygen atoms of phosphoric acid.

The close contacts for the pyridinium salts of the $H_2PO_4^-$ anion are summarized in table 5 below.

Table 5 Selected close contacts for crystals from the phosphoric acid reactions

Compound formula	Bonded atoms	Bond lengths
$(4\text{-}NH_2\text{-}C_5H_4NH^+)(H_2PO_4^-)$	N1…O002	2.77Å
	O002…N2	2.98Å
	O2…N2	2.95Å
	O1…O2	2.68Å
	O3…O4	2.67Å
$(4\text{-}OH\text{-}C_5H_4NH^+)(H_2PO_4^-)$	N1-O5	2.66Å
	O1-O2	2.55Å
	O2-O3	2.60Å
$(4\text{-}CO_2H\text{-}C_5H_4NH^+)(H_2PO_4^-)$	N1…O6	2.67Å
	O1…O4	2.57Å
	O2…O3	2.49Å
	O5…O6	2.57Å
$(4\text{-}CONH_2\text{-}C_5H_4NH^+)(H_2PO_4^-)$	N1…O2	2.64Å

	N2…O1	2.91Å
	N2…O5	2.91Å
	O4…O5	2.61Å
(4-CSNH$_2$-C$_5$H$_4$NH$^+$)(H$_2$PO$_4^-$)	N1…O4	2.68Å
	N2…S1	3.52Å
	O1…O6	2.67Å
	O3…O6	2.01Å
	O4…O5	2.69Å

17.3 Reactions with nitric acid (HNO$_3$)

17.3.1 4-Aminopyridine

Compound (4-NH$_2$-C$_5$H$_4$NH$^+$)(NO$_3^-$) (**37**) was prepared by the reaction of 4-aminopyridine with HNO$_3$ acid in methanol. Evaporation of the solvent under vacuum yielded the compound as a white powder. The ^{1}H NMR spectrum of the compound did not show any signal for the protonated hydrogen. X-ray diffractometry analysis revealed the structure of the compound in the monoclinic space group with a space group symbol P2$_1$/C$_1$ and centrosymmetric unit cell. In the crystal structure, the N1···O1 close contact is 2.78Å, N2···O1 close contact is 2.94Å and N2···O2 close contact is 2.95Å as shown in figure 46. In the crystal structure, separate layers of anions and cations are formed with the cations having close contacts with the anions through the amide nitrogen. The cations in one layer have their polarity pointing in the same direction and in the next layer, they point in the opposite direction.

Figure 46. Close contacts between nitrogen atoms of 4-aminopyridine and oxygen atoms of nitric acid.

17.3.2 4-methylaminopyridine

Compound (4-CH_3-NH_2-$C_5H_4NH^+$)(NO_3^-) (**38**) was synthesized by the reaction of 4-methylaminopyridine with HNO_3 acid in methanol. Evaporation of the solvent was carried out under vacuum and the compound obtained as a white powder. The ^{1}H NMR spectrum of the compound did not show any signal for the protonated hydrogen. X-ray diffractometry analysis revealed the structure of the compound in orthorhombic space group with a space group symbol Pmna and centrosymmetric unit cell. In the crystal structure, the N1⋯O1 close contact is 2.79Å and N2⋯O3 close contact is 2.97Å as shown in Figure 47. In the crystal structure, separate layers are formed with the anions and cations alternating each other. The polarity of cations in each layer points in the same direction but opposite to that in the next layer.
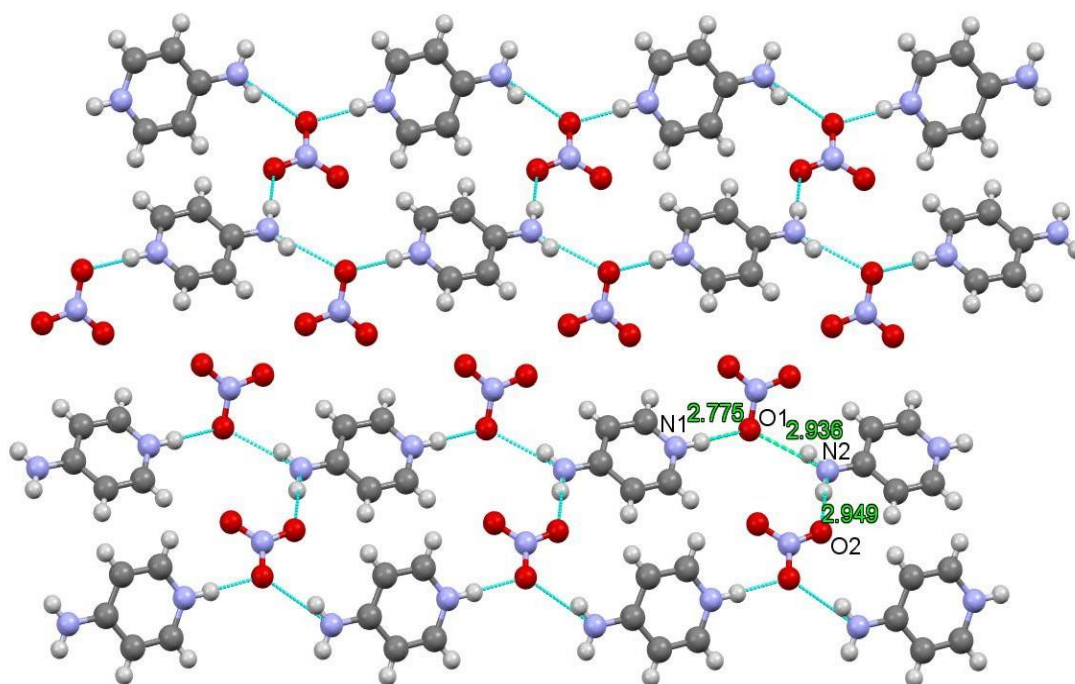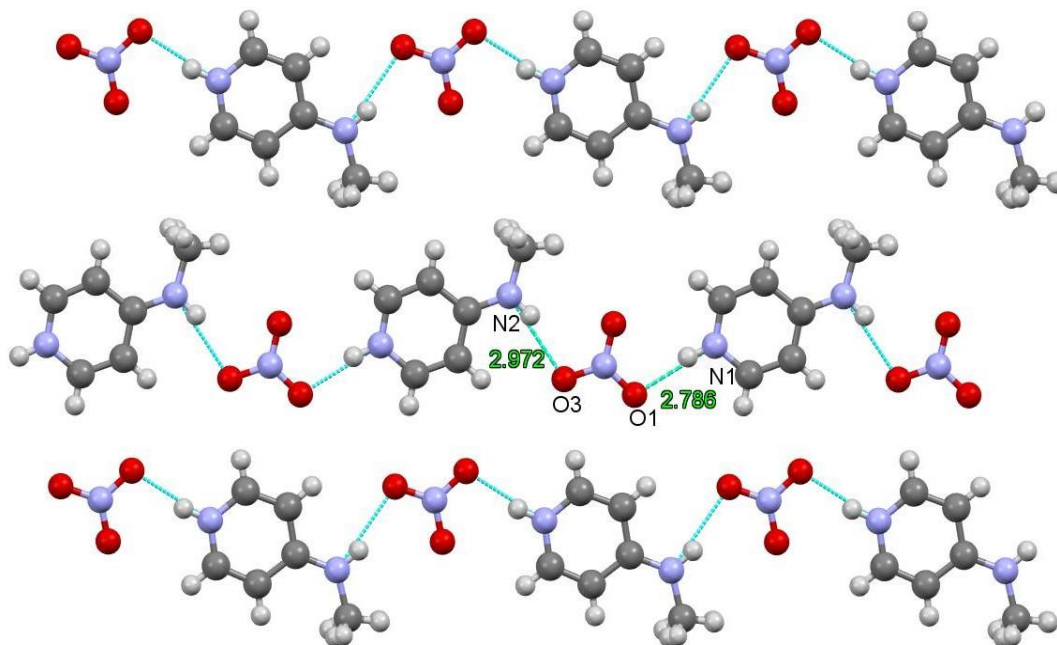
Figure 47. Close contacts between nitrogen atoms of 4-methylaminopyridine and oxygen atoms of nitric acid

17.3.3 4-hydroxypyridine

Compound $(4\text{-}OH\text{-}C_5H_4NH^+)(NO_3^-)$ (**39**) was prepared by the reaction of 4-hydroxypyridine with HNO_3 acid in methanol. Evaporation of the solvent was carried out under vacuum and the compound obtained as a white powder. No signal for the protonated hydrogen was obtained in the ^1H NMR spectrum of the compound. X-ray diffractometry revealed the structure of the compound in the triclinic space group with a space group symbol P_1. The unit cell enantiomorphic. Small SHG signal though with very low intensity about 1-5% that of urea reference was obtained from this reaction implying that the compound was NLO active. In the crystal structure, the N1···O3 close contact is 2.76Å, N3···O7 close contact is 2.79Å, O1···O2 close contact is 2.66Å and O5···O6 close contact is 2.66Å as shown in Figure 48. In the crystal structure, separate layers are formed with the anions and cations alternating each other. The polarity of cations in each layer points in the same direction but opposite to that in the next layer.
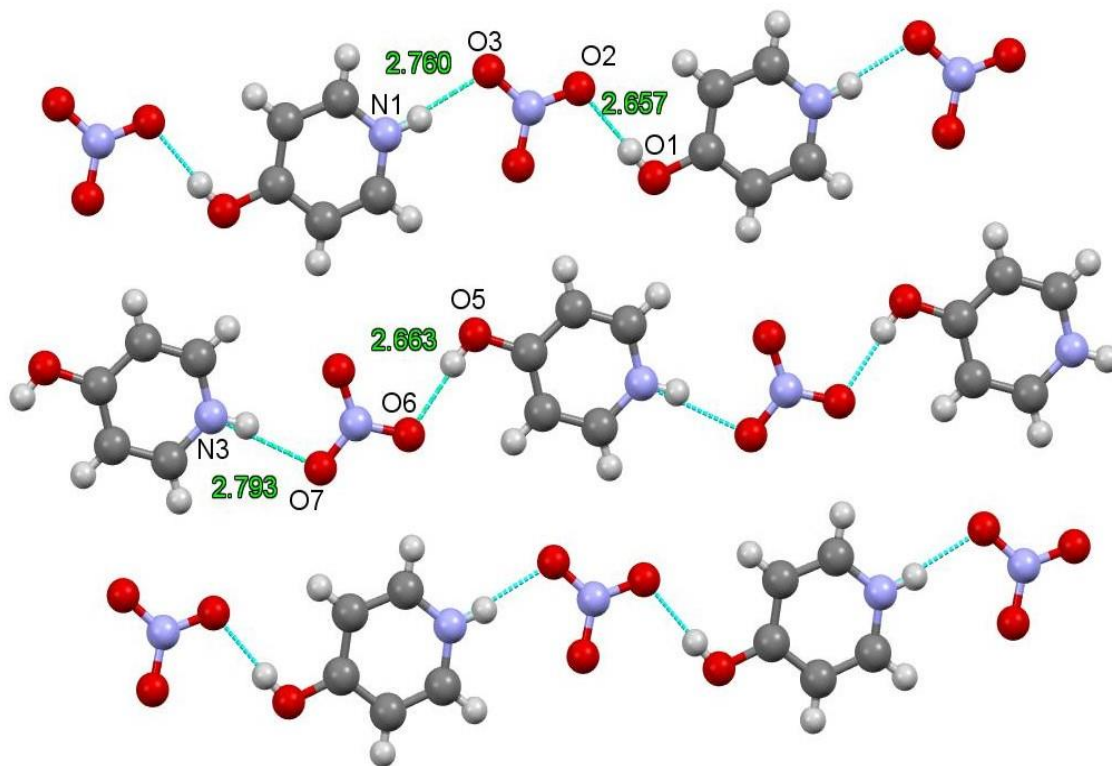
Figure 48. Close contacts between nitrogen and oxygen atoms of 4-hydroxypyridine and oxygen atoms of nitric acid.

17.3.4 4-mercaptopyridine

Compound (4-SH-C$_5$H$_4$NH$^+$)(NO$_3$$^-$) (**40**) was synthesized by the reaction of 4-mercaptopyridine with HNO$_3$ acid in methanol. Evaporation of the solvent was done under vacuum and the compound obtained as a yellow powder. ^{1}H NMR spectrum of the compound did not show any signal for the protonated hydrogen. No good quality crystals were obtained for X-ray diffractometry measurements.

17.3.5 Isonicotinic acid

Compound (4-CO$_2$H-C$_5$H$_4$NH$^+$)(NO$_3$$^-$) (**41**) was prepared by the reaction of isonicotinic acid with HNO$_3$ acid in methanol. Evaporation of the solvent was carried out under vacuum and the compound obtained as a white powder. ^{1}H NMR spectrum of the compound did not show any signal for the protonated hydrogen. X-ray diffractometry

revealed the crystal structure in the monoclinic space group with a space group symbol P2$_1$/n$_1$ and centrosymmetric unit cell. The crystal exhibited phase transition and the unit cell was different at different temperatures. In the crystal structure, the N1···O3 close contact is 2.73Å, the O1···O3 close contact is 2.58Å and the O2···O3 close contact is 2.98Å as shown in Figure 49. The layers in the crystal structure appear in a zig-zag manner with the cation polarity pointing in opposite directions. In addition to the close contacts formed between the anion and the protonated nitrogen, the anion also forms close contacts with both oxygens of isonicotinic acid.
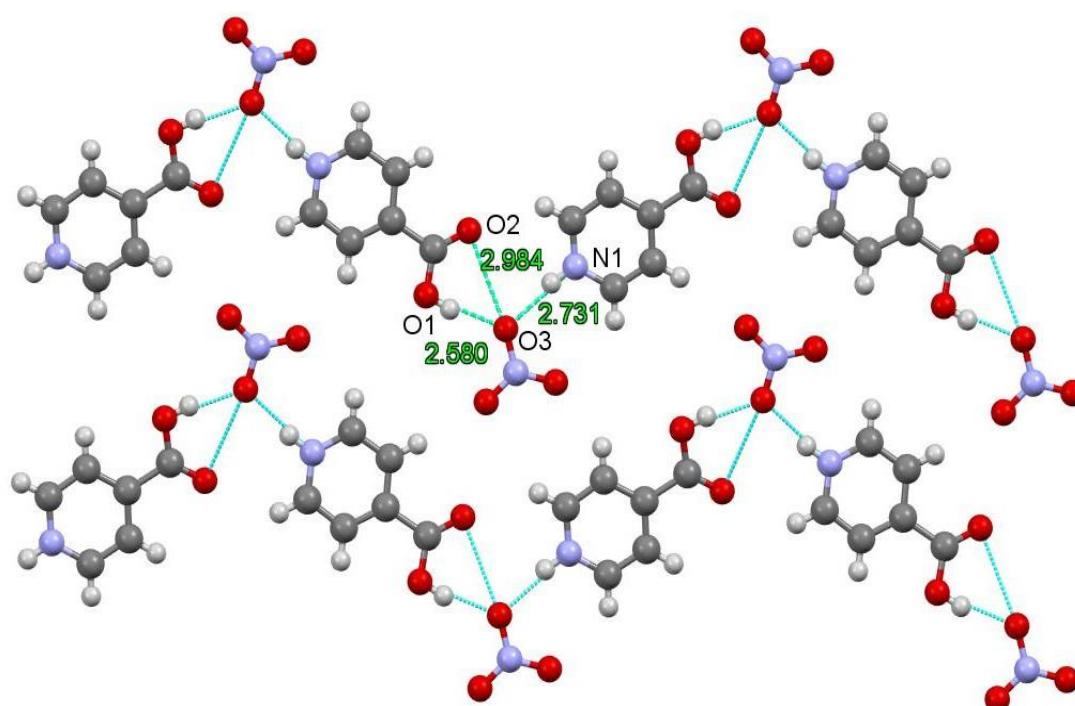
Figure 49. Close contacts between pyridine nitrogen and oxygen atoms of nitric acid and isonicotinic acid.

17.3.6 Isonicotinamide

Compound (4-CONH$_2$-C$_5$H$_4$NH$^+$)(NO$_3^-$) (**42**) was synthesized by the reaction of isonicotinamide with HNO$_3$ acid in methanol. Evaporation of the solvent was carried out under vacuum and the compound obtained as a white powder. The ^{1}H NMR spectrum of the compound did not show any signal for the protonated hydrogen. X-ray

diffractometry analysis revealed the structure of the compound in the monoclinic space group with a space group symbol $P2_1/n_1$ and centrosymmetric unit cell. In the crystal structure, the N1···O2 close contact is 2.76Å, N1···O4 close contact is 3.03Å, N2···O7 close contact is 2.91Å, N2···O13 close contact is 2.88Å, N4···O6 close contact is 2.70Å, N5···O3 close contact is 2.92Å, N5···O9 close contact is 2.94Å, N7···O10 close contact is 2.70Å, N8···015 close contact is 2.96Å, N10···O14 close contact is 2.71Å, N11···O1 close contact is 2.88Å and N11···O11 close contact is 2.94Å as shown in Figure 50. In the crystal structure, linear layers are formed which are cross linked through close contacts between the amide nitrogen and oxygen of isonicotinamide. The cation polarity points in opposite directions.
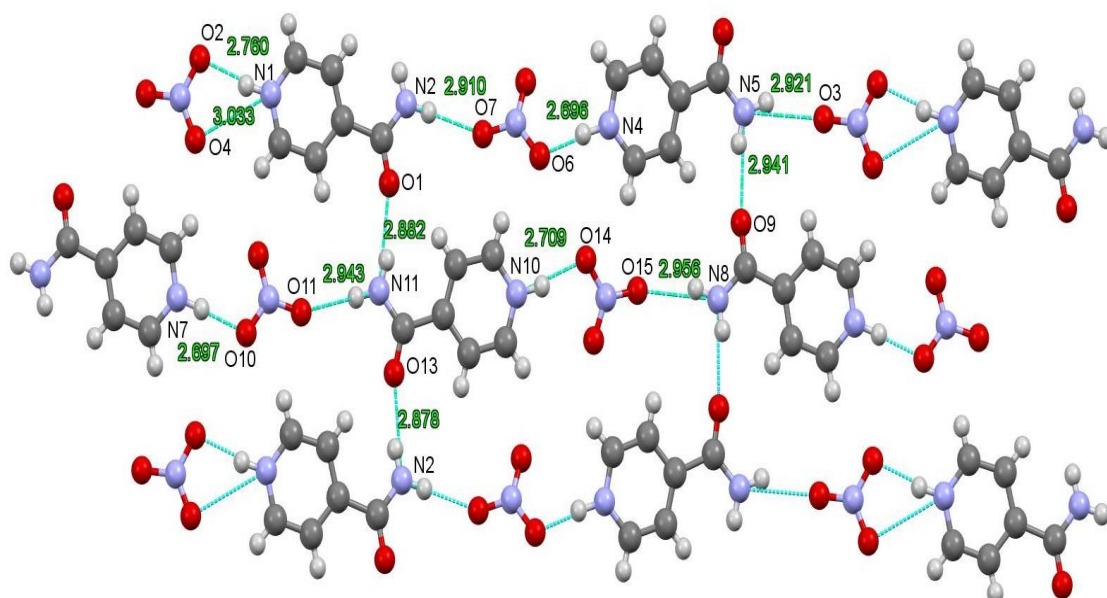
Figure 50. Close contacts between nitrogen and oxygen atoms of isonicotinamide and oxygen atoms of nitric acid.

17.3.7 Pyridinethioamide

Compound (4-CSNH$_2$-C$_5$H$_4$NH$^+$)(NO$_3^-$) (**43**) was prepared by the reaction of pyridinethioamide with HNO$_3$ acid in methanol. Evaporation of the solvent was carried out under vacuum and the compound obtained as an orange powder. The ^{1}H NMR spectrum of the compound did not show any signal for the protonated hydrogen. X-ray

diffractometry analysis revealed the structure of the compound in the monoclinic space group with a space group symbol $P2_1/C_1$ and centrosymmetric unit cell. In the crystal structure, the N1⋯O1 close contact is 2.75Å, S1⋯N2 close contact is 3.42Å and N2⋯O3 close contact is 2.99Å as shown in Figure 51. Cations in the crystal structure form linear layers with the cation polarity in opposite directions.
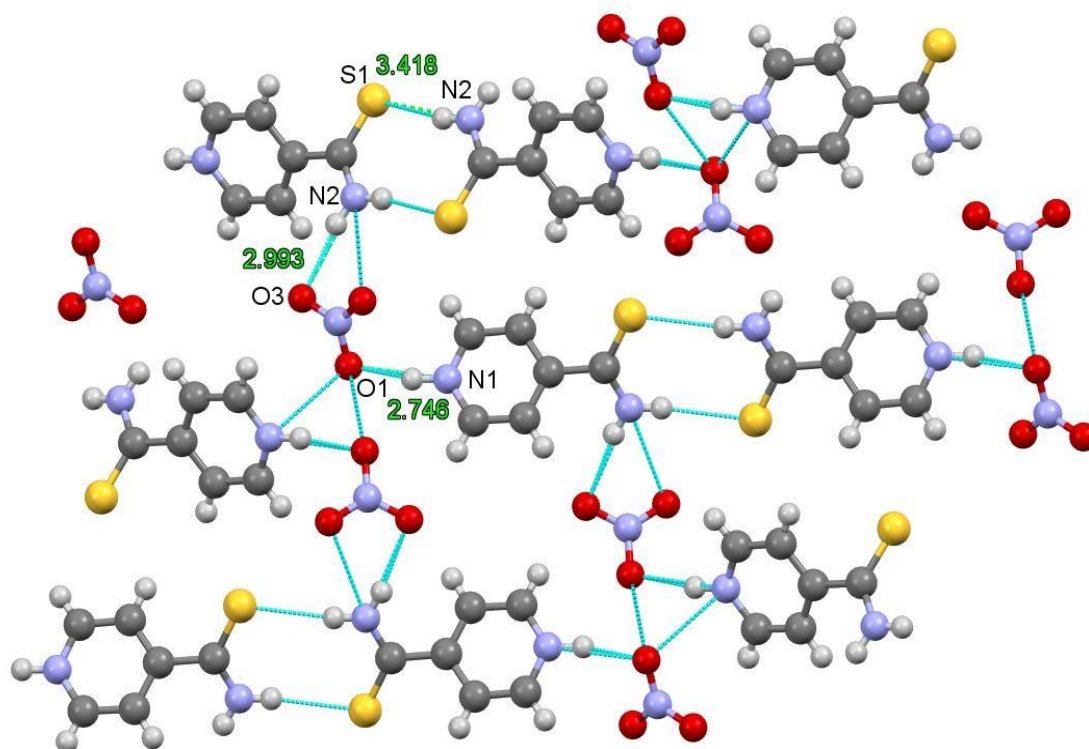
Figure 51. Close contacts between nitrogen and sulphur atoms of pyridinethioamide and oxygen atoms of nitric acid.

Close contacts for crystal structures from the nitric acid reactions are summarized in table 6 below.

Table 6 Selected close contacts for crystal structures from the nitric acid reactions

Compound formula	Bonded atoms	Close contacts
$(4\text{-}NH_2\text{-}C_5H_4NH^+)(NO_3^-)$	N1…O1	2.78Å
	N2…O1	2.94Å
	N2…O2	2.95Å
$(4\text{-}CH_3\text{-}NH_2\text{-}C_5H_4NH^+)(NO_3^-)$	N1…O1	2.79Å
	N2…O3	2.97Å
$(4\text{-}OH\text{-}C_5H_4NH^+)(NO_3^-)$	N1…O3	2.76Å
	N3…O7	2.79Å
	O1…O2	2.66Å
	O5-O6	2.66Å
$(4\text{-}CO_2H\text{-}C_5H_4NH^+)(NO_3^-)$	N1…O3	2.73Å
	O1…O3	2.58Å
	O2…O3	2.98Å
$(4\text{-}CONH_2\text{-}C_5H_4NH^+)(NO_3^-)$	N1…O2	2.76Å
	N1…O4	3.03Å
	N2…O7	2.91Å
	N2…O13	2.88Å
	N4…O6	2.70Å
	N5…O3	2.92Å
	N5…O9	2.94Å
	N7…O10	2.70Å
	N8…015	2.96Å
	N10…O14	2.71Å
	N11…O1	2.88Å
	N11…O11	2.94Å
$(4\text{-}CSNH_2\text{-}C_5H_4NH^+)(NO_3^-)$	N1-O1	2.75Å
	S1-N2	3.42Å
	N2-O3	2.99Å

17.4 Reactions with H_2SO_4 in 1:1 molar ratio

17.4.1 4-Aminopyridine

Compound $(4\text{-}NH_2\text{-}C_5H_4NH^+)(HSO_4^-)$ (**44**) was synthesized by the reaction of 4-aminopyridine with H_2SO_4 acid in methanol. Evaporation of the solvent was carried out under vacuum and the compound obtained as a white powder. The ^1H NMR spectrum of the compound did not show any signal for the protonated hydrogen. X-ray diffractometry analysis revealed two structures of the compound. One structure with five pyridinium cations to only four anions. This therefore means that one of the anions must be a dianion that has resulted from double deprotonation. This structure was in the monoclinic space group with a space group symbol P_1n_1 and non-centrosymmetric unit cell. The other structure had one sulphate dianion to two pyridinium cations one of which was disordered. The structure had a water molecule trapped in it. This structure was in the triclinic space group and noncentrosymmetric unit cell. Small SHG signal though with very low intensity about 1-5% that of urea reference was obtained from this reaction implying that the compound was NLO active. In the crystal structure, the N1···O2 close contact is 2.71Å, N2···O3 close contact is 2.82Å, N2···O4 close contact is 2.87Å, O1···O5 close contact is 2.80Å and O4···O5 close contact is 2.83Å as illustrated in Figure 52. In the crystal structure, alternating linear layers of anions and cations are formed with the cation polarity pointing in the same direction.
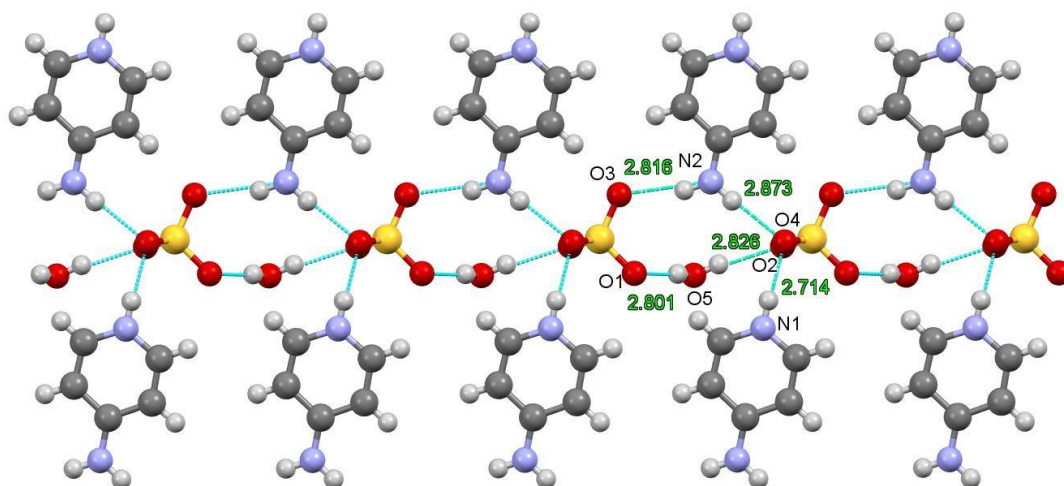
Figure 52. Close contacts between nitrogen atoms of 4-aminopyridine and oxygen atoms of sulphuric acid and water.

17.4.2 4-hydroxypyridine

Compound $(4\text{-OH-C}_5\text{H}_4\text{NH}^+)(\text{HSO}_4^-)$ (**45**) was prepared by the reaction of 4-hydroxypyridine with H_2SO_4 acid in methanol. Evaporation of the solvent was carried out under vacuum and the compound obtained as a white powder. The ^{1}H NMR spectrum of the compound did not show any signal for the protonated hydrogen. X-ray diffractometry analysis revealed the structure of the compound in the monoclinic space group with a space group symbol $P2_1/c1$ and centrosymmetric unit cell. In the crystal structure, the N1···O4 close contact is 2.84Å and O1···O2 close contact is 2.61Å as shown in Figure 53. This structure has been previously reported under DUJHOG at the CSD data base. Linear layers are formed in the crystal structure with the cation polarity pointing in opposite directions.
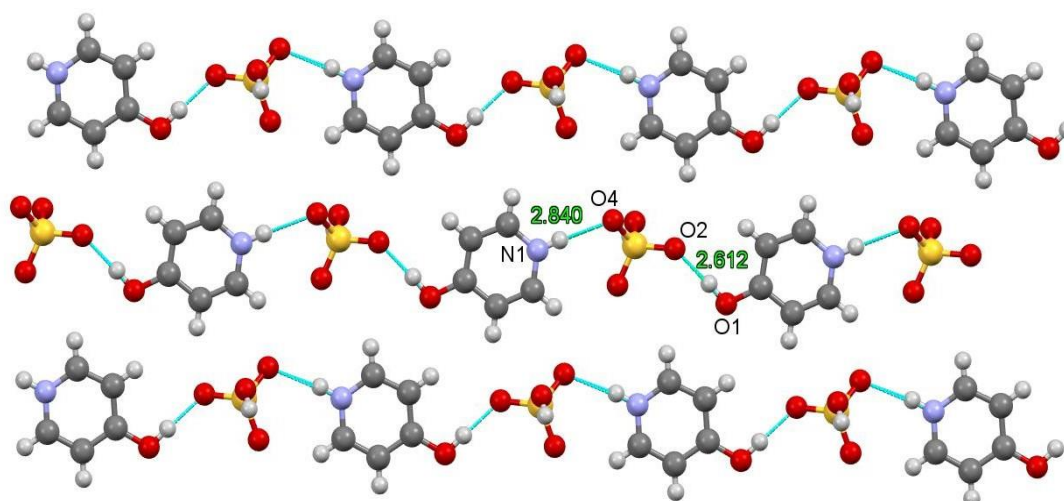

Figure 53. Close contact between nitrogen and oxygen atoms of 4-hydroxypyridine and oxygen atoms of sulphuric acid

17.4.3 4-mercaptopyridine

Compound (4-SH-C$_5$H$_4$NH$^+$)(HSO$_4^-$) (**46**) was prepared by the reaction of 4-mercaptopyridine with H$_2$SO$_4$ acid in methanol. Evaporation of the solvent was carried out under vacuum and the compound obtained as a yellow powder. The compound was not pure but was a mixture of other products as revealed by the ^{1}H NMR of the compound. Water molecules were incorporated into the crystal structure. X-ray diffractometry analysis revealed the structure of the compound in the orthorhombic space group with a space group symbol Pca2$_1$ and non-centrosymmetric unit cell. 4-Mercaptopyridine dimerized in this compound forming 4,4'-dipyridinium-disulfide as seen in Figure 43. Small SHG signal though with very low intensity about 1-5% that of urea reference was obtained from this reaction implying that the compound was NLO active. In the crystal structure, the N1⋯O1 close contact is 2.72Å, N2⋯O5 close contact is 2.76Å and O2⋯O5 close contact is 2.63Å as illustrated in Figure 54.. No specific arrangement of cations and anions could be observed in the crystal structure. Anions form close contacts with each other through the oxygen atoms. Cation pairs are formed by dimerization through the S-S bond.
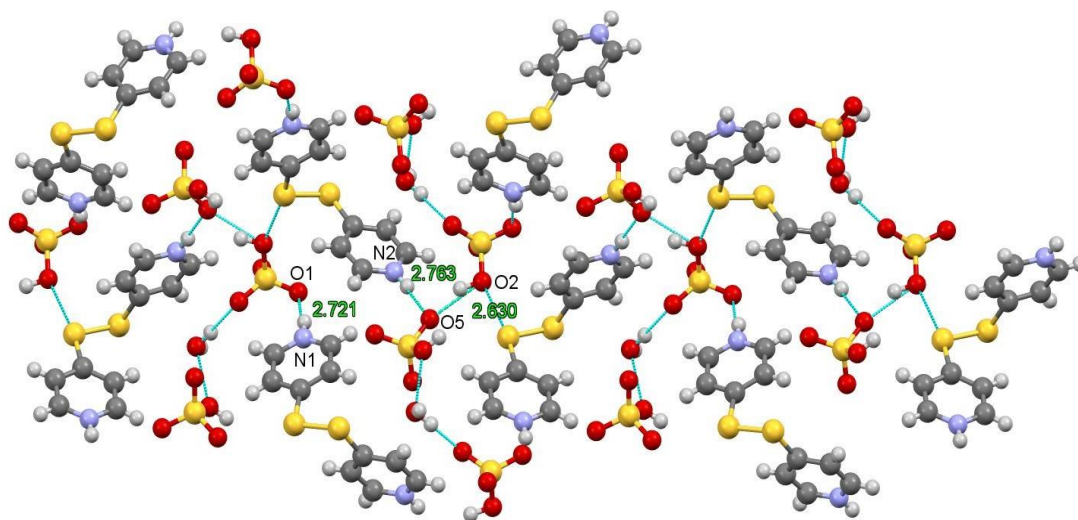
Figure 54. Close contacts between nitrogen atoms of 4-mercaptopyridine and oxygen atoms of sulphuric acid.

17.4.4 Isonicotinic acid

Compound (4-CO$_2$H-C$_5$H$_4$NH$^+$)(HSO$_4^-$) (**47**) was synthesized by the reaction of isonicotinic acid with H$_2$SO$_4$ acid in methanol. Evaporation of the solvent was carried out under vacuum and the compound obtained as a white powder. The ^{1}H NMR spectrum of the compound did not show any signal for the protonated hydrogen. X-ray diffractometry analysis revealed the structure of the compound in the monoclinic space group with the space group symbol P2$_1$/c1 and centrosymmetric unit cell. In the crystal structure, the N1···O5 close contact is 2.79Å, O2···O3 close contact is 2.65Å and O4···O5 close contact is 2.66Å as illustrated in Figure 55. Linear layers are formed in the crystal structure with the cation polarity pointing in opposite directions. The crystal structure has previously been reported in the CSD data base under the name BUFROK and BUFKET

Figure 55. Close contacts between nitrogen and oxygen atoms of isonicotinic acid and oxygen atoms of sulphuric acid.

17.4.5 Isonicotinamide

Compound (4-CONH$_2$-C$_5$H$_4$NH$^+$)(HSO$_4^-$) (**48**) was prepared by the reaction of isonicotinamide with H$_2$SO$_4$ acid in methanol. Evaporation of the solvent was carried out under vacuum and the compound obtained as a white powder. The ^{1}H NMR spectrum of the compound did not show any signal for the protonated hydrogen. X-ray diffractometry analysis revealed the structure of the compound in the monoclinic space group with a space group symbol P2$_1$/c1 and centrosymmetric unit cell. In the crystal structure, the N1···O5 close contact is 2.76Å, N2···O5 close contact is 2.96Å and O1···O2 close contact is 2.55Å as shown in Figure 56. The crystal structure consists of linear layers of anions and cations with polarity in opposite directions.
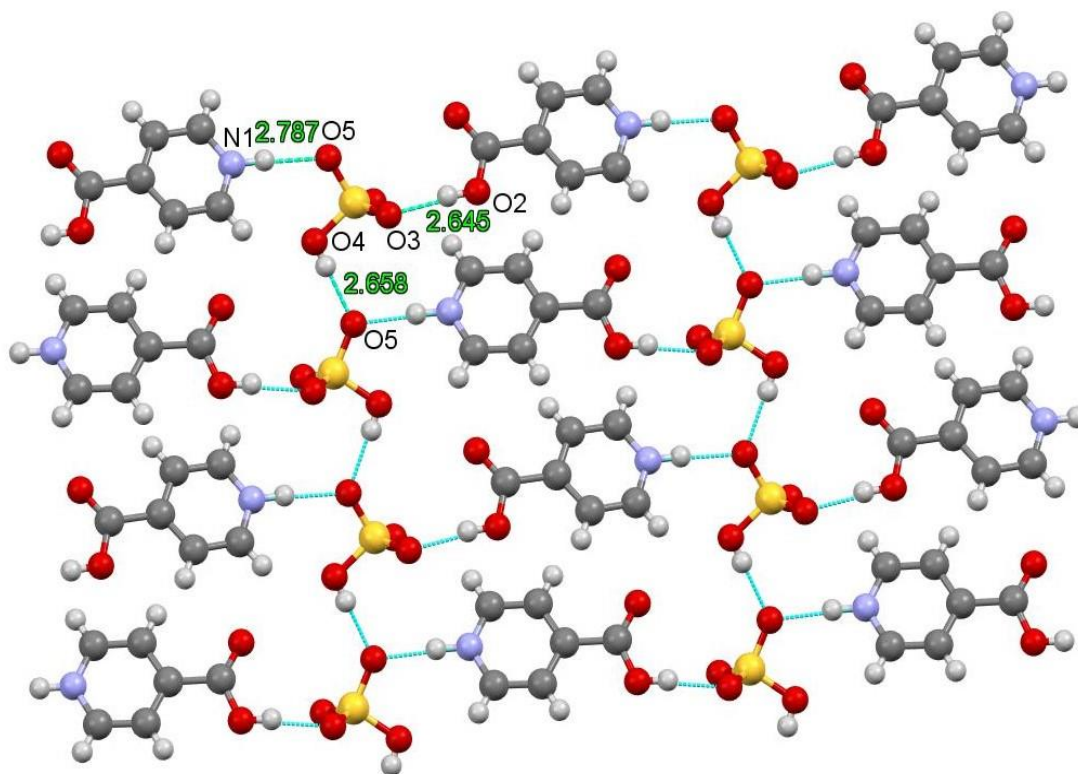

Figure 56. Close contacts between nitrogen and oxygen atoms of isonicotinamide and oxygen atoms of sulphuric acid.

17.4.6 4-Pyridinethioamide

Compound $(4\text{-}CSNH_2\text{-}C_5H_4NH^+)(HSO_4^-)$ (**49**) was synthesized by the reaction of 4-pyridinethioamide with H_2SO_4 acid in methanol. Evaporation of the solvent was carried out under vacuum and the compound obtained as an orange powder. The ^1H NMR spectrum of the compound did not show any signal for the protonated hydrogen. X-ray diffractometry analysis revealed the structure of the compound in the triclinic space group with a space group symbol P -1 and centrosymmetric unit cell. In the crystal structure, the N1···O1 close contacts is 2.75Å, N2···O3 close contact is 2.92Å, N2···O4 close contact is 2.93Å and O1···S1 close contacts is 3.31Å as illustrated in Figure 57. The crystal structure consists of linear layers of anions and cations with polarity in opposite directions.

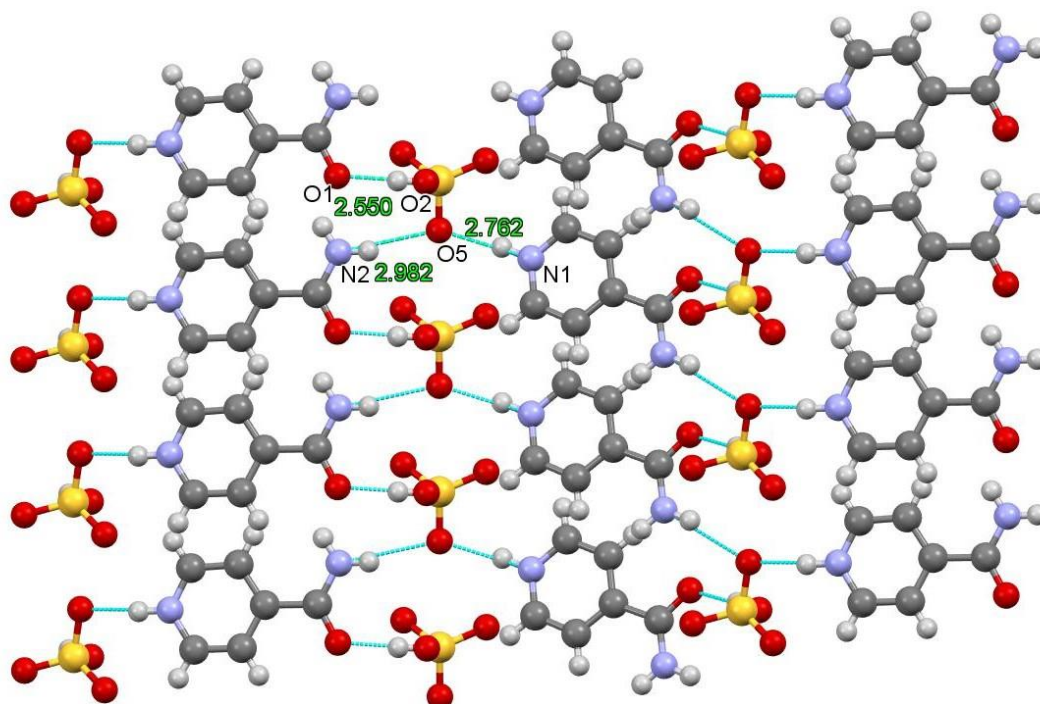Figure 57. Close contacts between nitrogen and sulphur atoms of 4-pyridinethioamide and oxygen atoms of sulphuric acid

The close contacts for the sulphuric acid (1:1) reactions are summarized in table 7 below.

Table 7. Selected close contacts for the sulphuric acid (1:1) reactions

Compound formula	Bonded atoms	Bond lengths
(4-NH$_2$-C$_5$H$_4$NH$^+$)(HSO$_4^-$)	N1…O2	2.71Å
	N2…O3	2.82Å
	N2…O4	2.87Å,
	O1…O5	2.80Å
	O4…O5	2.83Å
(4-OH-C$_5$H$_4$NH$^+$)(HSO$_4^-$)	N1…O4	2.84Å
	O1…O2	2.61Å
(4-SH-C$_5$H$_4$NH$^+$)(HSO$_4^-$)	N1…O1	2.72Å
	N2…O5	2.76Å
	O2…O5	2.63Å
(4-CO$_2$H-C$_5$H$_4$NH$^+$)(HSO$_4^-$)	N1…O5	2.79Å
	O2…O3	2.65Å
	O4…O5	2.66Å
(4-CONH$_2$-C$_5$H$_4$NH$^+$)(HSO$_4^-$)	N1…O5	2.76Å
	N2…O5	2.96Å
	O1…O2	2.55Å
(4-CSNH$_2$-C$_5$H$_4$NH$^+$)(HSO$_4^-$)	N1…O1	2.75Å
	N2…O3	2.92Å
	N2…O4	2.93Å
	O1…S1	3.31Å

17.5 Reactions with H_2SO_4 in 2:1 molar ratio

17.5.1 4-Aminopyridine

Compound $(4\text{-}NH_2\text{-}C_5H_4NH^+)(SO_4^{2-})$ (**50**) was prepared by the action of 4-aminopyridine with H_2SO_4 acid in 2:1 molar ratio in methanol. Evaporation of the solvent was carried out under vacuum and the compound obtained as a white powder. The ^{1}H NMR spectrum of the compound did not show any signal for the protonated hydrogen. X-ray diffractometry analysis revealed the structure of the compound with the asymmetric unit having a water molecule and two pyridinium cations. The crystal structure was in the triclinic space group with a space group symbol P-1 and centrosymmetric unit cell. Water molecules were trapped between anions in the crystal structure. Small SHG signal though with very low intensity about 1-5% that of urea reference was obtained from this reaction implying that the compound was NLO active. In the crystal structure, the N1···O1 close contact is 2.71Å, N2···O1 close contact is 2.87Å, N2···O3 close contact is 2.81Å, O2···O5 close contact is 2.82Å and O4···O5 close contact is 2.78Å as illustrated in Figure 58. The crystal structure consists of a linear arrangement of anions and cations with polarity in the same direction.
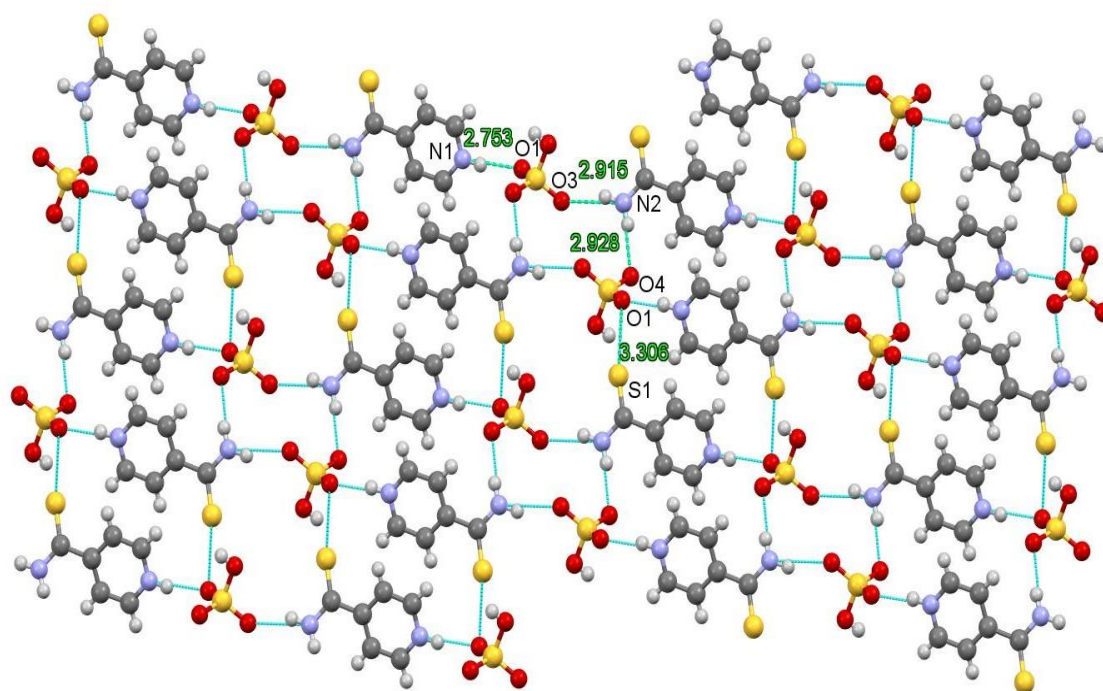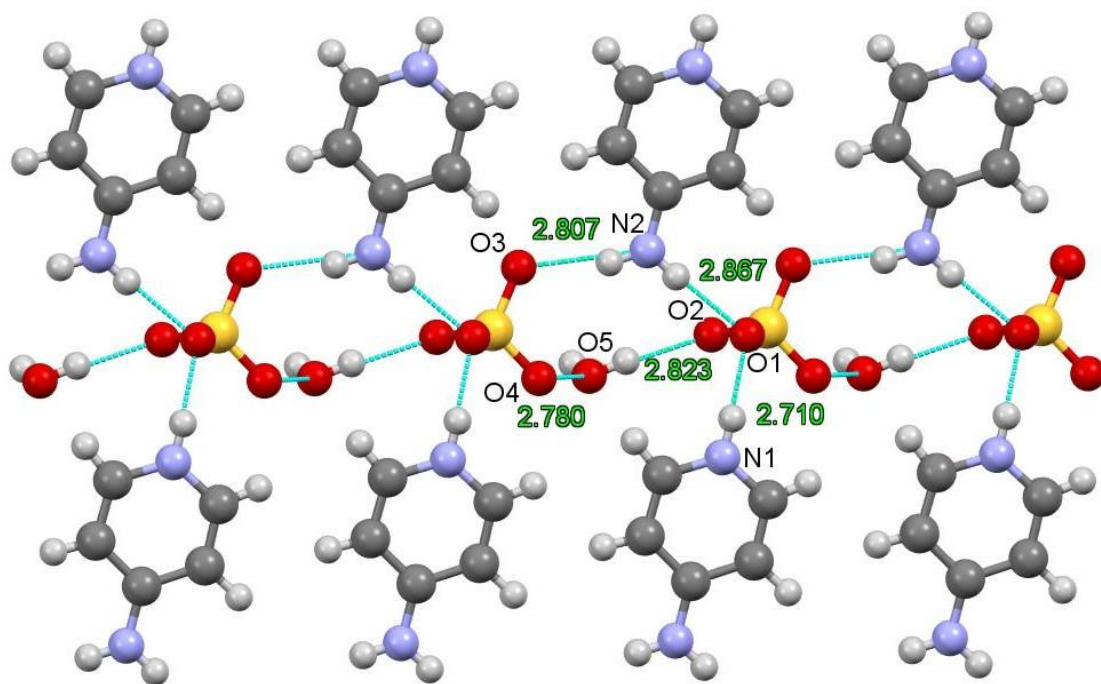
Figure 58. Close contacts between nitrogen atoms of 4-aminopyridine and oxygen atoms of sulphuric acid.

17.5.2 4-Hydroxypyridine

Compound $(4\text{-}OH\text{-}C_5H_4NH^+)(SO_4^{2-})$ (**51**) was synthesized by the reaction of 4-hydrroxypyridine with H_2SO_4 acid in 2:1 molar ratio in methanol. Evaporation of the solvent was carried out under vacuum and the compound obtained as a white powder. The ^1H NMR spectrum of the compound did not show any signal for the protonated hydrogen. X-ray diffractometry analysis revealed the structure of the compound with the asymmetric unit having a water molecule incorporated into it. The crystal structure was in the monoclinic space group with a space group symbol P 2₁/n 1 and centrosymmetric unit cell. In the crystal structure, the N1···O3 close contacts is 2.70Å and O1···O4 close contact is 2.55Å as shown in Figure 59. No specific arrangement of the anions and cations was observed in the crystal structure.

Figure 59. Close contacts between nitrogen and oxygen atoms of 4-hydroxypyridine and oxygen atoms of sulphuric acid.

17.5.3 4-mercaptopyridine

Compound (4-SH-C$_5$H$_4$NH$^+$)(SO$_4$$^{2-}$) (**52**) was prepared by the reaction of 4-mercaptopyridine with H$_2$SO$_4$ acid in 2:1 molar ratio in methanol. Evaporation of the solvent was carried out under vacuum and the compound obtained as an oily product. All attempts to crystallize the compound failed and crystals were not obtained.

17.5.4 Isonicotinic acid

Compound (4-CO$_2$H-C$_5$H$_4$NH$^+$)(SO$_4$$^{2-}$) (**53**) was synthesized by the reaction of isonicotinic acid with H$_2$SO$_4$ acid in 2:1 molar ratio in methanol. Evaporation of the solvent was carried out under vacuum and the compound obtained as a white product. The ^{1}H NMR spectrum of the compound did not show any signal for the protonated hydrogen. Double protonation by the acid was not complete as the asymmetric unit had three pyridinium cations to one sulphate and one hydrogen sulphate anions with a water molecule incorporated into the crystal structure. X-ray diffractometry revealed the structure of the compound as monoclinic space group with a space group symbol C 1

2/c 1 and centrosymmetric unit cell. In the crystal structure, the N1···O7 close contacts is 2.85Å, N2···O10 close contact is 2.66Å, N3···O13 close contact is 2.83Å, N3···O14 close contact is 2.95Å, O2···O15 close contact is 2.52Å, O4···O8 close contact is 2.57Å, O5···O11 close contact is 2.58Å and O9···O14 close contact is 2.48Å as shown in Figure 60. No specific arrangement of the anions and cations was observed in the crystal structure.
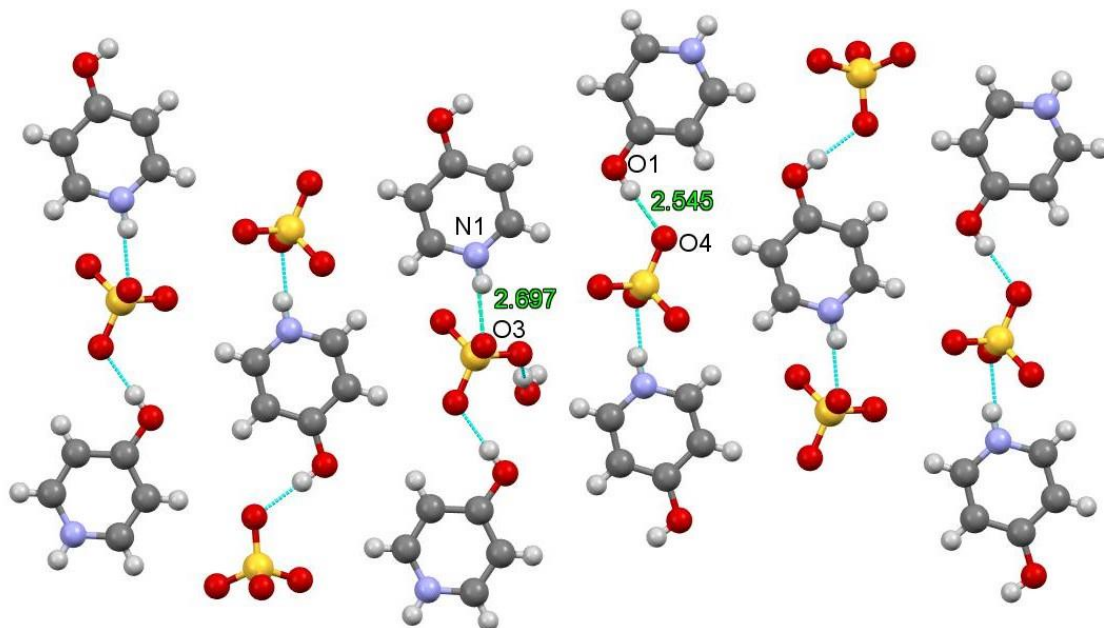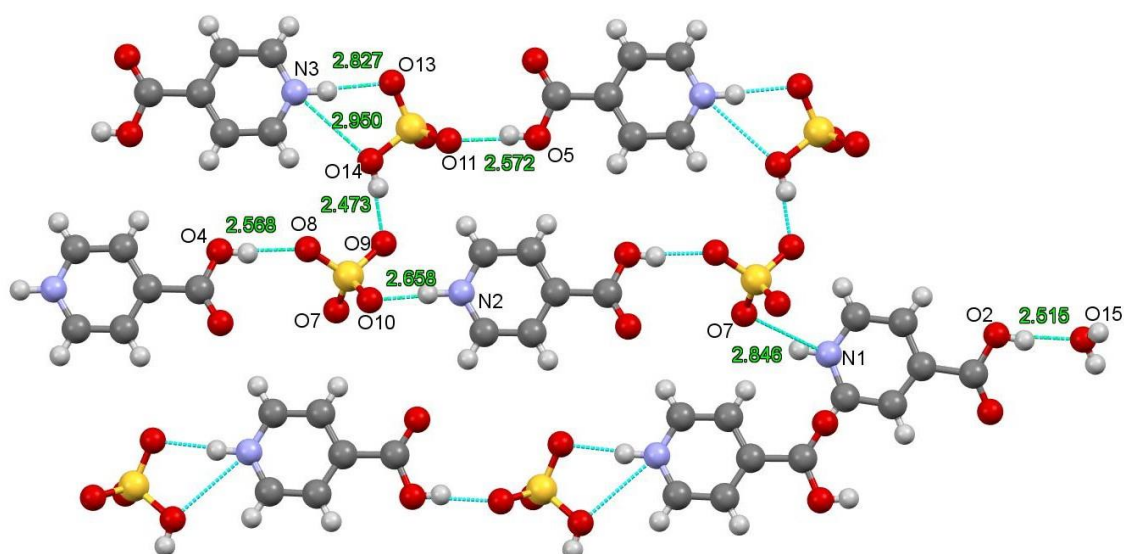

Figure 60. Close contacts between nitrogen and oxygen atoms of isonicotinic acid and oxygen atoms of sulphuric acid.

17.5.5 Isonicotinamide

Compound $(4\text{-}CONH_2\text{-}C_5H_4NH^+)(SO_4^{2-})$ (**54**) was prepared by the reaction of isonicotinamide with H_2SO_4 acid in 2:1 molar ratio in methanol. Evaporation of the solvent was carried out under vacuum and the compound was obtained as a white product. The ^1H NMR spectrum of the compound did not show any signal for the protonated hydrogen. X-ray diffractometry revealed the structure of the compound in the monoclinic space group with the space group symbol P 2₁/c 1 and centrosymmetric unit cell. The crystal structure had a water molecule incorporated into it. In the crystal structure, the N1···O4 close contacts is 2.58Å, N1···O3 close contact is 3.07Å, N2···O2

close contact is 2.91Å, N2···O3 close contact is 2.78Å, N3···O7 close contact is 2.57Å, N4···O1 close contact is 2.97Å and O5···O7 close contact is 2.77Å as illustrated in Figure 61. No specific arrangement of the anions and cations was observed in the crystal structure. Cations form dimers through close contacts with the oxygen atom and the amide nitrogen.
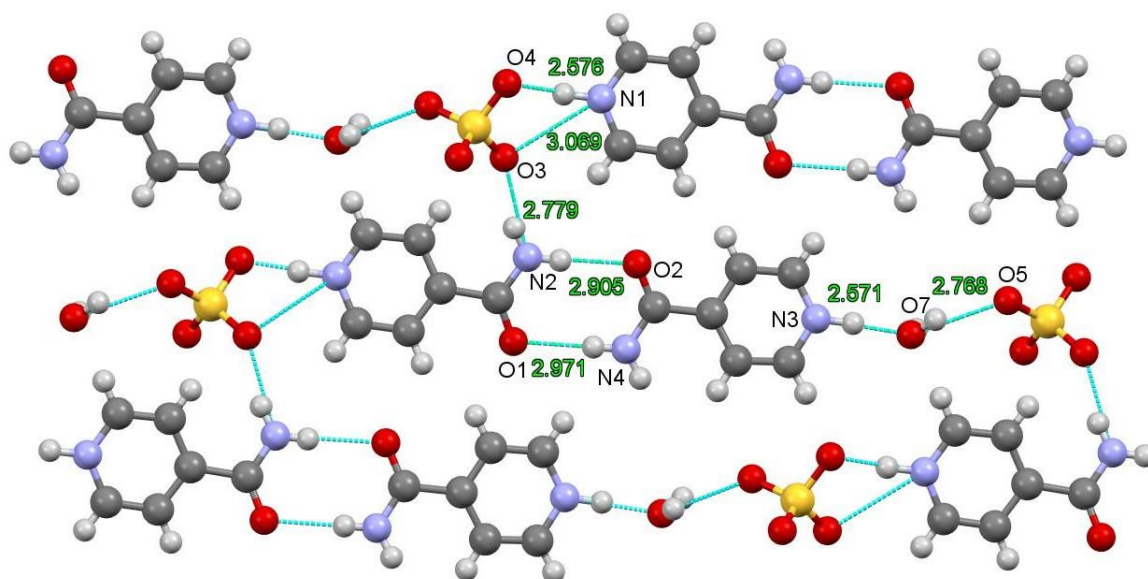
Figure 61. Close contacts between nitrogen and oxygen atoms of isonicotinamide and oxygen atoms of sulphuric acid and water.

17.5.6 4-pyridinethioamide

Compound (4-CSNH$_2$-C$_5$H$_4$NH$^+$)(SO$_4^{2-}$) (**55**) was synthesized by the reaction of 4-pyridinethioamide with H$_2$SO$_4$ acid in 2:1 molar ratio in methanol. Evaporation of the solvent was carried out under vacuum and the compound obtained as an orange product. The ^{1}H NMR spectrum of the compound did not show any signal for the protonated hydrogen. X-ray diffractometry revealed the structure of the compound in the monoclinic space group with the space group symbol P 2$_1$/c 1 and centrosymmetric unit cell. In the crystal structure, the N1···O1 close contacts is 2.67Å, N2···O3 close contact is 2.76Å, N2···S2 close contact is 3.37Å, N3···O5 close contact is 2.69Å, N4···S1 close

contact is 3.40Å, N4···O8 close contact is 2.74Å, N5···O5 close contact is 2.64Å, N5···O6 close contact is 3.05Å and N7···O2 close contact is 2.59Å as shown in Figure 62. In the crystal structure, cations have their polarity in opposite directions and form dimers through close contacts with the sulphur atom and the amide nitrogen.
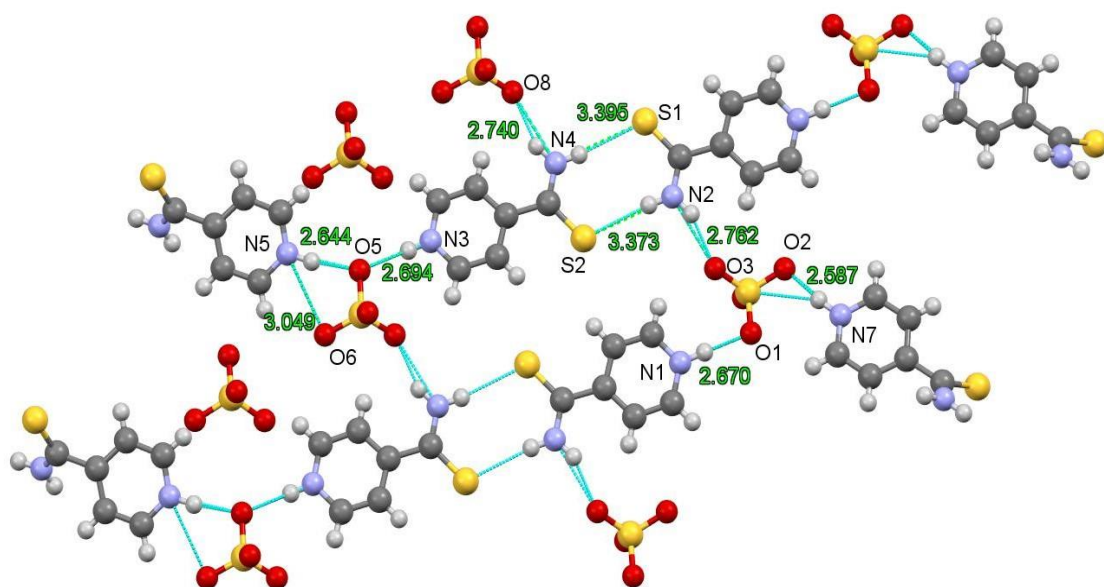
Figure 62. Close contacts between nitrogen and sulphur atoms of 4-pyridinethioamide and oxygen atoms of sulphuric acid.

Close contacts for crystals from the sulphuric acid (2:1) reactions are summarized in table 8 below.

Table 8 Selected close contacts for crystals from the sulphuric acid (2:1) reactions

Compound formula	Close contact atoms	Close contacts
$(4\text{-}NH_2\text{-}C_5H_4NH^+)(SO_4^{2-})$	N1…O1	2.71Å
	N2…O1	2.87Å
	N2…O3	2.81Å
	O2…O5	2.82Å
	O4…O5	2.78Å
$(4\text{-}OH\text{-}C_5H_4NH^+)(SO_4^{2-})$	N1…O3	2.70Å
	O1…O4	2.55Å
$(4\text{-}CO_2H\text{-}C_5H_4NH^+)(SO_4^{2-})$	N1…O7	2.85Å
	N2…O10	2.66Å
	N3…O13	2.83Å
	N3…O14	2.95Å,
	O2…O15	5.52Å
	O4…O8	2.57Å
	O5…O11	2.58Å
	O9…O14	2.48Å
$(4\text{-}CONH_2\text{-}C_5H_4NH^+)(SO_4^{2-})$	N1…O4	2.58Å
	N1…O3	3.07Å
	N2…O2	2.91Å
	N2…O3	2.78Å
	N3…O7	2.57Å
	N4…O1	2.97Å
	O5…O7	2.77Å
$(4\text{-}CSNH_2\text{-}C_5H_4NH^+)(SO_4^{2-})$	N1…O1	2.67Å
	N2…O3	2.76Å,
	N2…S2	3.37Å
	N3…O5	2.69Å
	N4…S1	3.40Å
	N4…O8	2.74Å
	N5…O5	2.64Å
	N5…O6	3.05Å
	N7…O2	2.59Å

These values on the tables for the close contacts are used to compare similar structures with different acids.

18 Comparing the crystal structure with different acids

18.1 4-aminopyridine structures

$(4\text{-}NH_2\text{-}C_5H_4NH^+)(H_2PO_4^-)$ crystal structure contained water molecules whose oxygen atoms formed bonds with the pyridine nitrogen and the amine nitrogen. The bond formed between the pyridine nitrogen and the oxygen of the water molecule has a close contact of 2.77Å which is even stronger than the close contact formed between the oxygen of $H_2PO_3^-$ anion and the amine nitrogen with a close contact of 2.95Å. The pyridine nitrogen did not form any close contacts with the oxygen of the $H_2PO_3^-$ anion as it was the case with nitric acid reactions where the pyridine nitrogen had close contacts with the oxygen atoms of the nitrate anion (NO_3^-). $(4\text{-}NH_2\text{-}C_5H_4NH^+)(HSO_4^-)$ and $(4\text{-}NH_2\text{-}C_5H_4NH^+)(SO_4^{2-})$ crystal structures had water molecules but the oxygen of the water molecule was not bonded to the pyridine nitrogen. Rather, the pyridine nitrogen formed bonds with the oxygen atoms of the HSO_4^- and the SO_4^{2-} anions. $(4\text{-}NH_2\text{-}C_5H_4NH^+)(H_2PO_4^-)$ and $(4\text{-}NH_2\text{-}C_5H_4NH^+)(NO_3^-)$ had their polarity pointing in opposite directions while $(4\text{-}NH_2\text{-}C_5H_4NH^+)(HSO_4^-)$ and $(4\text{-}NH_2\text{-}C_5H_4NH^+)(SO_4^{2-})$ had their polarity pointing in the same direction. The pyridine nitrogen to oxygen close contact in $(4\text{-}NH_2\text{-}C_5H_4NH^+)(HSO_4^-)$ and $(4\text{-}NH_2\text{-}C_5H_4NH^+)(SO_4^{2-})$ was the same (2.71Å). This similarity is also observed with $(4\text{-}NH_2\text{-}C_5H_4NH^+)(H_2PO_4^-)$ and $(4\text{-}NH_2\text{-}C_5H_4NH^+)(NO_3^-)$ structures with the pyridine nitrogen to oxygen close contact of 2.77Å and 2.78Å respectively. From this point of view, $(4\text{-}NH_2\text{-}C_5H_4NH^+)(H_2PO_4^-)$ and $(4\text{-}NH_2\text{-}C_5H_4NH^+)(NO_3^-)$ were closely related to each other just like $(4\text{-}NH_2\text{-}C_5H_4NH^+)(HSO_4^-)$ and $(4\text{-}NH_2\text{-}C_5H_4NH^+)(SO_4^{2-})$. $(4\text{-}NH_2\text{-}C_5H_4NH^+)(H_2PO_4^-)$, $(4\text{-}NH_2\text{-}C_5H_4NH^+)(NO_3^-)$ and $(4\text{-}NH_2\text{-}C_5H_4NH^+)(SO_4^{2-})$ were all centrosymmetric while $(4\text{-}NH_2\text{-}C_5H_4NH^+)(HSO_4^-)$ was noncentrosymmetric. This comparison is summarized in table 8 below.

Table 9 Comparison of 4-aminopyridine derivatives with different acids

4-NH$_2$-C$_5$H$_4$NH$^+$)(H$_2$PO$_4$$^-$)	(4-NH$_2$-C$_5$H$_4$NH$^+$)(NO$_3$$^-$)	(4-NH$_2$-C$_5$H$_4$NH$^+$)(HSO$_4$$^-$)	(4-NH$_2$-C$_5$H$_4$NH$^+$)(SO$_4$$^{2-}$)
Crystal contain water molecules with oxygen atoms forming contacts with the pyridine nitrogen and the amine nitrogen. No contact between the pyridine nitrogen and the H$_2$PO$_4$$^-$ anion as expected.	Crystal does not contain any water molecule and Pyridine nitrogen form contacts with the anion as expected.	Crystal contain water molecules but no close contacts with the pyridine nitrogen. Pyridine nitrogen form contacts with the anion as intended.	Crystal contain water molecules but no close contacts with the pyridine nitrogen. Pyridine nitrogen form contacts with the anion as expected.
polarity pointing in opposite directions	polarity pointing in opposite directions	polarity pointing in the same direction	polarity pointing in the same direction
pyridine nitrogen to oxygen close contact of 2.77Å	pyridine nitrogen to oxygen close contact of 2.78Å	pyridine nitrogen to oxygen close contact of 2.71Å	pyridine nitrogen to oxygen close contact of 2.71Å
Triclinic crystal system	Monoclinic crystal system	Monoclinic crystal system	Triclinic crystal system
Space group symbol is P-1	Space group symbol is P2$_1$/C$_1$	Space group symbol is P 1 n 1	Space group symbol is P -1
Centrosymmetric unit cell	Centrosymmetric unit cell	Centrosymmetric unit cell	Centrosymmetric unit cell

18.2 4-hydroxypyridine structures

With the hydroxypyridine structures, (4-OH-C$_5$H$_4$NH$^+$)(H$_2$PO$_4$$^-$) had the shortest and therefore the strongest pyridine nitrogen to oxygen bond with a bond length of 2.66Å. (4-OH-C$_5$H$_4$NH$^+$)(NO$_3$$^-$) and (4-OH-C$_5H_4NH^+$)(BF$_4$$^-$) had similar close contact values of 2.76Å and 2.78Å respectively. (4-OH-C$_5$H$_4$NH$^+$)(SO$_4$$^{2-}$) had pyridine to oxygen close contact of 2.70Å which is midway between that of (4-OH-C$_5$H$_4$NH$^+$)(NO$_3$$^-$) and (4-OH-C$_5H_4NH^+$)(H$_2PO_4$$^-$). (4-OH-C$_5H_4NH^+$)(HSO$_4$$^-$) had the longest and consequently the weakest pyridine nitrogen to oxygen bond length of 2.84Å. (4-OH-C$_5$H$_4$NH$^+$)(BF$_4$$^-$) presumably has the highest dipole moment as the pyridine nitrogen is bonded to Fluorine which is more electronegative than oxygen as it is the case with H$_3$PO$_4$, HNO$_3$ and

H_2SO_4 reactions. All the structures had their polarity in opposite directions effectively cancelling each other. All the structures were centrosymmetric. Only the hydroxypyridine derivative with Tetrafluoroboric acid formed dimers through the oxygen atoms. $(4-OH-C_5H_4NH^+)(H_2PO_4^-)$ and $(4-OH-C_5H_4NH^+)(NO_3^-)$ showed some NLO activity with small SHG signals. This comparison is summarized in table 9 below.

Table 10 Comparison of 4-hydroxypyridine derivatives with different acids

$(4-OH-C_5H_4NH^+)(BF_4^-)$	$(4-OH-C_5H_4NH^+)(H_2PO_4^-)$	$(4-OH-C_5H_4NH^+)(NO_3^-)$	$(4-OH-C_5H_4NH^+)(HSO_4^-)$	$(4-OH-C_5H_4NH^+)(SO_4^{2-})$
pyridine nitrogen to anion close contact of 2.78Å similar to that with HNO₃ acid	Shortest and consequently strongest pyridine nitrogen to anion close contact of 2.66Å.	pyridine nitrogen to anion close contact of 2.76Å similar to that with HBF₄	Longest and consequently weakest pyridine nitrogen to anion close contact of 2.84Å	Pyridine nitrogen to anion close contact of 2.70Å midway between that with the Nitric acid and phosphuric acid
Cation polarity in opposite directions	Cation polarity in opposite directions	Cation polarity in opposite directions	Cation polarity in opposite directions	Cation polarity in opposite directions
Centrosymmetric unit cell	Centrosymmetric unit cell	Centrosymmetric unit cell	Centrosymmetric unit cell	Centrosymmetric unit cell
Monoclinic crystal system	Orthorhombic crystal system	Triclinic crystal system	Monoclinic crystal system	Monoclinic crystal system
Space group symbol is P2₁/c	Space group symbol is Pbca	Space group symbol is P1	Space group symbol is P2₁/c 1	Space group symbol is P2₁/n 1
Cations formed dimers through oxygen atoms	Oxygen atoms of cations form close contacts with the anions	Oxygen atoms of cations form close contacts with the anions	Oxygen atoms of cations form close contacts with the anions	Oxygen atoms of cations form close contacts with the anions
No SHG signal obtained	showed some NLO activity with small SHG signals	showed some NLO activity with small SHG signals	No SHG signal obtained	No SHG signal obtained

19 Comparison of the crystal structures obtained in this synthetic work to literature

The crystal structures obtained during this synthetic work quite closely resemble those already known in existing literature. Existing literature reveals that Nicotinium hydrogen sulphate (compound **47** in sulphuric acid series 1:1 reactions) consist of distinct ions linked together through N−H···O and O−H···O hydrogen bonds.[55] The hydrogen bonds help to complement the coulombic interactions thereby further stabilizing the molecular crystal structure. The crystal structure of the compound belongs to the monoclinic space group with the space group symbol P 2_1/c 1 which is in exactly the same as that obtained in this work. The asymmetric unit has a protonated nicotinic acid and a HSO_4^- with the nicotinium cation planar in shape.[55] The cations and anions in the molecular crystal structure are alternately arranged and interconnected by intermolecular hydrogen bonds which stabilizes the entire molecular crystal structure.[57]

For dinicotinium sulphate (compound **53** in sulphuric acid reactions 2:1), existing literature reveals that the carbonyl groups of the two nicotinium cations in the asymmetric unit are twisted away from the pyridine ring.[56] The asymmetric unit has two nicotinium cations to one sulphate anion unlike the asymmetric unit obtained in this work with three nicotinium cations to one sulphate and one hydrogen sulphate anions and a water molecule incorporated into the crystal unit. The molecular structure of dinicotinium sulphate has one of the nicotinium cations interconnected to the sulphate anion through the O−atom of the sulphate anion and the other nicotinium cation forms an inverted -related close hydrogen loop.[56]

For 4-Aminopyridine dihydrogen phosphate (compound **30**), literature reveals that the crystal structure of the asymmetric unit has one water molecule.[58] It belongs to the triclinic space group with a space group symbol P-1. The compound forms a 1:1 dihydrogen phosphate monohydrate. All these is in good agreement with the one obtained in this work.

Pyridine thioamide phosphate (compound **36**) belongs to the monoclinic space group with a space group symbol C2/c same as that obtained during this work. The crystal structure is stabilized by N−H···S intermolecular hydrogen bond interactions.[59] In the crystal structure obtained in this work, cation form pairs through the sulphur atoms and

the amide nitrogen. The asymmetric unit of compound **36** is not disordered but in literature, the asymmetric unit is disordered.[59]

20 Conclusion

$C_5H_4NH^+$- X pyridinium cations bearing substituents X= NH_2, CH_3NH, SH, OH, COOH, $CONH_2$ and $CSNH_2$ were synthesized by the reaction of mineral acids (HBF_4, HNO_3, H_2SO_4 and H_3PO_4) with the corresponding pyridine derivatives in the presence of methanol as solvent. The synthesis becomes difficult when the pyridine derivative does not dissolve in methanol and water has to be added and the reaction mixture slightly warmed to enhance the dissolution. It even becomes more difficult when the end product is oily and needs to be further processed in an effort to obtain solid, crystalline products. Better yields were obtained for reactions in which the reactants just nicely dissolved in methanol without any difficulty. This implies that the extent to which the reactants dissolve in the reaction solvent plays a significant role in the success of the reaction. Crystal structures for the products were obtained by means of a network of physical methods and single crystal X-ray diffraction. During the synthesis, only compounds **26, 28, 30, 32, 35, 39, 44, 46** and **50** exhibited some small SHG signals with laser measurements though with very low intensities compared to that of urea (1-5% of the intensity of urea reference). Some compounds were centrosymmetric and display SHG signals confirming that non-centrosymmetry is not necessary a key factor to NLO activity. Most compounds with SHG signals have their anion and cation orderly arranged in the same direction thereby enhancing polarity. Dimerization occurred in 4-mercaptopyridine compounds of tetrafluoroboric acid and sulphuric acid (1:1 reaction). The H_3PO_4 series worked best as most compounds with the SHG signals are from reactions with this acid. The acetic acid series did not work out well presumably because the pKa value is too low for the protonation to take place.

Though the NMR signal for the protonated hydrogen of 4-aminopyridine with tetrafluoroboric acid was obtained, no good quality crystals were obtained for this compound, hence the NLO properties were not studied. Unpredictable phase transition occurred with isonicotinic acid in the nitric acid series resulting to different unit cells at different temperatures. This crystal structure has already been reported, CSD WOUZEF.

Intended goals for this work were almost entirely achieved because most of the target compounds were prepared, their crystal structures obtained and their NLO properties investigated. It may be useful and beneficial to try to investigate other characteristics of good NLO crystals such as phase matching, second order nonlinear susceptibility and wide optical transparency with these synthesized compounds.

21 Synthetic work

21.1 HBF₄ series

21.1.1 Synthesis of (4-NH₂-C₅H₄NH⁺)(BF₄⁻)

0.190g (2.109mmol) of 4-aminopyridine powder was dissolved in 30ml of methanol and 0.30ml (4.78mmol) of HBF₄ added. The reaction mixture was stirred at room temperature for one hour. The solvent was evaporated under vacuum and the product obtained as a white powder (0.319g, 85%). The product was soluble in acetonitrile, methanol, ethanol and THF but insoluble in dichloromethane and toluene. Recrystallization was done following the solvent diffusion. The product was separately dissolved in methanol, ethanol and acetonitrile (solvent 1) and then pentane, hexane, diethylether and toluene (solvent 2) was added. ^{1}H NMR (CD₃CN): δ 10.99 (m,1H,NH of pyridine), δ 7.50 (m,2H,C₅H₄N of pyridine), δ 6.85(m,2H,C₅H₄N of pyridine), δ 6.56 (br,s,2H, NH₂ of amine).The product was a clean powder and did not require any washing with diethylether. Analysis of the NMR spectrum proved that the product was pure.

21.1.2 Synthesis of (4-CH₃- NH₂-C₅H₄NH⁺)(BF₄⁻)

0.216g (1.997mmol) of 4-methylaminopyridine powder was dissolved in 30ml of methanol and 0.30ml (4.78mmol) of HBF₄ added. The reaction was mixture stirred at room temperature for one hour. The solvent was evaporated under vacuum obtaining C₆H₉N₂ as a white powder (0.195g, 50%). The product was soluble in acetonitrile, methanol and ethanol but insoluble in THF, toluene and dichloromethane. Recrystallization was done following the solvent diffusion. The product was separately

dissolved in methanol, ethanol and acetonitrile (solvent 1) and then pentane, hexane, diethylether and toluene (solvent 2) was added. The product was a clean powder and did not require any washing with diethylether. Analysis of the NMR spectrum proved that the product was pure. ^{1}H NMR (CD$_3$CN): δ 10.78 (m,1H, N of pyridine), δ 7.94 (m,2H,C$_5$H$_4$N of pyridine), δ 6.90 (br,s,1H,NH of amine), δ 6.84,(m,2H,C$_5$H$_4$N of pyridine), δ 2.93 (d,3H,CH_3 of methyl group).

21.1.3 Synthesis of (4-SH-C$_5$H$_4$NH$^+$)(BF$_4$$^-$)

0.224g (2.015mmol) of 4- mercaptopyridine powder was dissolved in 30ml of methanol and 0.30ml (4.78mmol) of HBF$_4$ was added. The reaction mixture stirred at room temperature for one hour thirty minutes. The solvent was evaporated under vacuum and a yellowish oily product was obtained with a yield of.(0.353g, 88%). The product was oily and required washing with diethylether several times and left in the fridge over the night. Analysis of the NMR spectrum suggest a mixture of products that makes the spectrum complicated and difficult to be interpreted. Therefore, the product was not a pure one. The product was soluble in acetonitrile, methanol, ethanol and THF but insoluble in dichloromethane and toluene. Recrystallization was done following the solvent diffusion. The product was separately dissolved in methanol, ethanol and acetonitrile (solvent 1) and then pentane, hexane, diethylether and toluene (solvent 2) was added. The crystals obtained after recrystallization were analyzed and found out that they were colorless though the bulk product had a yellow colour. This further confirms that the bulk product was not pure but contains a mixture of products as earlier suggested from the NMR spectrum.

21.1.4 Synthesis of (4-OH-C$_5$H$_4$NH$^+$)(BF$_4$$^-$)

 0.194g (2.040mmol) of 4-hydroxypyridine powder was dissolved in 30ml of methanol and 0.30ml (4.78mmol) of HBF$_4$ was added. The reaction mixture was stirred at room temperature for one hour fifteen minutes. The solvent was evaporated under vacuum and the product was washed with diethylether. The product obtained was a white powder (0.419g, 112%). The high percentage yield suggests the presence of solvent or the acid

in the product. The product was soluble in acetonitrile, methanol, ethanol and THF but insoluble in dichloromethane and toluene. Recrystallization was done by separately dissolving the powdered product in methanol, ethanol and acetonitrile (solvent 1) and then pentane, hexane, diethylether and toluene (solvent 2) was added. ^{1}H NMR (CD$_3$CN): δ 10.13 (m,1H, OH or NH), δ 8.37 (m,2H, C$_5$H$_4$N of pyridine), δ 7.28 (m,2H,C$_5$H$_4$N of pyridine).

21.1.5 Synthesis of (4-CO$_2$H--C$_5$H$_4$NH$^+$)(BF$_4^-$)

0.248g (2.014mmol) of isonicotinic acid was dissolved in 30ml of methanol and 0.30ml (4.78mmol) of HBF$_4$ was added. The solution formed was cloudy but became clear upon addition of 0.30ml of HBF$_4$. The reaction mixture was stirred at room temperature for one hour. The solvent was evaporated under vacuum and the product was washed with diethylether. The product was a white powder (0.344g, 81%). The product was soluble in acetonitrile, methanol, ethanol and THF but insoluble in dichloromethane and toluene. Recrystallization was done by separately dissolving the powdered product in methanol, ethanol and acetonitrile (solvent 1) and then pentane, hexane, diethylether and toluene (solvent 2) was added. ^{1}H NMR (CD$_3$CN): δ 8.88 (m,2H, C$_5$H$_4$N of pyridine), δ 8.47 (m, 2H, C$_5$H$_4$N of pyridine).

21.1.6 Synthesis of (4-CONH$_2$-C$_5$H$_4$NH$^+$)(BF$_4^-$)

0.258g (2.113mmol) of isonicotine amide powder was dissolved in 30ml of methanol and 0.30ml (4.78mmol) of HBF$_4$ was added. The clear solution became cloudy upon addition of HBF$_4$ and the reaction mixture stirred at room temperature for one hour. The cloudy solution became clear again upon immersion in a warm water bath for the evaporation of the solvent. The product was obtained as a white powder (0.489g, 110%). The high percentage yield suggests the presence of solvent or acid in the product. The product was soluble in acetonitrile, methanol, ethanol and THF but insoluble in dichloromethane and toluene. Recrystallization was done by separately dissolving the powdered product in methanol, ethanol and acetonitrile (solvent 1) and then pentane, hexane, diethylether and toluene (solvent 2) was added. ^{1}H NMR (CD$_3$CN): δ 8.58

(m,4H,C$_5$H$_4$N of pyridine), δ 7.32 (br,s,1H,NH$_2$ of amide), δ 6.72 (br, s, 1H,NH$_2$ of amide).

21.1.7 Synthesis of (4-CSNH$_2$-C$_5$H$_4$NH$^+$)(BF$_4$$^-$)

0.280g (2.026mmol) of pyridinethioamide powder was dissolved in 30ml of methanol resulting in a yellow solution. 0.30ml (4.78mmol) of HBF$_4$ was added the yellow solution turned red. The reaction mixture was stirred at room temperature for one hour. The solvent was evaporated under vacuum and the product (0.491g,107%) obtained as an orange powder. The high percentage yield suggests the presence of either the solvent or the acid in the product. The product was soluble in acetonitrile, methanol, ethanol and THF but insoluble in dichloromethane and toluene. Recrystallization was done by separately dissolving the powdered product in methanol, ethanol and acetonitrile (solvent 1) and then pentane, hexane, diethylether and toluene (solvent 2) was added. ^{1}H NMR (CD$_3$CN): δ 8.74 (m,2H, C$_5$H$_4$N of pyridine), δ 8.21 (m,2H, C$_5$H$_4$N of pyridine).

21.2 H$_3$PO$_4$ series

21.2.1 Synthesis of (4-NH$_2$-C$_5$H$_4$NH$^+$)(H$_2$PO$_4$$^-$)

0.190g (2.109mmol) of 4-aminopyridine and 0.197g (2.010mmol) of H$_3$PO$_4$ were weighed and dissolved in 30ml of methanol. A cloudy solution was obtained which became clear upon addition of a small amount of water. The reaction mixture was stirred at room temperature for two hours. The solvent was evaporated under vacuum. The product was obtained as a white powder with a yield of 0.449g (116%). The high percentage yield suggests the presence of solvent in the product. The signal for the protonated product was not obtained from the NMR results. The yield and the absence of the pure 4-aminopyridine signal from the spectrum suggest that the reaction did occur. This reaction was repeated in water with 4-aminopyridne in excess (two to one reaction). An oily product was obtained which became powder after washing with methanol. The yield was 0.155g (54%). The NMR spectrum for this product closely

resembled that of pure 4-aminopyridine suggesting that the product might just have been excess 4-aminopyridine. Both products were soluble in water but insoluble in DCM, THF, ethanol, methanol, toluene and acetonitrile. Recrystallization was done following the solvent-layering technique. The product was separately dissolved in water (solvent 1) and then pentane, hexane, diethylether, DCM, THF, methanol, ethanol, acetonitrile and toluene (solvent 2) was added. The crystals were measured, and the results revealed that both products from the 1:1 and the 2:1 reaction have the same crystal structure as shown in figure 1 below. The product from the 2:1 reaction showed some NLO activity with Laser measurements though the signal was weak but the product from the 1:1 reaction did not show any signal. ^{1}H NMR (CD$_3$CN): δ 8.05 (m,2H,C$_5$H$_4$N of pyridine), δ 6.52 (m,2H,C$_5$H$_4$N of pyridine), δ 4.75 (br,s,2H, NH$_2$ of amine).

This structure for this compound has previously been reported in the CSD data base under the number 959235 and name SODCUS01.

21.2.2 Synthesis of (4-CH$_3$-NH$_2$-C$_5$H$_4$NH$^+$)(H$_2$PO$_4^-$)

0.138g (1.276mmol) of 4-methylaminopyridine and 0.196g (2.000mmol) of H$_3$PO$_4$ were weighed and dissolved in 30ml of methanol. The reaction mixture was stirred at room temperature for one hour forty minutes. The solvent was evaporated under vacuum. An oily product was obtained which was left in the freezer. The product remained oily and was difficult to be processed.

21.2.3 Synthesis of (4-SH-C$_5$H$_4$NH$^+$)(H$_2$PO$_4^-$)

0.225g (2.024mmol) of 4-mercaptopyridine was weighed and 0.200g (2.041mmol) of H$_3$PO$_4$ added and dissolved in 30ml of methanol. A yellow solution was obtained and stirred at room temperature for two hours thirty minutes. Evaporation of the solvent was carried out under vacuum. An oily product was obtained and left in the freezer. The product remained as an oil hence cannot be processed.

21.2.4 Synthesis of (4-OH-C$_5$H$_4$NH$^+$)(H$_2$PO$_4^-$)

0.196g (2.000mmol) of H$_3$PO$_4$ was weighed and 0.191g of 4-hydroxypyridine was added and dissolved in 30ml of methanol. The reaction mixture was stirred at room temperature for two hours. The product was obtained as a white powder after evaporation under vacuum. The yield was 0.350g (90.44%). The signal for the protonated product was not obtained from the ^{1}H NMR results. The yield and the absence of the pure 4-hydroxypyridine signal from the spectrum suggest that the reaction did occur. The product was soluble in water and methanol but insoluble in DCM, THF, ethanol, toluene and acetonitrile. Recrystallization was done following the solvent-layering technique. The product was separately dissolved in methanol, and water (solvent 1) and then pentane, hexane, diethylether, DCM, THF, ethanol, acetonitrile and toluene (solvent 2) was added. ^{1}H NMR (CD$_3$CN): δ 8.33 (m,2H, C$_5$H$_4$N of pyridine), δ 7.28 (m,2H,C$_5$H$_4$N of pyridine).

21.2.5 Synthesis of (4-CO$_2$H-C$_5$H$_4$NH$^+$)(H$_2$PO$_4^-$)

0.199g (2.031mmol) of H$_3$PO$_4$ was weighed and 0.248g of isonicotinic acid was added and dissolved in 30ml of methanol. A cloudy solution was obtained which became clear after heating in a water bath. The reaction mixture was stirred at room temperature for three hours. Evaporation was done under vacuum and the product obtained as a white powder with a yield of 0.322g (72.04%). The signal for the protonated product was not obtained from the ^{1}H NMR results. The yield and the absence of the pure isonicotinic acid signal from the spectrum suggest that the reaction had taken place. The product was soluble in water but insoluble in methanol, DCM, THF, ethanol, toluene and acetonitrile. Recrystallization was done following the solvent-layering technique. The product was dissolved in water (solvent 1) and then methanol, pentane, hexane, diethylether, DCM, THF, ethanol, acetonitrile and toluene (solvent 2) was added. ^{1}H NMR (CD$_3$CN): δ 8.95 (m,2H, C$_5$H$_4$N of pyridine), δ 8.45 (m, 2H, C$_5$H$_4$N of pyridine).

21.2.6 Synthesis of (4-CONH$_2$-C$_5$H$_4$NH$^+$)(H$_2$PO$_4^-$)

0.198g (2.021mmol) of H$_3$PO$_4$ was weighed and 0.247g of isonicotinamide was added and dissolved in 30ml of methanol. The reaction mixture was stirred at room temperature for one hour thirty minutes. Evaporation was done under vacuum and the product obtained as a white powder with a yield of 0.404g (90.79%). The product was soluble in water, methanol and ethanol but insoluble in DCM, THF, toluene and acetonitrile. The signal for the protonated product was not obtained from the ^{1}H NMR results. The yield and the absence of the pure isonicotine amide signal from the spectrum suggest that the reaction had occur. Recrystallization was done following the solvent-layering technique. The product was dissolved separately in water, methanol and ethanol (solvent 1) and then pentane, hexane, diethylether, DCM, THF, acetonitrile and toluene (solvent 2) was added. ^{1}H NMR (CD$_3$CN): δ 8.68 (m,4H,C$_5$H$_4$N of pyridine), δ 7.34 (br,s,1H,NH$_2$ of amide), δ 6.52 (br, s, 1H,NH$_2$ of amide).

21.2.7 Synthesis of (4-CSNH$_2$-C$_5$H$_4$NH$^+$)(H$_2$PO$_4^-$)

0.203g (2.072mmol) of H$_3$PO$_4$ was weighed and 0.276g of pyridinethioamide was added and dissolved in 30ml of methanol. A golden yellow solution was obtained. The reaction mixture was stirred at room temperature for two hours. Evaporation was done under vacuum and the product obtained as an orange powder with a yield of 0.540g (112.73%). The high percentage yield suggests the presence of solvent in the product. The product was soluble in water, methanol and ethanol but insoluble in DCM, THF, toluene and acetonitrile. The signal for the protonated product was not obtained from the ^{1}H NMR results. The yield and the absence of the pure 4-aminopyridine signal from the spectrum suggest that the reaction occurred. Recrystallization was done following the solvent-layering technique. The product was dissolved separately in water, methanol and ethanol (solvent 1) and then pentane, hexane, diethylether, DCM, THF, acetonitrile and toluene (solvent 2) was added. ^{1}H NMR (CD$_3$CN): δ 8.90 (m,2H, C$_5$H$_4$N of pyridine), δ 8.31 (m,2H, C$_5$H$_4$N of pyridine).

This structure has previously been reported in the CSD data base under the number 74418 and name FOWSOA

21.3 HNO₃ series

21.3.1 Synthesis of (4-NH₂-C₅H₄NH⁺)(NO₃⁻)

0.188g (2.087mmol) of 4-aminopyridine and 0.78ml (1.476mmol) of 2M HNO_3 were weighed and dissolved in 30ml of methanol. The reaction mixture was stirred at room temperature for two hours forty-five minutes. Evaporation of the solvent was done under vacuum. The product was obtained as a white powder with a yield of 0.280g (97.80%). The product was soluble in methanol, ethanol and water but insoluble in acetonitrile, toluene, THF and DCM. Recrystallization was done following the solvent-layering technique. The product was separately dissolved in methanol and ethanol (solvent 1), then pentane, hexane, diethylether and toluene was added (solvent 2). The crystal structure has previously been reported in the CSD data base under the name DATACOR. ^{1}H NMR (MeOD): δ 8.05 (m,2H,C₅H₄N of pyridine), δ 6.87(m,2H,C₅H₄N of pyridine),

21.3.2 Synthesis of (4-CH₃-NH₂-C₅H₄NH⁺)(NO₃⁻)

0.053g (0.490mmol) of 4-methylaminopyridine and 0.19ml (0.380mmol) of 2M HNO_3 were weighed and dissolved in 30ml of methanol. The reaction mixture was stirred at room temperature for two hours forty minutes. Evaporation was done under vacuum. The product was obtained as a white powder. The yield was 0.072g (93.51%). The product was soluble in methanol, ethanol, acetonitrile and water but insoluble in toluene, THF and DCM. Recrystallization was done following the solvent-layering technique. The product was separately dissolved in methanol, acetonitrile and ethanol (solvent 1), then pentane, hexane, diethylether and toluene was added (solvent 2). The crystals obtained were not good enough to be measured. ^{1}H NMR (CD₃CN): δ 7.97 (m,2H,C₅H₄N of pyridine), δ 7.205 (br,s,1H,NH of amine), δ 6.79 (m,2H,C₅H₄N of pyridine), δ 2.93 (d,3H,CH₃ of methyl group).

21.3.3 Synthesis of (4-SH-C₅H₄NH⁺)(NO₃⁻)

0.223g (2.006mmol) of 4-mercaptopyridine was weighed and 0.78ml (1.476mmol) of 2M HNO₃ was added and dissolved in 30ml of methanol. A yellow solution was obtained which was stirred at room temperature for one hour thirty minutes. Evaporation was done under vacuum and the product obtained as a yellow powder with a yield of 0.302g (94.08%). The product was soluble in methanol, ethanol, acetonitrile and water but insoluble in toluene, THF and DCM. Recrystallization was done following the solvent-layering technique. The product was separately dissolved in methanol, acetonitrile and ethanol (solvent 1), then pentane, hexane, diethylether and toluene was added (solvent 2). ^{1}H NMR (CD₃CN): δ 8.18 (m,2H, C₅H_4N of pyridine), δ 7.69 (m,2H,C₅H_4N of pyridine).

21.3.4 Synthesis of (4-OH-C₅H₄NH⁺)(NO₃⁻)

0.191g (2.008mmol) of 4-hydroxypyridine was weighed and 0.78ml (1.476mmol) of 2M HNO₃ was added and dissolved in 30ml of methanol. The reaction mixture was stirred at room temperature for two hours. The product was obtained as a grey powder after evaporation under vacuum. The yield was 0.266g (92.04%). The product was soluble in methanol and water but insoluble in DCM, THF, toluene and acetonitrile. Recrystallization was done following the solvent-layering technique with methanol as solvent 1 and pentane, hexane, acetonitrile, ethanol, diethylether, toluene, DCM,THF as solvent 2. ^{1}H NMR (CD₃CN): δ 8.49 (m,2H, C₅H_4N of pyridine), δ 7.26(m,2H,C₅H_4N of pyridine).

21.3.5 Synthesis of (4-CO₂H-C₅H₄NH⁺)(NO₃⁻)

0.246g (1.998mmol) of isonicotinic acid was weighed and 0.78ml (1.476mmol) of 2M HNO₃ was added and dissolved in 30ml of methanol by warming in a water bath. The reaction mixture was stirred at room temperature for two hours thirty minutes. Evaporation was done under vacuum and the product obtained as white powder with a

yield of 0.317g (92.15%). The product was soluble in methanol, ethanol and water but insoluble in DCM, THF, toluene and acetonitrile. Recrystallization was done following the solvent-layering technique with methanol and ethanol as solvent 1 and pentane, hexane, diethylether, toluene, as solvent 2. The crystal was measured at 170K because it exploded at 120K. The unit cell was different at 120K because the crystal exhibited phase transition at low temperatures. This crystal structure has already been reported, CSD WOUZEF. ^{1}H NMR (MeOD): δ 10.53 (m,2H, C_5H_4N of pyridine), δ 9.96 (m, 2H, C_5H_4N of pyridine).

21.3.6 Synthesis of (4-$CONH_2$-$C_5H_4NH^+$)(NO_3^-)

0.245g (2.006mmol) of isonicotinamide was weighed and 0.78ml (1.476mmol) of 2M HNO_3 was added and dissolved in 30ml of methanol. A cloudy solution was obtained which became clear upon slight warming in a water bath. The reaction mixture was stirred at room temperature for two hours. A white powder with a yield of 0.317g (92.42%) was obtained after evaporation under vacuum. The product was soluble in water and only slightly soluble in methanol but insoluble in ethanol, acetonitrile, toluene, THF and DCM. Recrystallization was done following the solvent-layering technique. The product was dissolved in water (solvent 1), then pentane, hexane, diethylether, DCM, THF, ethanol, acetonitrile and toluene (solvent 2) was added. ^{1}H NMR (MeOD): δ 8.98 (m,4H,C_5H_4N of pyridine), δ 8.32 (m,1H,NH_2 of amide).

21.3.7 Synthesis of (4-$CSNH_2$-$C_5H_4NH^+$)(NO_3^-)

0.277g (2.004mmol) of pyridinethioamide was weighed and 0.78ml (1.476mmol) of 2M HNO_3 was added and dissolved in 30ml of methanol. An orange solution was obtained which was stirred at room temperature for two hours. Evaporation was done under vacuum and the product obtained as an orange powder with a yield of 0.355g (94.67%). The product was soluble in water and methanol, slightly soluble in acetonitrile, ethanol and THF but insoluble in toluene and dichloromethane. Recrystallization was done following the solvent-layering technique. The product was dissolved in water, methanol, ethanol and acetonitrile (solvent 1) and then pentane, hexane, diethylether, DCM and

toluene (solvent 2) was added. ^{1}H NMR (MeOD): δ 10.36 (m,2H, C$_5$H$_4$N of pyridine), δ 9.69 (m,2H, C$_5$H$_4$N of pyridine).

21.4 H$_2$SO$_4$ series 1:1 reactions

21.4.1 Synthesis of (4-NH$_2$-C$_5$H$_4$NH$^+$)(HSO$_4^-$)

0.189g (2.098mmol) of 4-aminopyridine was weighed and 0.78ml (1.560mmol) of 2M H$_2$SO$_4$ was added and dissolved in 30ml of methanol. The reaction mixture was stirred at room temperature for two hours. Evaporation was done under vacuum and the product washed with diethylether. A white powder was obtained with a yield of 0.282g (82.46%). The product was soluble in water and methanol but insoluble in ethanol, acetonitrile, toluene, THF and DCM. Recrystallization was done following the solvent-layering technique with the product dissolved separately in water and methanol (solvent 1) then pentane, hexane, diethylether, toluene, acetonitrile, DCM, THF and ethanol added (solvent 2). Two crystal structures were obtained from this reaction. One of the structures obtained from the crystal analysis was abit abnormal because there were five pyridium cations to only four anions. These suggest that one of the anions must be a dianion which might have resulted from double protonation. This can be seen clearly from the S-O bond lengths in the crystal structure. The structure was noncentrosymmetric. The other structure had one sulphate dianion to two pyridium cations, one of which was disordered. ^{1}H NMR (MeOD):), δ 9.22 (m,2H,C$_5$H$_4$N of pyridine), δ 8.01 (m,2H,C$_5$H$_4$N of pyridine).

21.4.2 Synthesis of (4-SH-C$_5$H$_4$NH$^+$)(HSO$_4^-$)

0.223g (2.006mmol) of 4-mercaptopyridine was weighed and 0.78ml (1.560mmol) of 2M H$_2$SO$_4$ was added and dissolved in 30ml of methanol. A yellow solution was obtained which was stirred at room temperature for two hours. Evaporation was done under vacuum and an oily yellow product was obtained and left in the freezer for one week. A yellow sticky powder was then obtained with a yield of 0.374g (99.47%). The

product was soluble in methanol, ethanol and water but insoluble in acetonitrile, toluene, THF and DCM. The NMR spectrum was complicated and suggest a mixture of products. Recrystallization was done following the solvent-layering technique. The product was separately dissolved in methanol, water and ethanol (solvent 1), then acetonitrile, pentane, hexane, diethylether and toluene was added (solvent 2).

21.4.3 Synthesis of (4-OH-C₅H₄NH⁺)(HSO₄⁻)

0.194g (2.040mmol) of 4-hydroxypyridine was weighed and 0.78ml (1.560mmol) of 2M H_2SO_4 was added and dissolved in 30ml of methanol. The reaction mixture was stirred at room temperature for three hours. Evaporation was done under vacuum and the product washed with diethylether and obtained as white powder. The yield was 0.320g (92.22%). The product was soluble in methanol, ethanol and water but insoluble in DCM, THF, toluene and acetonitrile. Recrystallization was done following the solvent-layering technique by separately dissolving the product in methanol, ethanol and water (solvent 1) and pentane, hexane, acetonitrile, diethylether, toluene, DCM,THF added (solvent 2). The crystal structure has previously been reported in the CSD data base under the name DUJHOG. ¹H NMR (MeOD): δ 6.71 (m,2H, C₅H₄N of pyridine), δ 5.49 (m,2H,C₅H₄N of pyridine).

21.4.4 Synthesis of (4-CO₂H-C₅H₄NH⁺)(HSO₄⁻)

0.248g (2.307mmol) of isonicotinic acid was weighed and 0.78ml (1.560mmol) of 2M H_2SO_4 was added and dissolved in 30ml of methanol. The reaction mixture was stirred at room temperature for two hours. Evaporation was done under vacuum and the product was washed with diethylether and obtained as a white powder with a yield of 0.320g (79.80%). The product was soluble in methanol, ethanol and water but insoluble in DCM, THF, toluene and acetonitrile. Recrystallization was done following the solvent-layering technique by separately dissolving the product in methanol and ethanol (solvent 1) and pentane, hexane, diethylether, toluene, (solvent 2). . ¹H NMR (MeOD): δ 10.24 (m,2H, C₅H₄N of pyridine), δ 9.73 (m, 2H, C₅H₄N of pyridine). The crystal

structure has previously been reported in the CSD data base under the name BUFROK and BUFKET

21.4.5 Synthesis of (4-CONH$_2$-C$_5$H$_4$NH$^+$)(HSO$_4^-$)

0.259g (2.121mmol) of isonicotinamide was weighed and 0.78ml (1.560mmol) of 2M H$_2$SO$_4$ was added and dissolved in 30ml of methanol. A cloudy solution was obtained which became clear upon slight warming in a water bath. The reaction mixture was stirred at room temperature for two hours thirty minutes. A white powder with a yield of 0.405g (98.30%) was obtained after evaporation under vacuum. The product was soluble in water but insoluble in methanol, ethanol, acetonitrile, toluene, THF and DCM. Recrystallization was done following the solvent-layering technique. The product was dissolved in water (solvent 1) and then methanol, pentane, hexane, diethylether, DCM, THF, ethanol, acetonitrile and toluene (solvent 2) was added. The crystal structure has previously been reported at room temperature in the CSD data base under the name HILLY. ^{1}H NMR (D$_2$O): δ 9.11 (m,2H,C$_5$*H*$_4$N of pyridine), δ 8.43 (m,2H,C$_5$*H*$_4$N of pyridine).

21.4.6 Synthesis of (4-CSNH$_2$-C$_5$H$_4$NH$^+$)(HSO$_4^-$)

0.203g (1.469mmol) of 4-pyridinethioamide was weighed and 0.78ml (1.560mmol) of 2M H$_2$SO$_4$ was added and dissolved in 30ml of methanol. An orange solution was obtained which was stirred at room temperature for one hour. Evaporation was done under vacuum and the product obtained as an orange powder with a yield of 0.350g (98.31%). The product was soluble in water, methanol, acetonitrile, ethanol but insoluble in THF, toluene and dichloromethane. Recrystallization was done following the solvent-layering technique. The product was separately dissolved in water, methanol, ethanol and acetonitrile (solvent 1) and then pentane, hexane, diethylether, DCM and toluene (solvent 2) was added. ^{1}H NMR (CD$_3$CN): δ 8.75 (m,2H, C$_5$*H*$_4$N of pyridine), δ 8.20 (m,2H, C$_5$*H*$_4$N of pyridine).

21.5 H$_2$SO$_4$ series 2:1 reactions

21.5.1 Synthesis of (4-NH$_2$-C$_5$H$_4$NH$^+$)(SO$_4$$^{2-}$)

0.189g (2.098mmol) of 4-aminopyridine was weighed and 0.39ml (0.780mmol) of 2M H$_2$SO$_4$ was added and dissolved in 30ml of methanol. The reaction mixture was stirred at room temperature for three hours twenty-five minutes. Evaporation was done under vacuum and the product washed with diethylether. A white powder was obtained with a yield of 0.252g (94.92%). The product was soluble in water and methanol but insoluble in ethanol, acetonitrile, toluene, THF and DCM. Recrystallization was done following the solvent-layering technique with the product dissolved separately in water and methanol (solvent 1) then pentane, hexane, diethylether, toluene, acetonitrile, DCM, THF and ethanol added (solvent 2). ^{1}H NMR (CD$_3$CN):), δ 7.94 (m,2H,C$_5$$H$$_4$N of pyridine), δ 6.84 (m,2H,C$_5$$H$$_4$N of pyridine).

21.5.2 Synthesis of (4-SH-C$_5$H$_4$NH$^+$)(SO$_4$$^{2-}$)

0.223g (2.006mmol) of 4-mercaptopyridine was weighed and 0.39ml (0.78mmol) of 2M H$_2$SO$_4$ was added and dissolved in 30ml of methanol. A yellow solution was obtained which was stirred at room temperature for three hours. Evaporation was done under vacuum and an oily yellow product was obtained and left in the freezer for two weeks. The product remained oily and was difficult to be processed.

21.5.3 Synthesis of (4-OH-C$_5$H$_4$NH$^+$)(SO$_4$$^{2-}$)

0.194g (2.040mmol) of 4-hydroxypyridine was weighed and 0.39ml (0.78mmol) of 2M H$_2$SO$_4$ was added and dissolved in 30ml of methanol. The reaction mixture was stirred at room temperature for two hours. Evaporation was done under vacuum and the product obtained as white powder with a yield of 0.225g (83.18%). The product was soluble in methanol and water but insoluble in ethanol, DCM, THF, toluene and acetonitrile.

Recrystallization was done following the solvent-layering technique by separately dissolving the product in methanol and water (solvent 1) and ethanol, pentane, hexane, acetonitrile, diethylether, toluene, DCM,THF (solvent 2). ^{1}H NMR (MeOD): δ 8.22 (m,2H, C$_5$H$_4$N of pyridine), δ 6.98 (m,2H,C$_5$H$_4$N of pyridine).

21.5.4 Synthesis of (4-CO$_2$H-C$_5$H$_4$NH$^+$)(SO$_4^{2-}$)

0.248g (2.307mmol) of isonicotinic acid was weighed and 0.39ml (0.78mmol) of 2M H$_2$SO$_4$ was added and dissolved in 30ml of methanol. The reaction mixture was stirred at room temperature for two hours in a warm water bath. Evaporation was done under vacuum and the product obtained as a white powder with a yield of 0.330g (101.69%). The product was only soluble in water but insoluble in methanol, ethanol, DCM, THF, toluene and acetonitrile. Recrystallization was done following the solvent-layering technique by separately dissolving the product in water (solvent 1) and methanol, ethanol, pentane, hexane, diethylether, toluene, (solvent 2) added. ^{1}H NMR (D$_2$O): δ 9.01 (m,2H, C$_5$H$_4$N of pyridine), δ 8.52 (m, 2H, C$_5$H$_4$N of pyridine).

21.5.5 Synthesis of (4-CONH$_2$-C$_5$H$_4$NH$^+$)(SO$_4^{2-}$)

0.259g (2.121mmol) of isonicotinamide was weighed and 0.39ml (0.78mmol) of 2M H$_2$SO$_4$ was added and dissolved in 30ml of methanol. A cloudy solution was obtained which became clear upon slight warming in a water bath. The reaction mixture was stirred at room temperature for two hours. A white powder with a yield of 0.312g (93.00%) was obtained after evaporation under vacuum. The product was soluble in water and methanol but insoluble in ethanol, acetonitrile, toluene, THF and DCM. Recrystallization was done following the solvent-layering technique. The product was dissolved in water and methanol (solvent 1) and then pentane, hexane, diethylether, DCM, THF, ethanol, acetonitrile and toluene (solvent 2) was added. ^{1}H NMR (MeOD): δ 8.91 (m,2H,C$_5$H$_4$N of pyridine), δ 8.19 (m,2H,C$_5$H$_4$N of pyridine).

21.5.6 Synthesis of (4-CSNH$_2$-C$_5$H$_4$NH$^+$)(SO$_4$$^{2-}$)

0.203g (1.469mmol) of 4-pyridinethioamide was weighed and 0.39ml (0.78mmol) of 2M H$_2$SO$_4$ was added and dissolved in 30ml of methanol. An orange solution was obtained which was stirred at room temperature for one hour forty minutes. Evaporation was done under vacuum and the product obtained as an orange powder with a yield of 0.333g (119.14%). The product was soluble in water, methanol and ethanol but insoluble in acetonitrile, THF, toluene and dichloromethane. Recrystallization was done following the solvent-layering technique. The product was separately dissolved in water, methanol and ethanol (solvent 1) then acetonitrile, pentane, hexane, diethylether, DCM and toluene (solvent 2) was added. ^{1}H NMR (MeOD): δ 8.81 (m,2H, C$_5$*H*$_4$N of pyridine), δ 8.11 (m,2H, C$_5$*H*$_4$N of pyridine).

Similar reactions were carried out using the same ligands with KH$_2$PO$_4$ and acetic acid. However, no reaction actually occurred though one structure was obtained with acetic acid and 4-aminopyridine as reported below.

21.6 Synthesis of (4-NH$_2$-C$_5$H$_4$NH$^+$)(CH$_3$COO$^-$)

0.189g (2.098mmol) of 4-aminopyridine powder was dissolved in 30ml of methanol and 0.13ml (5.25mmol) of acetic acid added. The reaction mixture was stirred at room temperature for two hours thirty minutes. The solvent was evaporated under vacuum and the product obtained as a white powder (0.312g, 70%). The product was soluble in acetonitrile, methanol, ethanol and THF but insoluble in dichloromethane and toluene. Recrystallization was done following the solvent diffusion. The product was separately dissolved in methanol, ethanol and acetonitrile (solvent 1) and then pentane, hexane, diethylether and toluene (solvent 2) was added. ^{1}H NMR (CD$_3$CN): δ 11.36 (b,1H,N*H* of pyridine), δ 8.06 (m,2H,C$_5$*H*$_4$N of pyridine), δ 6.66 (m,2H,C$_5$*H*$_4$N of pyridine), δ 5.60 (br,s,2H, N*H*$_2$ of amine). The NMR spectrum and the yield suggest that the reaction did occur.

References

(1) Dhanuskodi, S.; Vasantha, K. Structural, Thermal and Optical Characterizations of a NLO Material: L-Alaninium Oxalate. *Cryst. Res. Technol.* **2004**, *39* (3), 259–265.

(2) Nalwa, H. S.; Miyata, S. *Nonlinear Optics of Organic Molecules and Polymers*; CRC Press, 1997.

(3) Chemla, D. S. *Nonlinear Optical Properties of Organic Molecules and Crystals V1.*; Elsevier Science, 1987.

(4) Yu, J.; Cui, Y.; Wu, C.; Yang, Y.; Wang, Z.; O'Keeffe, M.; Chen, B.; Qian, G. Second-Order Nonlinear Optical Activity Induced by Ordered Dipolar Chromophores Confined in the Pores of an Anionic Metal-Organic Framework. *Angew. Chemie Int. Ed.* **2012**, *51* (42), 10542–10545.

(5) Britto Dhas, S. A. M.; Natarajan, S. Growth and Characterization of L-Prolinium Tartrate – A New Organic NLO Material. *Cryst. Res. Technol.* **2007**, *42* (5), 471–476.

(6) Fleck, M.; Petrosyan, A. M. Difficulties in the Growth and Characterization of Non-Linear Optical Materials: A Case Study of Salts of Amino Acids. *J. Cryst. Growth* **2010**, *312* (15), 2284–2290.

(7) Second Harmonic Generation https://newton.ex.ac.uk/research/biomedical-old/multiphoton/advantages/shg.html (accessed Mar 26, 2018).

(8) Hobden, M. V. Phase-Matched Second-Harmonic Generation in Biaxial Crystals. *J. Appl. Phys.* **1967**, *38* (11), 4365–4372.

(9) Hora, H. Y. R. Shen, The Principles of Nonlinear Optics, John Wiley & Sons, New York, 1984, 576 Pages. *Laser Part. Beams* **1986**, *4* (2), 318.

(10) Byer, R. L. Nonlinear Optical Phenomena in Oxides and Application to a Tunable Coherent Spectrometer. *J. Solid State Chem.* **1975**, *12* (3–4), 156–171.

(11) Chao, T.-L.; Chang, W.-J.; Wen, S.-H.; Lin, Y.-Q.; Chang, B.-C.; Lii, K.-H. Titanosilicates with Strong Phase-Matched Second Harmonic Generation Responses. *J. Am. Chem. Soc.* **2016**, *138* (29), 9061–9064.

(12) Ding, Y. J.; Kang, J. U.; Khurgin, J. B. Theory of Backward Second-Harmonic and Third-Harmonic Generation Using Laser Pulses in Quasi-Phase-Matched Second-Order Nonlinear Medium. *IEEE J. Quantum Electron.* **1998**, *34* (6), 966–974.

(13) Rose, A.; Smith, D. R. Overcoming Phase Mismatch in Nonlinear Metamaterials [Invited]. *Opt. Mater. Express* **2011**, *1* (7), 1232.

(14) Yu, J.; Cui, Y.; Wu, C.; Yang, Y.; Wang, Z.; O'Keeffe, M.; Chen, B.; Qian, G. Second-Order Nonlinear Optical Activity Induced by Ordered Dipolar Chromophores Confined in the Pores of an Anionic Metal-Organic Framework. *Angew. Chemie Int. Ed.* **2012**, *51* (42), 10542–10545.

(15) Pfitzner, A.; Baumann, F.; Kaim, W. TeS2.− Radical Anions in CuBrCu1.2TeS2. *Angew. Chemie Int. Ed.* **1998**, *37* (13–14), 1955–1957.

(16) He, J.; Zeller, M.; Hunter, A. D.; Xu, Z. White Light Emission and Second Harmonic

Generation from Secondary Group Participation (SGP) in a Coordination Network. *J. Am. Chem. Soc.* **2012**, *134* (3), 1553–1559.

(17) Boyd, G. D.; Ashkin, A. Theory of Parametric Oscillator Threshold with Single-Mode Optical Masers and Observation of Amplification in LiNb O 3. *Phys. Rev.* **1966**, *146* (1), 187–198.

(18) Zhang, B.; Zhao, Y.-M.; Yong, G.-P. Phosphorescence, near-Infrared Absorption and Nonlinear Optical Property of a New Chiral Organic Crystal. *Funct. Mater. Lett.* **2014**, *7* (2), 1450011.

(19) Britto Dhas, S. A. M.; Natarajan, S. Growth and Characterization of L-Prolinium Tartrate – A New Organic NLO Material. *Cryst. Res. Technol.* **2007**, *42* (5), 471–476.

(20) Materials Research Society., T.; ScienceDirect (Online service), P. *Materials Letters.*; North-Holland, 1982.

(21) Bosshard, C. *Organic Nonlinear Optical Materials*; Gordon and Breach, 1995.

(22) Fejer, M. M.; Magel, G. A.; Jundt, D. H.; Byer, R. L. Quasi-Phase-Matched Second Harmonic Generation: Tuning and Tolerances. *IEEE J. Quantum Electron.* **1992**, *28* (11), 2631–2654.

(23) Dhanuskodi, S.; Vasantha, K. Structural, Thermal and Optical Characterizations of a NLO Material: L-Alaninium Oxalate. *Cryst. Res. Technol.* **2004**, *39* (3), 259–265.

(24) SOHLER, W. Second-Order Nonlinear Guided Wave Interactions. *Mod. Probl. Condens. Matter Sci.* **1991**, *29*, 1–71.

(25) Midwinter, J. E.; Warner, J. The Effects of Phase Matching Method and of Uniaxial Crystal Symmetry on the Polar Distribution of Second-Order Non-Linear Optical Polarization. *Br. J. Appl. Phys.* **1965**, *16* (8), 1135–1142.

(26) Verbiest, T.; Houbrechts, S.; Kauranen, M.; Clays, K.; Persoons, A. Second-Order Nonlinear Optical Materials: Recent Advances in Chromophore Design. *J. Mater. Chem* **1997**, *7* (11), 2175–2189.

(27) An Overview of Nonlinear Optics, Crystal Growth and Characterization Techniques.

(28) Halasyamani, P. S.; Zhang, W. Viewpoint: Inorganic Materials for UV and Deep-UV Nonlinear-Optical Applications. **2017**.

(29) Saravana Kumar, G.; Murugakoothan, P. Synthesis, Spectral Analysis, Optical and Thermal Properties of New Organic NLO Crystal: N,N'-Diphenylguanidinium Nitrate (DPGN). *Spectrochim. Acta Part A Mol. Biomol. Spectrosc.* **2014**, *131*, 17–21.

(30) Kanis, D. R.; Ratner, M. A.; Marks', T. J. Design and Construction of Molecular Assemblies with Large Second-Order Optical Nonlinearities. *Quantum Chemical Aspects*; 1994; Vol. 94.

(31) Di Bella, S.; Ratner, M. A.; Marks, T. J. Design of Chromophoric Molecular Assemblies with Large Second-Order Optical Nonlinearities. A Theoretical Analysis of the Role of Intermolecular Interactions; *J. Am. Chem. Soc.* **1992**; *114,* 5842-5849.

(32) Liu, X.; Yang, Z.; Wang, D.; Cao, H.; Liu, X.; Yang, Z.; Wang, D.; Cao, H. Molecular Structures and Second-Order Nonlinear Optical Properties of Ionic Organic Crystal Materials. *Crystals* **2016**, *6* (12), 158.

(33) Smith, G.; Wermuth, U. D. Guanidinium 3-Nitro-Benzoate. *Acta Crystallogr. Sect. E. Struct. Rep. Online* **2010**, *66* (Pt 8), o1946.

(34) Ray, P. C. Size and Shape Dependent Second Order Nonlinear Optical Properties of Nanomaterials and Their Application in Biological and Chemical Sensing. *Chem. Rev.* **2010**, *110* (9), 5332–5365.

(35) Liu, X.; Yang, Z.; Wang, D.; Cao, H. Molecular Structures and Second-Order Nonlinear Optical Properties of Ionic Organic Crystal Materials. 2016.

(36) Jen, S.-H.; Gonella, G.; Dai, H.-L. The Effect of Particle Size in Second Harmonic Generation from the Surface of Spherical Colloidal Particles. I: Experimental Observations †.

(37) Thirupugalmani, K.; Karthick, S.; Shanmugam, G.; Kannan, V.; Sridhar, B.; Nehru, K.; Brahadeeswaran, S. Second- and Third-Order Nonlinear Optical and Quantum Chemical Studies on 2-Amino-4-Picolinium-Nitrophenolate-Nitrophenol: A Phasematchable Organic Single Crystal. *Opt. Mater. (Amst).* **2015**, *49*, 158–170.

(38) Evans, C.C.; Bagieu-Beucher, M.; Masse, R. and Nicoud, J.-F. Nonlinearity Enhancement by Solid-State Proton Transfer: A New Strategy for the Design of Nonlinear Optical Materials. *Chem. Mater.* **1998**, *10*, 847-854.

(39) Srinivasan, P.; Vidyalakshmi, Y.; Gopalakrishnan, R. Studies on the Synthesis, Growth, Crystal Structure, and Nonlinear Optical Properties of a Novel Nonlinear Optical Crystal: L -Argininium-4-Nitro Phenolate Monohydrate (LARP). *Cryst. Growth Des.* **2008**, *8* (7), 2329–2334.

(40) Karabacak, M.; Yilan, E. Molecular Structure, Spectroscopic (FT-IR, FT-Raman, 13C and 1H NMR, UV), Polarizability and First-Order Hyperpolarizability, HOMO and LUMO Analysis of 4'-Methylbiphenyl-2-Carbonitrile. *Spectrochim. Acta Part A Mol. Biomol. Spectrosc.* **2012**, *87*, 273–285.

(41) Devi, T. U.; Lawrence, N.; Babu, R. R.; Ramamurthi, K.; Bhagavannarayana, G. *Studies on L-Valinium Picrate Single Crystal: A Promising NLO Crystal*; 2009; Vol. 8.

(42) Srinivasan, P.; Kanagasekaran, T.; Gopalakrishnan, R. A Highly Efficient Organic Nonlinear Optical Donor−Acceptor Single Crystal: L -Valinium Picrate. *Cryst. Growth Des.* **2008**, *8* (7), 2340–2345.

(43) Aramburu, I.; Ortega, J.; Folcia, C. L.; Etxebarria, J.; Illarramendi, M. A.; Breczewski, T. Accurate Determination of Second Order Nonlinear Optical Coefficients from Powder Crystal Monolayers Related Articles Accurate Determination of Second Order Nonlinear Optical Coefficients from Powder Crystal Monolayers. *Addit. Inf. J. Appl. Phys. V C* **2011**, *109*, 74313.

(44) Hinchliffe, A. *Chemical Modelling : Applications and Theory. Vol. 1, A Review of the Literature Published up to June 1999*; Royal Society of Chemistry, 2000.

(45) Alfaify, S.; Shkir, M.; Arora, M.; Irfan, A.; Algarni, H.; Abbas, H.; Muhammad, S.; Al-Sehemi, A. G. *Molecular Structure, Vibrational, Photophysical and Nonlinear Optical Properties of L-Threoninium Picrate: A First-Principles Study*.

(46) Ramya, K.; Raja, C. R. Studies on the Growth and Characterization of L-Arginine Maleate Dihydrate Crystal Grown from Liquid Diffusion Technique. *J. Miner. Mater. Charact. Eng.* **2016**, *04* (02), 143–153.

(47) Vasantha, K.; Dhanuskodi, S. Single Crystal Growth and Characterization of Phase-Matchable l-Arginine Maleate: A Potential Nonlinear Optical Material. *J. Cryst. Growth* **2004**, *269*, 333–341.

(48) *GROWTH AND CHARACTERIZATION OF L-ALANINIUM MALEATE SINGLE CRYSTALS 6.1*

Introduction.

(49) Natarajan, S.; Britto, S. A. M.; Ramachandran, E. Growth, Thermal, Spectroscopic, and Optical Studies of L-Alaninium Maleate, a New Organic Nonlinear Optical Material. **2006**.

(50) Balasubramanian, D.; Jayavel, R.; Murugakoothan, P. Studies on the Growth Aspects of Organic L-Alanine Maleate: A Promising Nonlinear Optical Crystal. *Nat. Sci.* **2009**, *01* (03), 216–221.

(51) Thukral, K.; Vijayan, N.; Singh, B.; Bdikin, I.; Haranath, D.; Maurya, K. K.; Philip, J.; Soumya, H.; Sreekanth, P.; Bhagavannarayana, G. Growth, Structural and Mechanical Analysis of a Single Crystal of l -Prolinium Tartrate: A Promising Material for Nonlinear Optical Applications. *CrystEngComm* **2014**, *16* (39), 9245–9254.

(52) Padmaja, L.; Vijayakumar, T.; Hubert Joe, I.; Reghunadhan Nair, C. P.; Jayakumar, V. S. Vibrational Spectral Studies and the Non-Linear Optical Properties of a Novel NLO Material: L-Prolinium Tartrate. *J. Raman Spectrosc.* **2006**, *37* (12), 1427–1441.((

(53) Siva, V.; Kumar, S. S.; Shameem, A.; Raja, M.; Athimoolam, S.; Bahadur, S. A. Structural, Spectral, Quantum Chemical and Thermal Studies on a New NLO Crystal: Guanidinium Cinnamate. *J. Mater. Sci. Mater. Electron.* **2017**, *28* (17), 12484–12496.

(54) Arumanayagam, T.; Murugakoothan, P. Studies on Optical and Mechanical Properties of New Organic NLO Crystal: Guanidinium 4-Aminobenzoate (GuAB). *Mater. Lett.* **2011**, *65* (17–18), 2748–2750.

(55) Chen, L.-Z. Nicotinium Hydrogen Sulfate. *Acta Crystallogr. Sect. E Struct. Reports Online* **2009**, *65* (10), o2350–o2350.

(56) Chen, L.-Z. Isonicotinium Hydrogen Sulfate. *Acta Crystallogr. Sect. E Struct. Reports Online* **2009**, *65* (10), o2349–o2349.

(57) Athimoolam, S.; Rajaram, R. K. Dinicotinium Sulfate. *Acta Crystallogr. Sect. E Struct. Reports Online* **2005**, *61* (8), o2764–o2767.

(58) Hursthouse, M. B.; Montis, R.; Niitsoo, L.; Sarson, J.; Threlfall, T. L.; Asiri, A. M.; Khan, S. A.; Obaid, A. Y.; Al-Harbi, L. M. Anhydrates and/or Hydrates in Nitrate, Sulphate and Phosphate Salts of 4-Aminopyridine, (4-AP) and 3,4-Diaminopyridine (3,4-DAP): The Role of the Water Molecules in the Hydrates. *CrystEngComm* **2014**, *16* (11), 2205.

(59) Zahid, M.; Khawar Rauf, M.; Bolte, M.; Hameed, S.; IUCr. Adamantane-1-Thioamide. *Acta Crystallogr. Sect. E Struct. Reports Online* **2009**, *65* (8), o1891–o1891.

Appendix I. Crystallographic tables

Table 11 Crystallographic data for 4-Me-APYH$^+$ BF$_4$$^{-b}$, 4-MerPyH$^+$ BF$_4$$^{-b}$, 4-HydPyH$^+$ BF$_4$$^{-b}$, IsonicAcidH$^+$ BF$_4$$^{-b}$, IsonicAmideH$^+$ BF$_4$$^{-b}$ and PyThioAmideH$^+$ BF$_4$$^{-b}$

	4-Me-APYH$^+$ BF$_4$$^{-b}$	4-MerPyH$^+$ BF$_4$$^{-b}$	4-HydPyH$^+$ BF$_4$$^{-b}$	IsonicAcidH$^+$ BF$_4$$^{-b}$	IsonicAmideH$^+$ BF$_4$$^{-b}$	PyThioAmideH$^+$ BF$_4$$^{-b}$
formula	C$_6$ H$_9$ B F$_4$ N$_2$	C$_5$ H$_6$ B F$_4$ N S	C$_5$ H$_6$ B F$_4$ N O	C$_6$ H$_6$ B F$_4$ N O$_2$	C$_6$ H$_7$ B F$_4$ N$_2$ O	C$_6$ H$_7$ B F$_4$ N$_2$ S
Fw	195.96	198.98	182.92	210.93	209.95	226.01
cryst. system	Orthorhombic	Monoclinic	Monoclinic	Monoclinic	Monoclinic	Monoclinic
space group	P b c a	P2$_1$/c	P2$_1$/c	P2$_1$/c	C 1 c 1	P2$_1$/c
a [Å]	14.493(3)	5.2607(11)	5.2190(10)	5.3902(11)	5.1016(10)	9.873(2)
b [Å]	13.542(3)	17.339(4)	14.616(3)	13.424(3)	23.720(5)	8.4385(18)
c [Å]	17.355(4)	9.0150(18)	9.4747(19)	11.453(2)	7.3591(15)	11.328(2)
α [°]	90	90	90	90	90	90
β [°]	90	101.80(3)	102.16(3)	816.2(3)	109.80(3)	105.86(3)
γ [°]	90	90	90	90	90	90
V [Å^3]	3406.4(12)	804.9(3)	706.5(3)	816.2(3)	837.9(3)	907.9(3)
Z	16	4	4	4	4	4
T, °C	170	170	170	170	170	170
ρ_{calcd} [g cm^{-3}]	1.528	1.642	1.720	1.717	1.664	1.653
μ(Mo Kα) [mm^{-1}]	0.153	0.410	0.185	0.181	0.171	0.378

crystal size [mm^3]	0.22 0.16, 2.04	0.2,0.04,0.2	0.38, 0.2, 0.04	0.56, 0.48, 0.24	0.3, 0.24, 0.2	0.32, 0.2, 0.16
F(000)	1600	400	368	424	424	456
θ range, deg	2.347-25.022	2.349-25.026	2.603, 25.024	2.358-25.027	3.407-25.022	2.144-25.018
reflns. collected	14792	5434	2821	4130	2504	4969
unique reflns.	1637	850	998	1244	1162	1446
R_{int}	0.1148	0.0727	0.0330	0.0234	0.0186	0.0229
reflns [I>2σ(I)]	2998	1432	1250	1435	1176	1594
R$_1$ [I>2σ(I)][c]	0.1200	0.0760	0.0524	0.0529	0.0279	0.0287
wR_2 (all data)[d]	0.3287	0.1516	0.1078	0.1281	0.0691	0.0721
GOF on F^2	1.054	1.164	1.070	1.072	1.079	1.073
completeness	0.997	0.999	1.070	0.996	0.992	0.994

[a] λ (CuKα) = 1.54184 Å. [b] λ (MoKα) = 0.71073 Å. [c] $R_1 = \Sigma ||F_o|-|F_c||/ \Sigma |F_o|$. [d] $wR_2 = [\Sigma w(F_o^2-F_c^2)^2/\Sigma wF_o^4]^{1/2}$.

Table 12 Crystallographic data for 4-APYH$^+$ H$_2$PO$_4^{-b}$, 4-HydPyH$^+$ H$_2$PO$_4^{-b}$, IsonicAcidH$^+$ *H$_2$PO$_4^{-b}$*, IsonicAmideH$^+$ H$_2$PO$_4^{-b}$, PyThioAmideH$^+$ H$_2$PO$_4^{-b}$

	4-APYH$^+$H$_2$PO$_4^{-b}$	4-HydPyH$^+$ H$_2$PO$_4^{-b}$	IsonicAcidH$^+$ H$_2$PO$_4^{-b}$	IsonicAmideH$^+$ H$_2$PO$_4^{-b}$	PyThioAmideH$^+$ H$_2$PO$_4^{-b}$
formula	C$_5$ H$_{11}$ N$_2$ O$_5$ P	C$_5$ H$_8$ N O$_5$ P	C$_6$ H$_6$ B F$_4$ N O$_2$	C$_6$ H$_9$ N$_2$ O$_5$ P	C$_{12}$ H$_{21}$ N$_4$ O$_{12}$ P$_3$ S$_2$
Fw	210.13	193.09	221.10	220.12	570.36
cryst. system	Triclinic	orthorhombic	Monoclinic	Monoclinic	Monoclinic
space group	P -1	P b c a	C2/c	C 1 c 1	C2/c
a [Å]	7.2785(4)	6.8401(14)	16.3686(9)	4.7730(10)	24.526(5)
b [Å]	7.9141(4)	13.099(3)	4.7806(2)	23.609(5)	8.1216(16)
c [Å]	8.9022(6)	17.835(4)	23.2260(11)	8.2782(17)	11.359(2)
α [°]	77.651(6)	90	90	90	90
β [°]	71.756(5)	90	92.777(5)	105.57(3)	101.50(3)
γ [°]	67.405(5)	90	90	90	90
V [Å^3]	447.07(4)	1598.0(6)	1815.34(15)	902.8(3)	2217.2(8)
Z	2	8	8	4	4
T, °C	120(2)	170	120.00(10)	170	170
ρ$_{calcd}$ [g cm^{-3}]	1.561	1.605	1.618	1.619	1.709
μ(Mo Kα) [mm^{-1}]	0.302	0.328	0.308	0.304	0.526
crystal size [mm^3]	0.38, 0.28, 0.25	0.22, 0.16, 0.04	0.205,0.134,0.092	0.42, 0.22, 0.04	0.2, 0.16, 0.08
F(000)	220	800	912	456	1176

θ range, deg	3.14-27.44	2.284-24.998	2.492- 25.024	3.073-25.004	2.647-25.025
reflns. collected	5766	10376	6008	2414	5960
unique reflns.	1842	1191	1569	1153	1614
R_{int}	0.0122	0.0491	0.0491	0.0286	0.0482
reflns [$I>2\sigma(I)$]	2031	1408	1649	1186	1962
R_1 [$I>2\sigma(I)$][c]	0.0270	0.0370	0.1180	0.0323	0.0437
wR_2 (all data)[d]	0.0791	0.0866	0.3759	0.0723	0.1024
GOF on F^2	1.147	1.094	1.848	1.078	1.077
completeness	0.997	0.999	0.999	0.995	0.999

[a] λ (CuKα) = 1.54184 Å. [b] λ (MoKα) = 0.71073 Å. [c] $R_1 = \Sigma ||F_o|-|F_c|| / \Sigma |F_o|$. [d] $wR_2 = [\Sigma w(F_o^2-F_c^2)^2/\Sigma wF_o^4]^{1/2}$.

Table 13 Crystallographic data for 4-APYH$^+$ NO$_3^{-b}$, 4-Me-APYH$^+$ NO$_3^{-a}$, 4-HydPyH$^+$ NO$_3^{-b}$, IsonicAcidH$^+$ NO$_3^{-a}$, IsonicAmideH$^+$ NO$_3^{-b}$ and PyThioAmideH$^+$ NO$_3^{-b}$

	4-APYH$^+$ NO$_3^{-b}$	4-Me-APYH$^+$ NO$_3^{-a}$	4-HydPyH$^+$ NO$_3^{-b}$	IsonicAcidH$^+$ NO$_3^{-a}$	IsonicAmideH$^+$ NO$_3^{-b}$	PyThioAmideH$^+$ NO$_3^{-b}$
formula	C$_5$H$_7$N$_3$O$_3$	C$_6$H$_9$N$_3$O$_3$	C$_5$H$_6$N$_2$O$_4$	C$_6$H$_6$N$_2$O$_5$	C$_6$H$_7$N$_3$O$_4$	C$_6$H$_7$N$_3$O$_3$S
Fw	157.14	171.16	158.12	186.13	185.15	201.21
cryst. system	Monoclinic	Orthorhombic	Triclinic	Monoclinic	Monoclinic	Monoclinic
space group	P2$_1$/C$_1$	Pmna	P$_1$	P2$_1$/n$_1$	P2$_1$/n$_1$	P2$_1$/C$_1$
a [Å]	9.1734(3)	10.0342(3)	3.6168(5)	6.6774(2)	12.4131(3)	12.3880(3)
b [Å]	6.9225(3)	6.2314(2)	9.2803(14)	8.1740(2)	10.0323(2)	3.71920(10)
c [Å]	10.8271(4)	12.8549(5)	9.887(2)	14.1384(4)	24.8669(5)	18.2157(5)
α [°]	90	90	95.209(14)	90	90	90
β [°]	93.624(4)	90	94.040(13)	90.612(2)	95.271(2)	105.69(3)
γ [°]	90	90	91.332(11)	90	90	90
V [Å^3]	686.18(5)	803.78(5)	329.52(10)	771.64(4)	3083.63(12)	807.97(4)
Z	4	4	2	4	16	4
T, °C	120.01(10)	120.01(10)	120.01(10)	170.01(10)	119.96(11)	120.00(10)
ρ$_{calcd}$ [g cm^{-3}]	1.521	1.414	1.594	1.602	1.595	1.654
μ(Mo Kα) [mm^{-1}]	0.127	0.984	0.140	1.249	0.136	0.337
crystal size [mm^3]	0.56,0.14,0.12	0.3,0.125,0.033	0.236,0.72,0.27	0.205,0.164,0.11	0.288,0.234,0.175	0.548,0.313,0.226
F(000)	328	360	164	384	1536	416

θ range, deg	2.225-25.026	5.593-66.533	2.074-25.015	6.254-66.554	2.190-25.025	2.323-25.022
reflns. collected	2424	1711	2099	2877	12150	2884
unique reflns.	1037	707	1573	1203	4605	1322
R_{int}	0.0149	0.0197	0.0238	0.0183	0.0191	0.0201
reflns [$I>2\sigma(I)$]	1209	777	1719	1353	5415	1432
R_1 [$I>2\sigma(I)$][c]	0.0367	0.0357	0.0642	0.0351	0.0363	0.0301
wR_2 (all data)[d]	0.1000	0.0966	0.1775	0.1001	0.0972	0.0761
GOF on F^2	1.121	1.101	1,080	1.054	1.056	1.070
completeness	0.999	0.996	0.997	0.996	0.997	0.999

[a] λ (CuKα) = 1.54184 Å. [b] λ (MoKα) = 0.71073 Å. [c] $R_1 = \Sigma||F_o|-|F_c||/ \Sigma|F_o|$. [d] $wR_2 = [\Sigma w(F_o^2-F_c^2)^2/\Sigma wF_o^4]^{\frac{1}{2}}$.

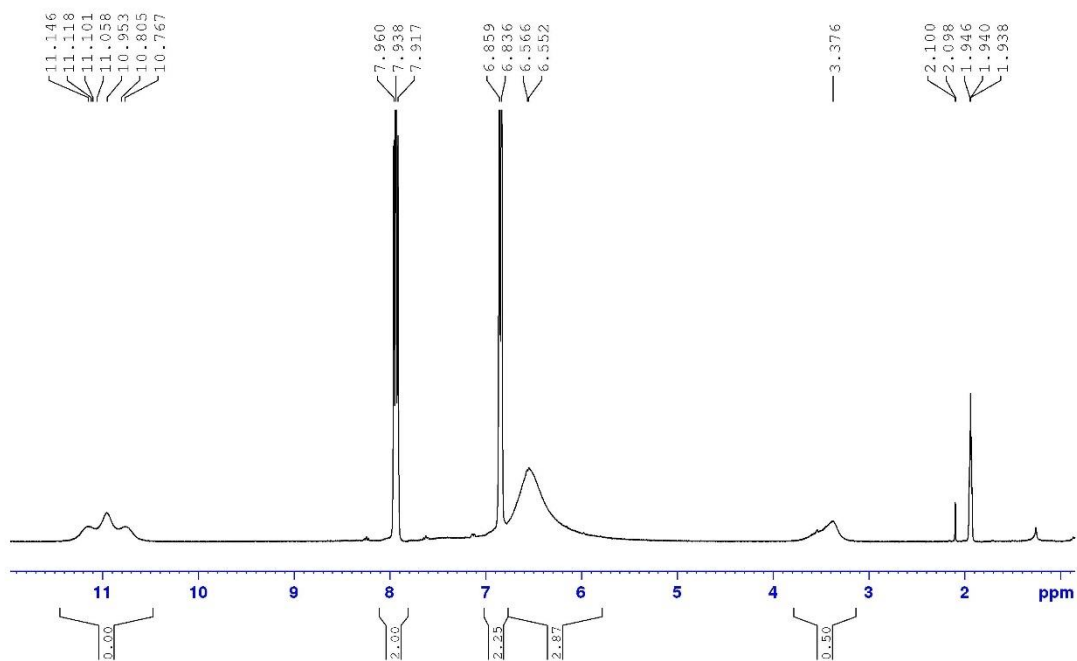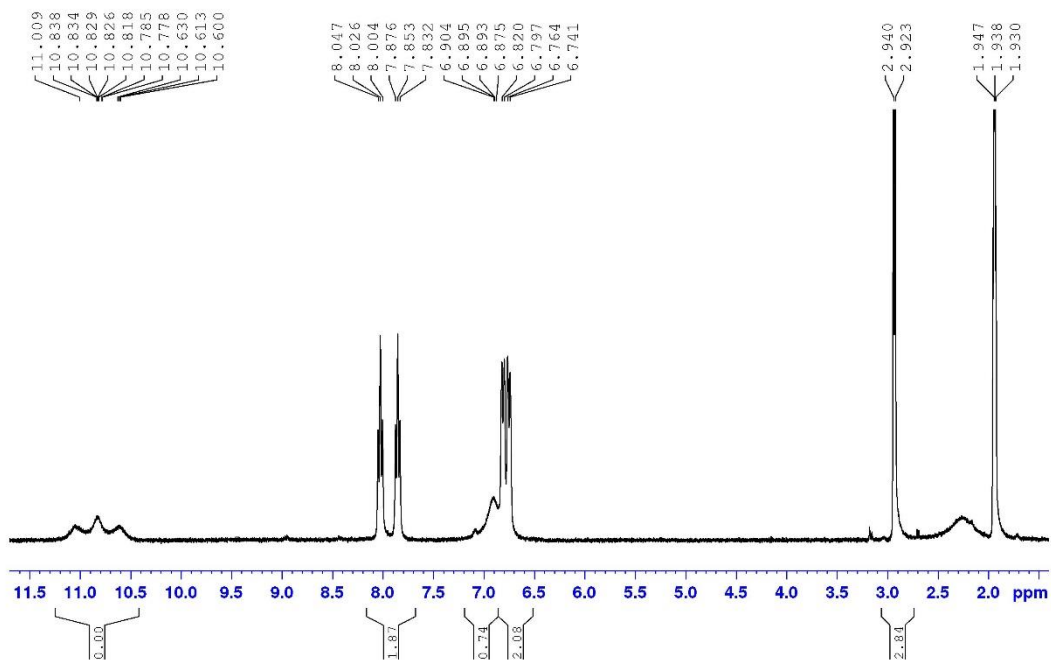**Table 14** Crystallographic data for, 4-APYH$^+$ HSO$_4^{-a}$ 4-MerPyH$^+$ HSO$_4^{-a}$, 4-HydPyH$^+$ HSO$_4^{-a}$, IsonicAcidH$^+$ HSO$_4^{-a}$, IsonicAmideH$^+$ HSO_4^{-a} and PyThioAmideH$^+$ HSO_4^{-a}

	4-APYH$^+$ HSO_4^{-a}	4-MerPyH$^+$HSO$_4^{-a}$	4-HydPyH$^+$HSO$_4^{-a}$	IsonicAcidH$^+$ HSO$_4^{-a}$	IsonicAmideH$^+$ HSO_4^{-a}	PyThioAmideH$^+$ HSO_4^{-a}
formula	C$_{25}$ H$_{38}$ N$_{10}$ O$_{16}$ S$_4$	C$_{10}$ H$_{14}$ N$_2$ O$_9$ S$_4$	C$_5$ H$_7$ N O$_5$ S	C$_6$ H$_7$ N O$_6$ S	C$_6$ H$_8$ N$_2$ O$_5$ S	C$_6$ H$_8$ N$_2$ O$_4$ S$_2$
Fw	862.89	434.47	193.18	221.19	220.20	236.26
cryst. system	Monoclinic	Orthorhombic	Monoclinic	Monoclinic	Monoclinic	Triclinic
space group	P 1 n 1	P c a 21	P 2$_1$/c 1	P 2$_1$/c 1	P 2$_1$/c 1	P -1
a [Å]	10.0996(3)	16.6684(4)	10.4105(3)	8.2339(2)	5.1325(2)	7.5977(5)
b [Å]	18.7186(4)	5.64650(10)	10.6316(3)	11.4617(3)	19.9931(8)	8.1758(6)
c [Å]	10.4276(3)	17.5976(4)	6.6685(2)	9.4324(3)	8.0165(4)	8.7581(6)
α [°]	90	90	90	90	90	97.469(5)
β [°]	110.921(3)	90	96.805(3)	109.080(3)	98.553(4)	99.504(6)
γ [°]	90	90	90	90	90	115.077(7)
V [Å^3]	1841.38(9)	1656.25(6)	732.87(4)	841.27(4)	813.46(6)	473.65(6)
Z	2	4	4	4	4	2
T, °C	120.00(10)	120.01(10)	120.01(10)	120.01(10)	120.01(10)	120.00(10)
ρ_{calcd} [g cm^{-3}]	1.556	1.742	1.751	1.746	1.798	1.657
μ(Mo Kα) [mm^{-1}]	0.343	5.765	3.884	3.571	3.629	5.087
crystal size [mm^3]	0.314,0.201,0.071	0.572,0.186,0.156	0.196,0.152,0.033	0.496,0.169,0.089	0.231,0.194,0.121	0.394,0.233,0.163

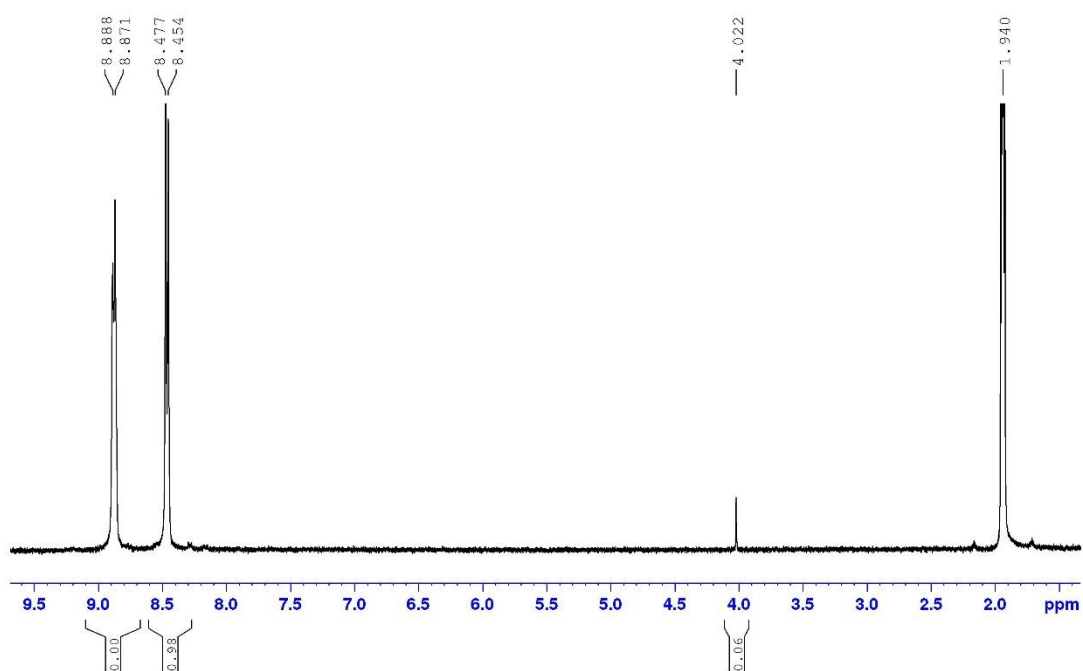| $F(000)$	900	896	400	456	456	244
θ range, deg	2.176- 25.026	5.027-66.596	5.971-66.567	5.686-66.521	4.423-66.589	5.254-66.585
reflns. collected	6972	3706	2536	2871	2753	2786
unique reflns.	4098	2230	1191	1403	1284	1598
R_{int}	0.0224	0.0263	0.0218	0.0186	0.0267	0.0188
reflns [$I>2\sigma(I)$]	4324	2247	1283	1474	1437	1650
R_1 [$I>2\sigma(I)$][c]	0.0311	0.0368	0.0298	0.0317	0.0350	0.0313
wR_2 (all data)[d]	0.0724	0.0966	0.0802	0.0880	0.0930	0.0865
GOF on F^2	1.058	1.050	1.083	1.078	1.079	1.053
completeness	0.999	0.995	0.998	0.993	0.999	0.987

[a] λ (CuKα) = 1.54184 Å. [b] λ (MoKα) = 0.71073 Å. [c] $R_1 = \Sigma||F_o|-|F_c||/ \Sigma|F_o|$. [d] $wR_2 = [\Sigma w(F_o^2-F_c^2)^2/\Sigma wF_o^4]^{\frac{1}{2}}$.

Table 15 Crystallographic data for, 4-APYH$^+$ SO$_4^{2-a}$ 4-MerPyH$^+$ SO$_4^{2-a}$, 4-HydPyH$^+$ SO$_4^{2-a}$, IsonicAcidH$^+$ SO$_4^{2-a}$, IsonicAmideH$^+$ SO_4^{2-a} ,PyThioAmideH$^+$ SO$_4^{2-a}$ and 4-APYH$^+$ CH$_3$COO^{-b}.

	4-APYH$^+$$SO_4^{2-a}$	4-HydPyH$^+$SO$_4^{2-a}$	IsonicAcidH$^+$SO$_4^{2-a}$	IsonicAmideH$^+$$SO_4^{2-}$ [a]	PyThioAmideH$^+$ SO_4^{2-a}	4-APYH$^+$ CH$_3$COO$^-$ [b]
formula	C$_{10}$ H$_{16}$ N$_4$ O$_5$ S	C$_{10}$ H$_{14}$ N$_2$ O$_7$ S	C$_{18}$ H$_{21}$ N$_3$ O$_{15}$ S$_2$	C$_{12}$ H$_{16}$ N$_4$ O$_7$ S	C$_{24}$ H$_{28}$ N$_8$ O$_8$ S$_6$	C$_9$ H$_{14}$ N$_2$ O$_4$
Fw	304.33	306.29	583.50	360.35	748.90	214.22
cryst. system	Triclinic	Monoclinic	Monoclinic	Monoclinic	Monoclinic	Triclinic
space group	P -1	P 2$_1$/n 1	C 1 2/c 1	P 2$_1$/c 1	P 2$_1$/c 1	P -1
a [Å]	6.4355(3)	7.08630(10)	19.9497(4)	12.9533(3)	8.47880(10)	7.5691(15)
b [Å]	8.4033(3)	19.9615(4)	11.7888(2)	7.0194(2)	41.2294(5)	7.9194(16)
c [Å]	12.4621(6)	9.3689(2)	20.8660(3)	16.4101(3)	8.82450(10)	9.2765(19)
α [°]	96.255(4)	90	90	90	90	88.86(3)
β [°]	97.498(4)	101.876(2)	105.631(2)	96.513(2)	91.1510(10)	77.25(3)
γ [°]	95.385(4)	90	90	90	90	85.75(3)
V [Å^3]	660.20(5)	1296.89(4)	4725.84(15)	1482.45(6)	3084.21(6)	540.9(2)
Z	2	4	8	4	4	2
T, °C	120.00(10)	120.00(10)	121(1)	120.01(10)	120.01(10)	170
ρ_{calcd} [g cm^{-3}]	1.531	1.569	1.640	1.615	1.613	1.315

μ(Mo Kα) [mm^{-1}]	2.451	2.576	2.819	2.396	4.645	0.104
crystal size [mm^3]	0.415,0.228,0.042	0.415,0.196,0.127	0.306,0.074,0.042	0.251,0.162,0.031	0.403,0.221,0.135	0.5, 0.4, 0.12
F(000)	320	640	2416	752	1552	228
θ range, deg	5.328- 66.482	4.430- 66.597	4.603-66.588	5.426-66.595	5.127- 5.127	2.766-25.023
reflns. collected	4231	4478	7685	5382	11420	3467
unique reflns.	2071	2117	3834	2387	4791	1577
R_{int}	0.0312	0.0177	0.0149	0.0187	0.0262	0.0268
reflns [$I>2\sigma(I)$]	2309	2290	4155	2618	5436	1879
R_1 [$I>2\sigma(I)$][c]	0.0552	0.0307	0.0281	0.0316	0.0337	0.0494
wR_2 (all data)[d]	0.1489	0.0844	0.0781	0.0937	0.0943	0.1310
GOF on F^2	1.067	1.048	1.052	1.037	1.041	1.129
completeness	0.996	0.996	0.994	0.996	0.998	0.984

[a] λ (CuKα) = 1.54184 Å. [b] λ (MoKα) = 0.71073 Å. [c] $R_1 = \Sigma||F_o|-|F_c||/ \Sigma|F_o|$. [d] $wR_2 = [\Sigma w(F_o^2-F_c^2)^2/\Sigma wF_o^4]^{1/2}$.

Appendix 2. ^{1}H NMR spectra

VA0118 CD3CN, 4-AMINOPYRIDINE + HBF4
5.02.2018

11.146
11.118
11.101
11.058
10.953
10.805
10.767

7.960
7.938
7.917

6.859
6.836
6.566
6.552

3.376

2.100
2.098
1.946
1.940
1.938

VA0218 CD3CN, 4-METHYLAMINOPYRIDINE + HBF4
8.02.2018

11.009
10.838
10.834
10.829
10.826
10.818
10.778
10.630
10.613
10.600

8.047
8.026
8.004
7.876
7.853
7.832
6.904
6.895
6.893
6.875
6.820
6.797
6.764
6.741

2.940
2.923

1.947
1.938
1.930

VA0318 CD3CN, 4-MERCAPTOPYRIDINE + HBF4
12.02.2018

8.683
8.660
8.579
8.556
8.340
8.319
8.126
8.106
8.072
8.049
7.858
7.837

1.940

9.5 9.0 8.5 8.0 7.5 7.0 6.5 6.0 5.5 5.0 4.5 4.0 3.5 3.0 2.5 2.0 ppm

0.00
1.24
4.53
1.17
1.00
4.37
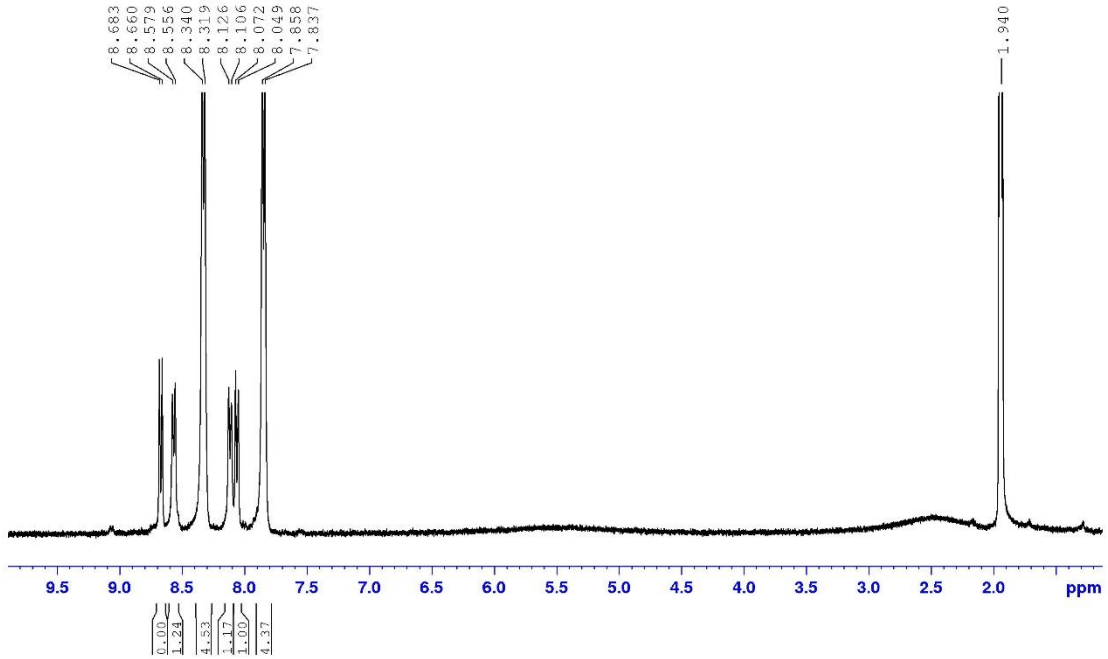
VA0418 CD3CN, 4-HYDROXYPYRIDINE + HBF4
13.02.2018

10.132
10.119

8.392
8.371
8.347

7.293
7.271

2.126
1.948
1.940
1.932
1.729
1.712
1.697
1.296
1.284
1.278

10.5 10.0 9.5 9.0 8.5 8.0 7.5 7.0 6.5 6.0 5.5 5.0 4.5 4.0 3.5 3.0 2.5 2.0 1.5 1.0 ppm

0.00
1.78
1.86
13.36
0.65
0.96
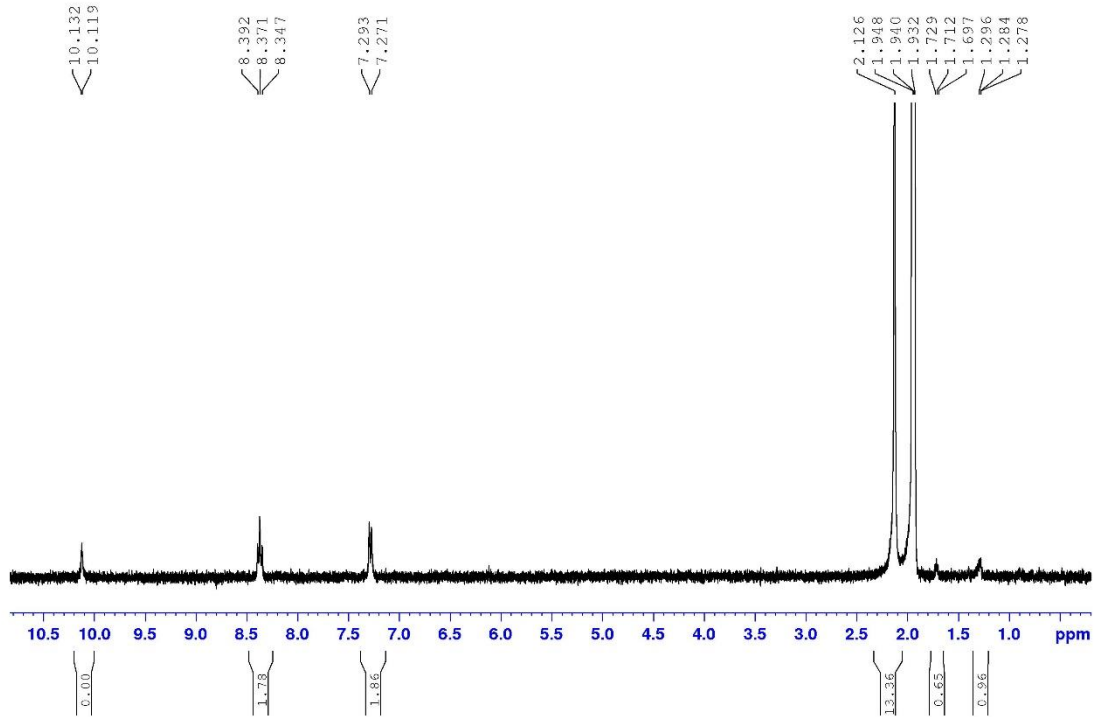
VA0518 CD3CN, ISONICOTINIC ACID + HBF4
20.02.2018

VA0618 CD3CN, ISONICOTINE AMIDE PYRIDINE + HBF4
15.02.2018
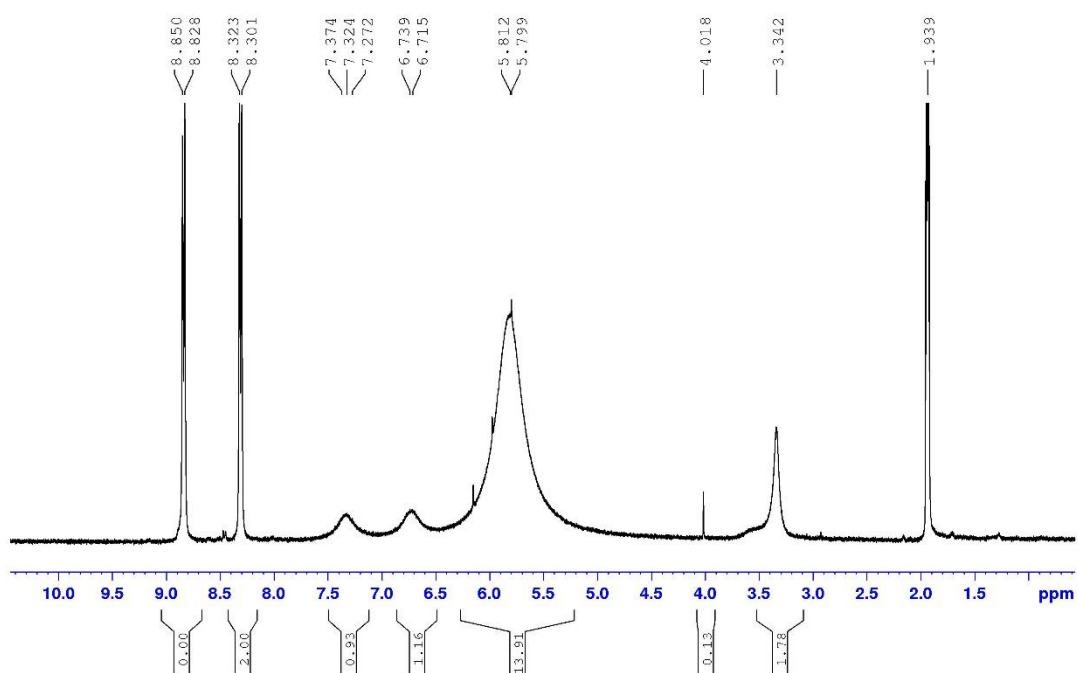
VA0718 CD3CN, PYRIDINE THIOIMIDE + HBF4
20.02.2018

8.751
8.728
8.217
8.195
6.122
5.944
5.766
2.908
1.940

10.0 9.5 9.0 8.5 8.0 7.5 7.0 6.5 6.0 5.5 5.0 4.5 4.0 3.5 3.0 2.5 2.0 1.5 ppm

1.00
0.83
0.25
0.10

VA0818 CD3CN, 4-AMINOPYRIDINE + ACETIC ACID
27.02.2018

11.361
8.066
8.044
6.672
6.650
5.600
1.936

11 10 9 8 7 6 5 4 3 2 1 0 ppm

1.00
1.08
1.09
0.86
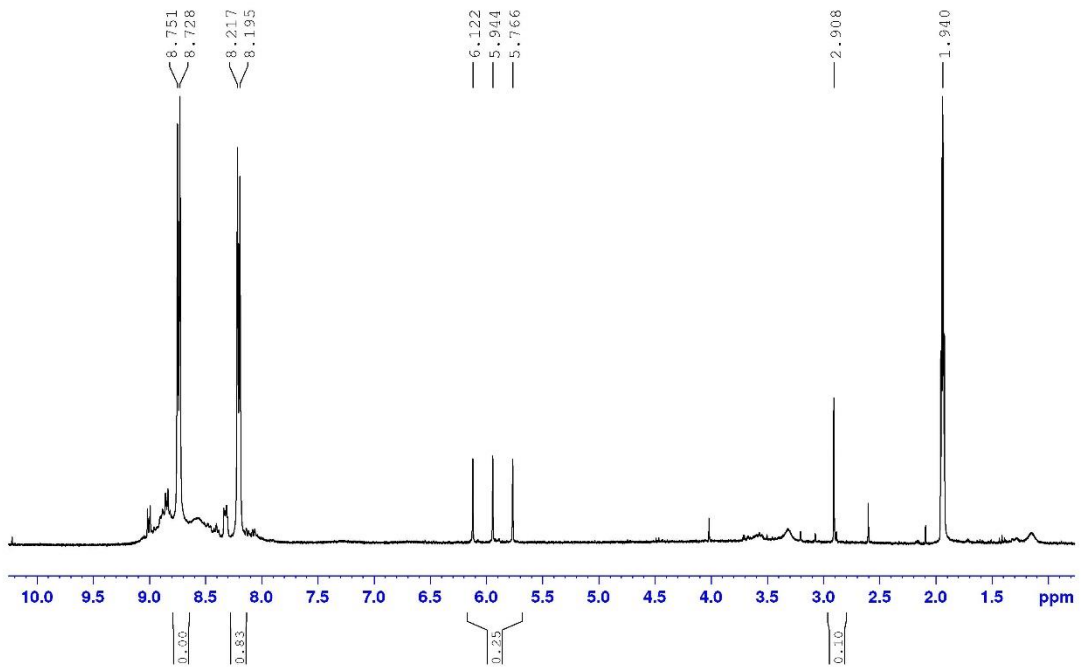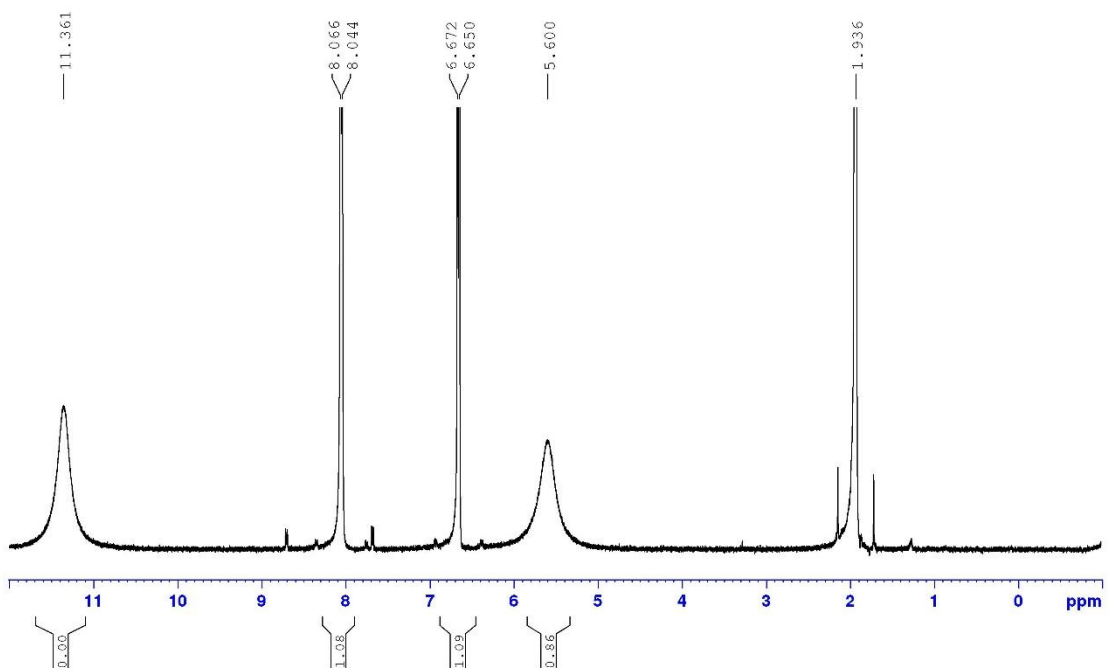
VA1018 CD3CN, 4-MERCAPTOPYRIDINE + ACETIC ACID
27.02.2018
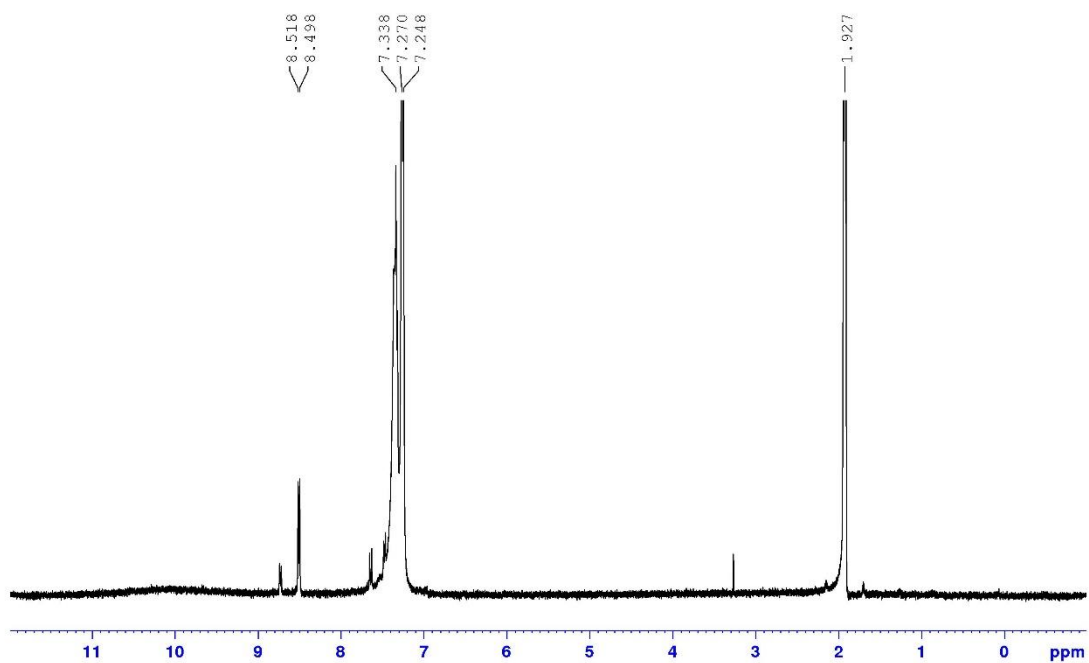
VA1118 CD3CN, 4-HYDROXYPYRIDINE + ACETIC ACID
07.03.2018
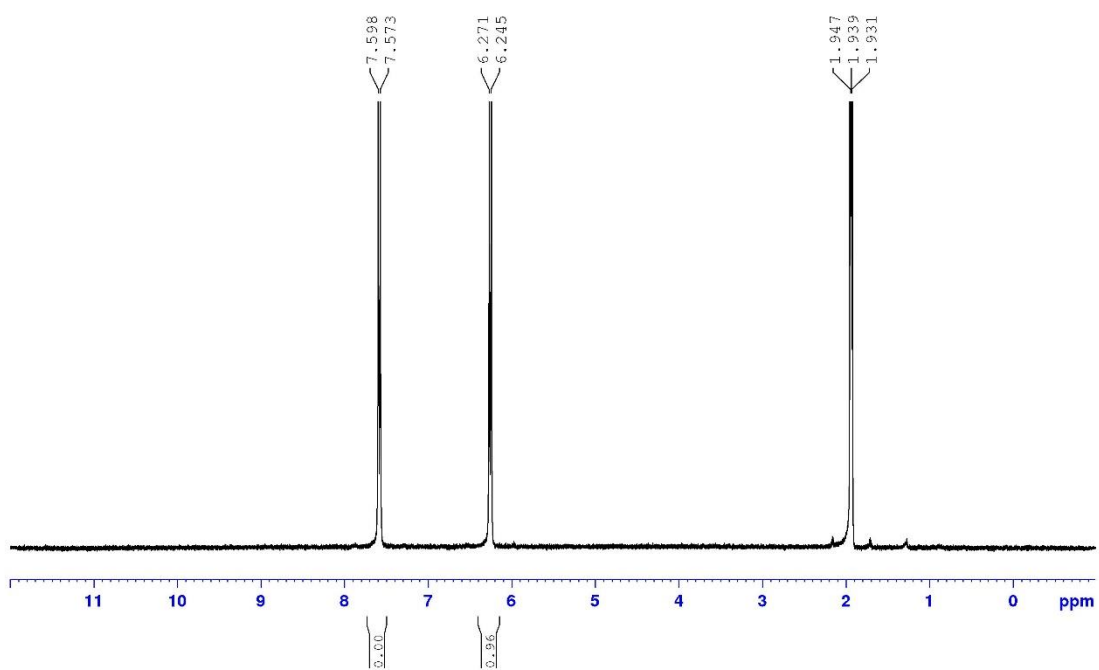
VA1318 CD3CN, 4-ISONICOTINAMIDE+ ACETIC ACID
08.03.2018
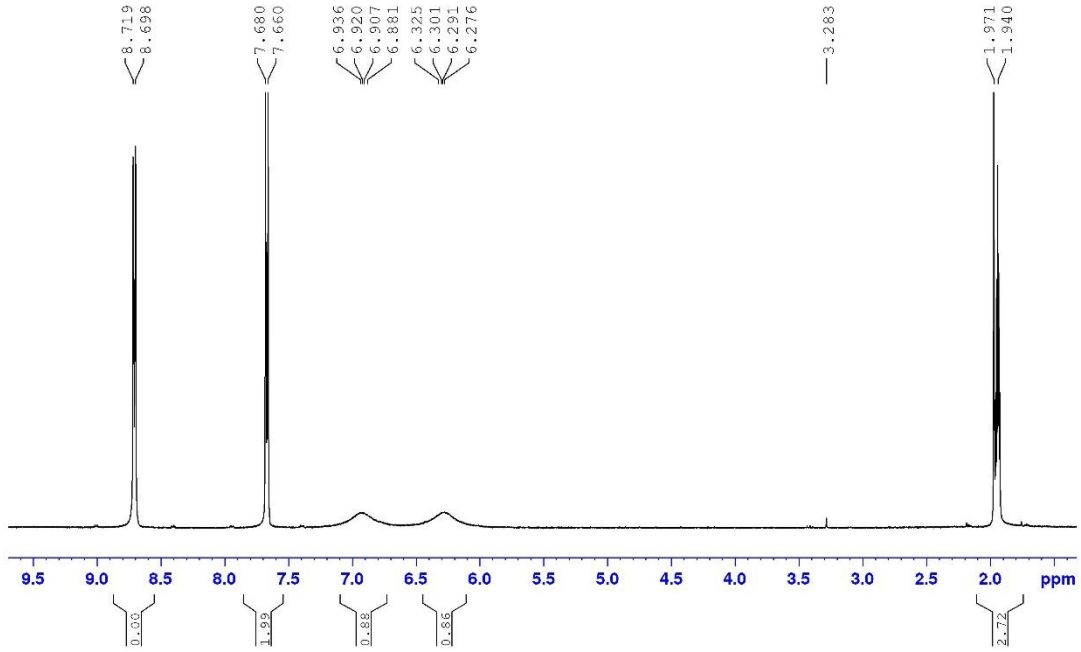
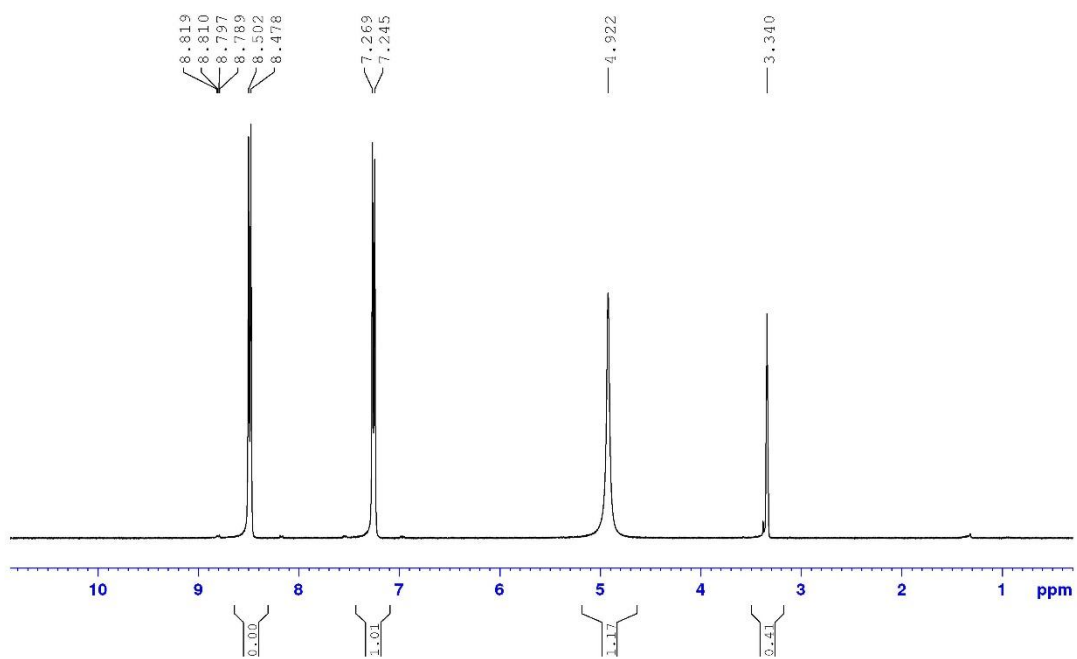VA1418 CD3CN, 4-PYRIDINETHIOAMIDE+ ACETIC ACID
08.03.2018
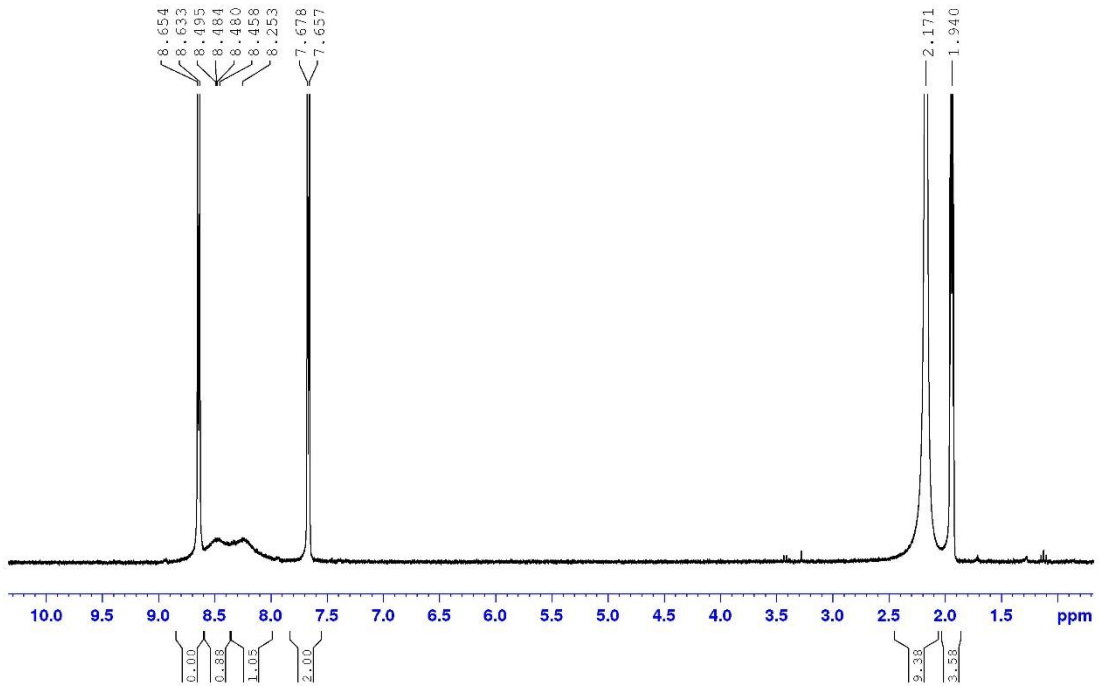
VA1618 CD3CN, 4-AMINOPYRIDINE+ AMMONIUM CARBONATE
22.03.2018
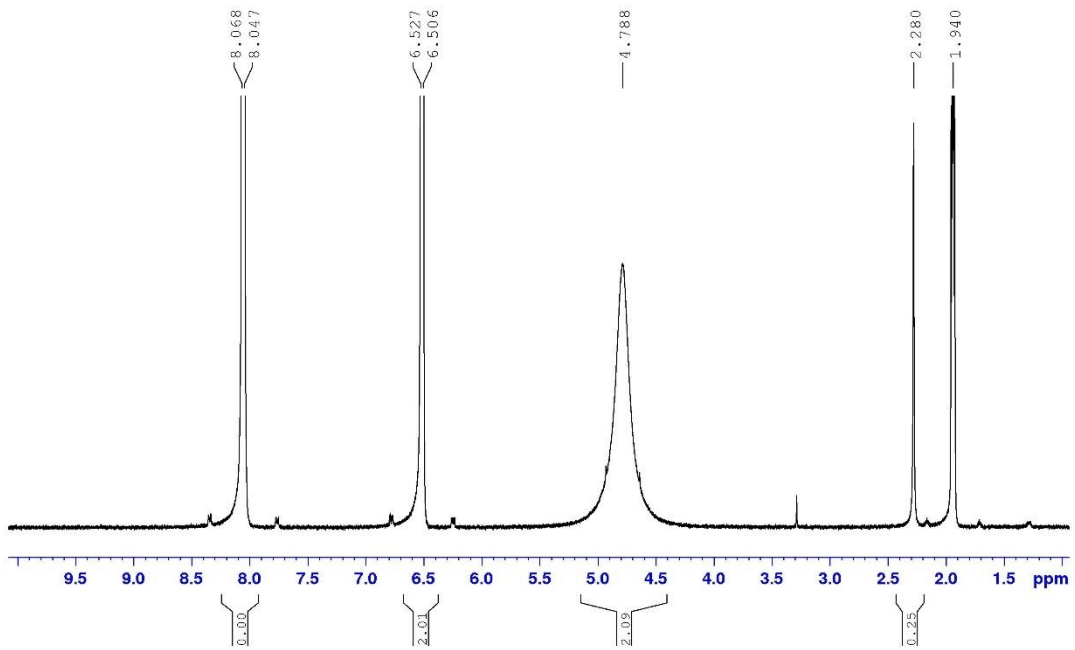
VA1718 CD3CN, 4-METHYLAMINOPYRIDINE+ AMMONIUM CARBONATE
22.03.2018
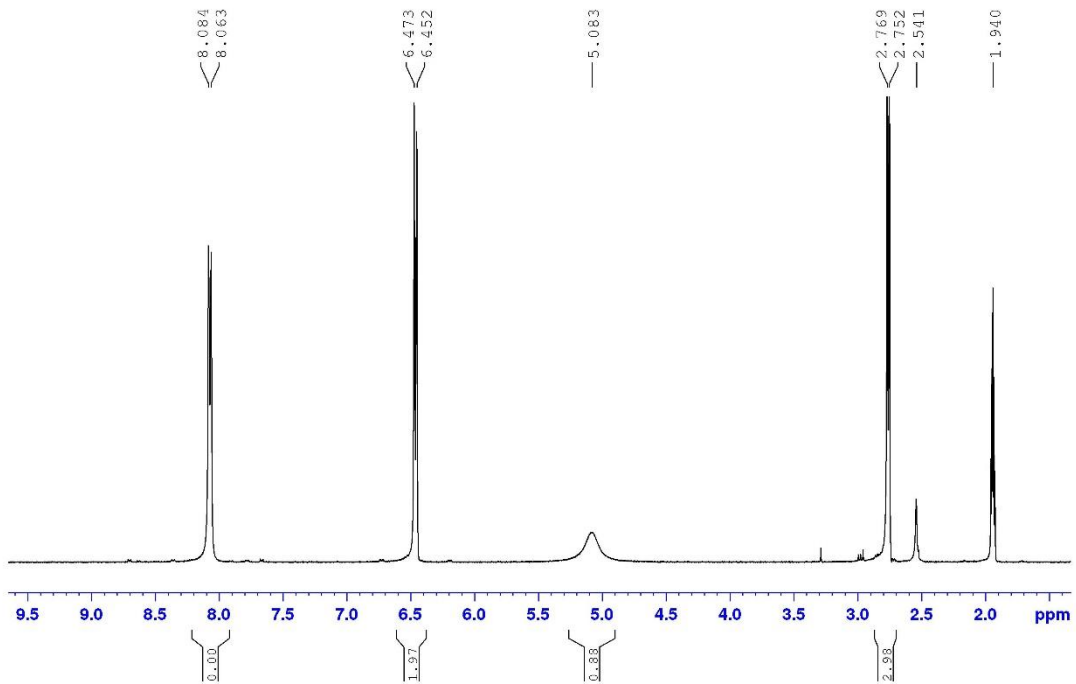
VA1818 D2O, 4-METHYLAMINOPYRIDINE+ PHOSPHURIC ACID
3.4.2018
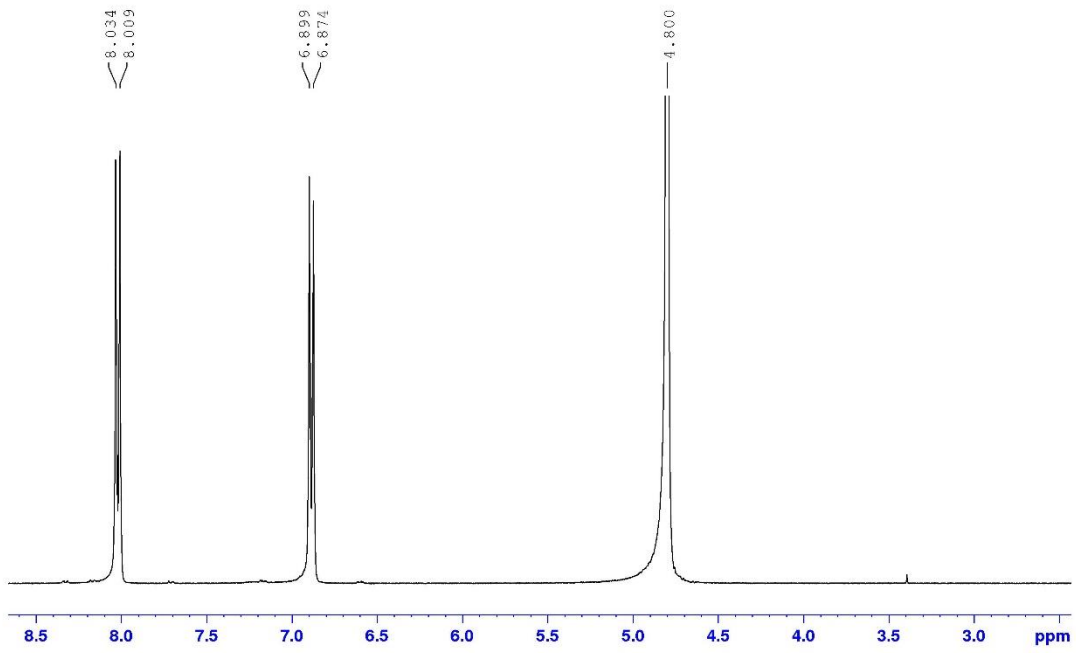
VA1918 D2O, 4-METHYLAMINOPYRIDINE+ PHOSPHURIC ACID
6.4.2018
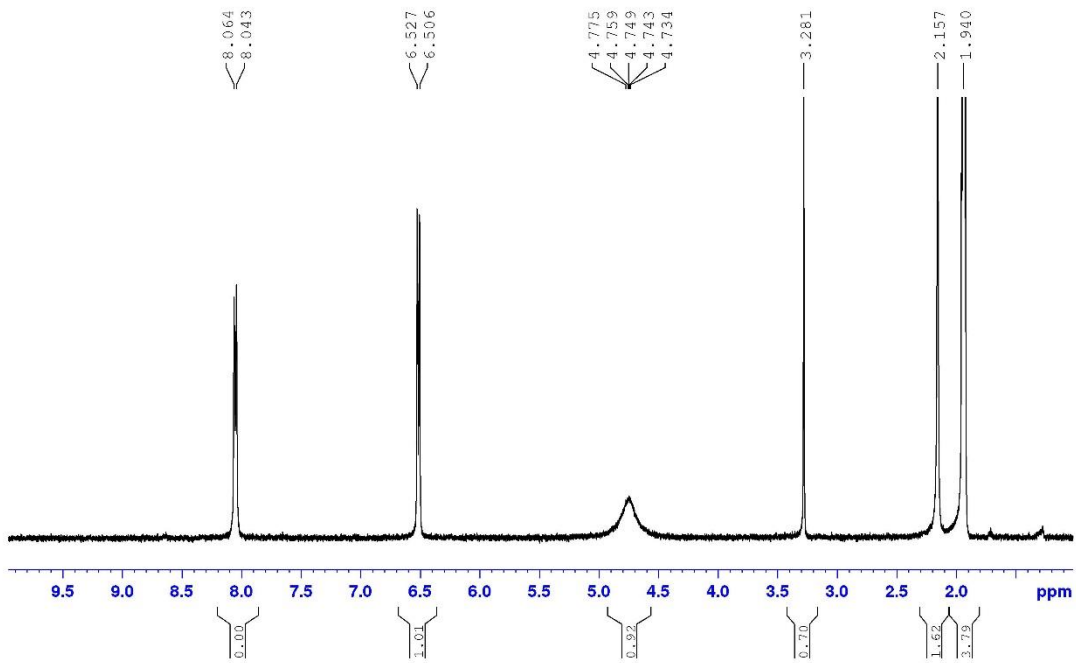
VA2118 CD3CN, 4-HYDROXYPYRIDINE+ PHOSPHURIC ACID
13.4.2018
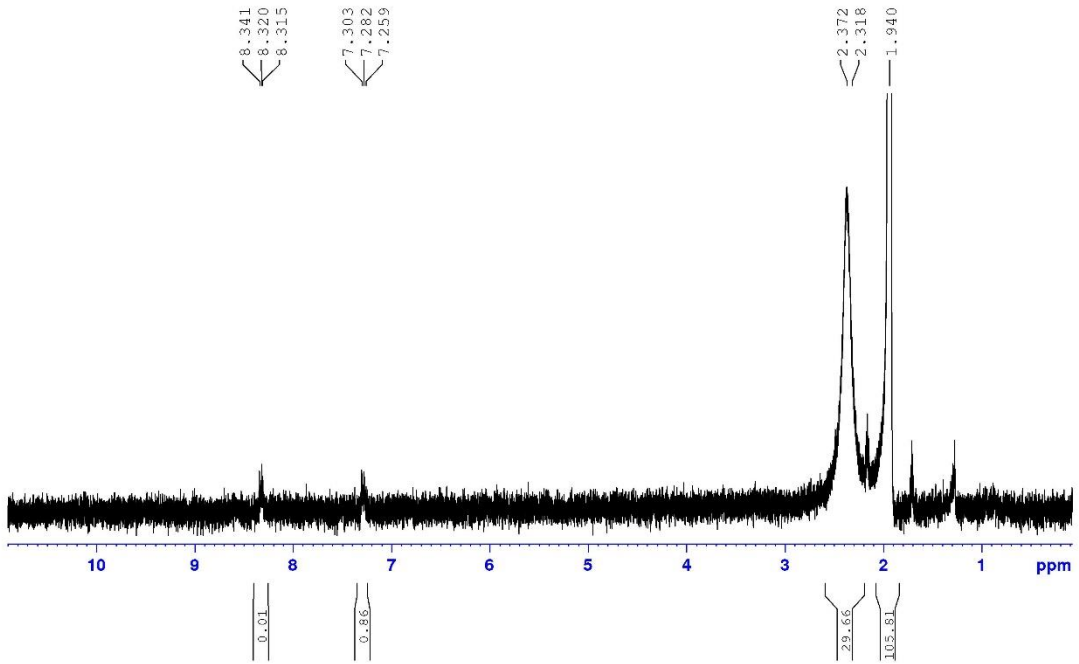
VA2218 CD3CN, 4-ISONICOTINIC ACID+ PHOSPHURIC ACID
13.4.2018
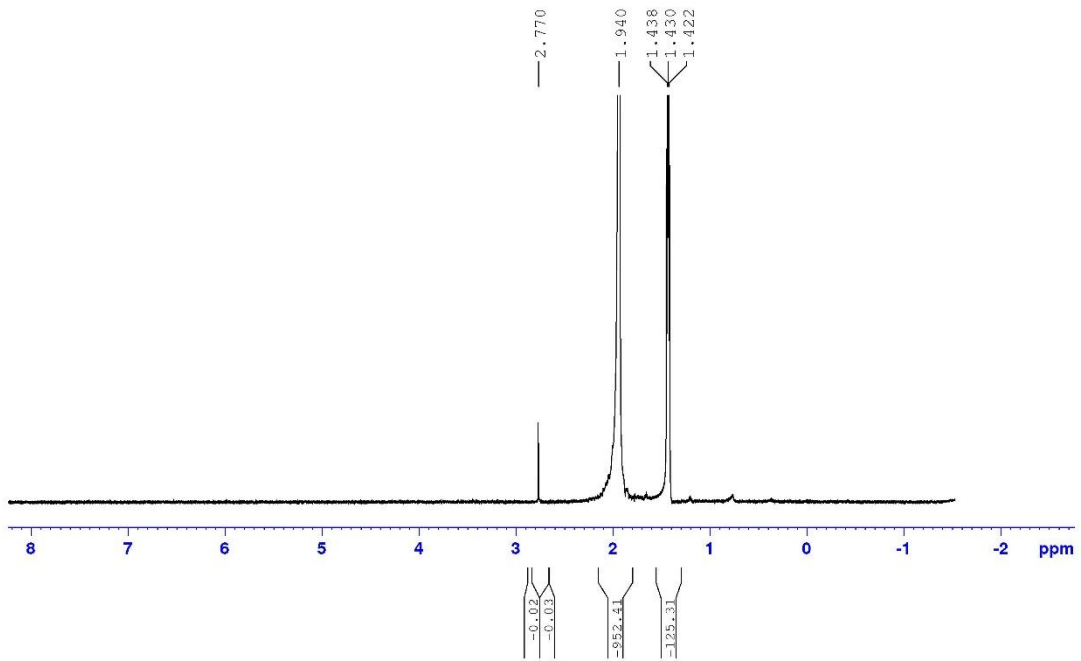
VA2318 CD3CN, 4-ISONICOTINEAMIDE+ PHOSPHURIC ACID
13.4.2018

—2.195
—1.940

7.0   6.5   6.0   5.5   5.0   4.5   4.0   3.5   3.0   2.5   2.0   1.5   1.0   0.5   0.0   ppm

0.00   3.08
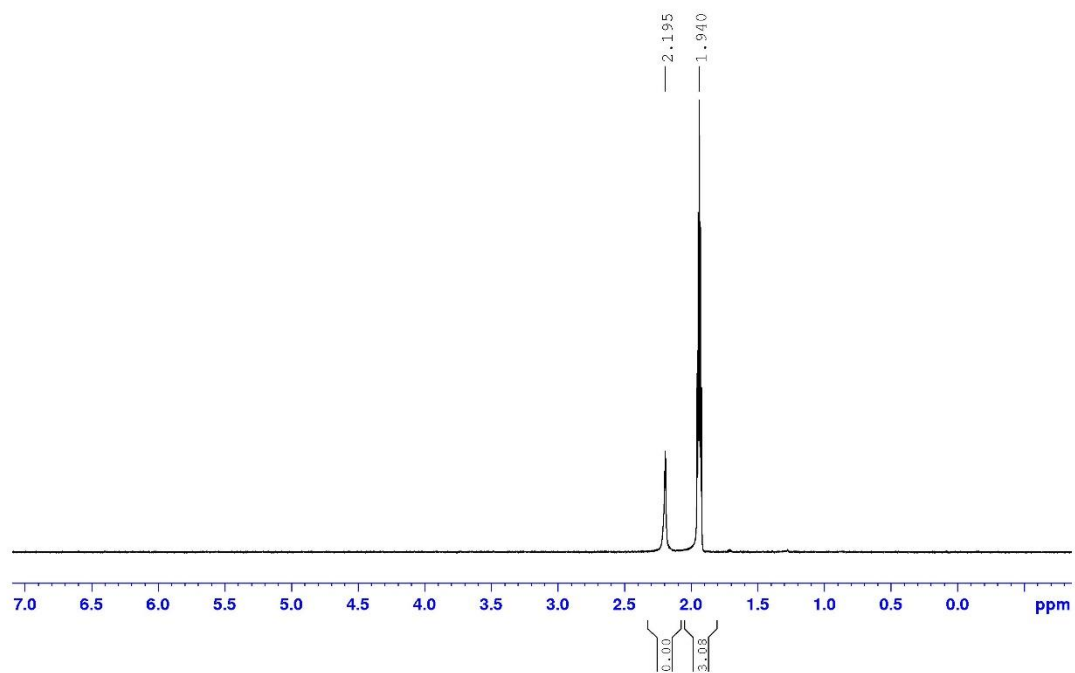
VA2418 D2O, 4-PYRIDINE THIOIMIDE + PHOSPHURIC ACID
2.5.2018

8.913
8.892
8.319
8.298

4.800

11.0   10.5   10.0   9.5   9.0   8.5   8.0   7.5   7.0   6.5   6.0   5.5   5.0   4.5   4.0   3.5   3.0   ppm

0.00   1.00   5.99
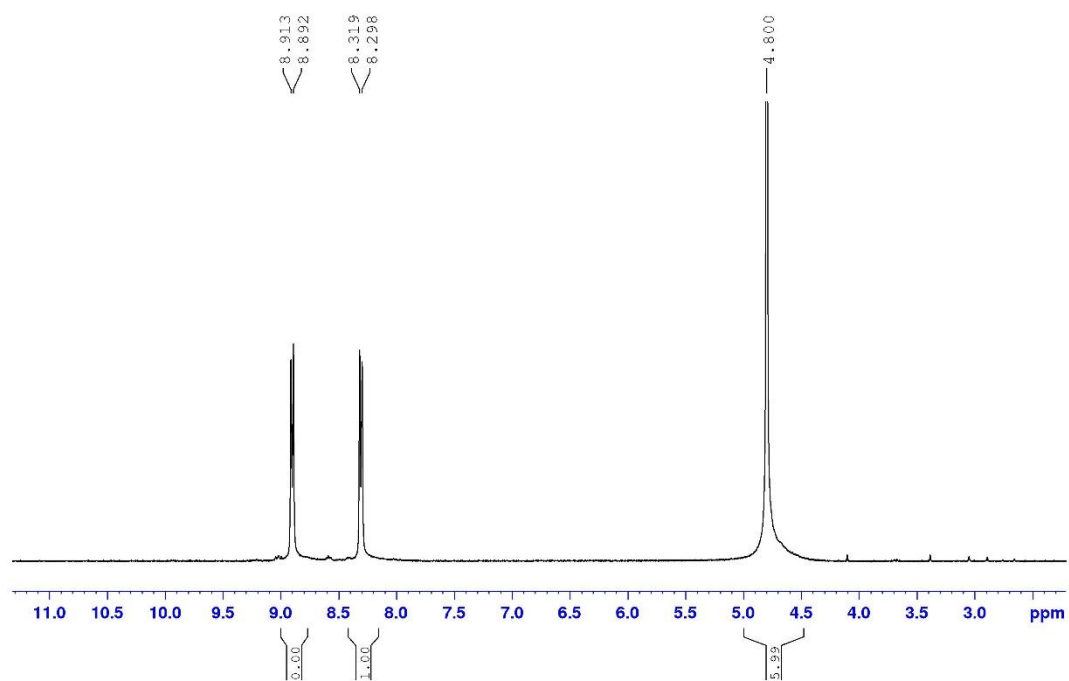
VA2518, ISONICOTINIC ACID + PHOSPHURIC ACID
2.05.2018
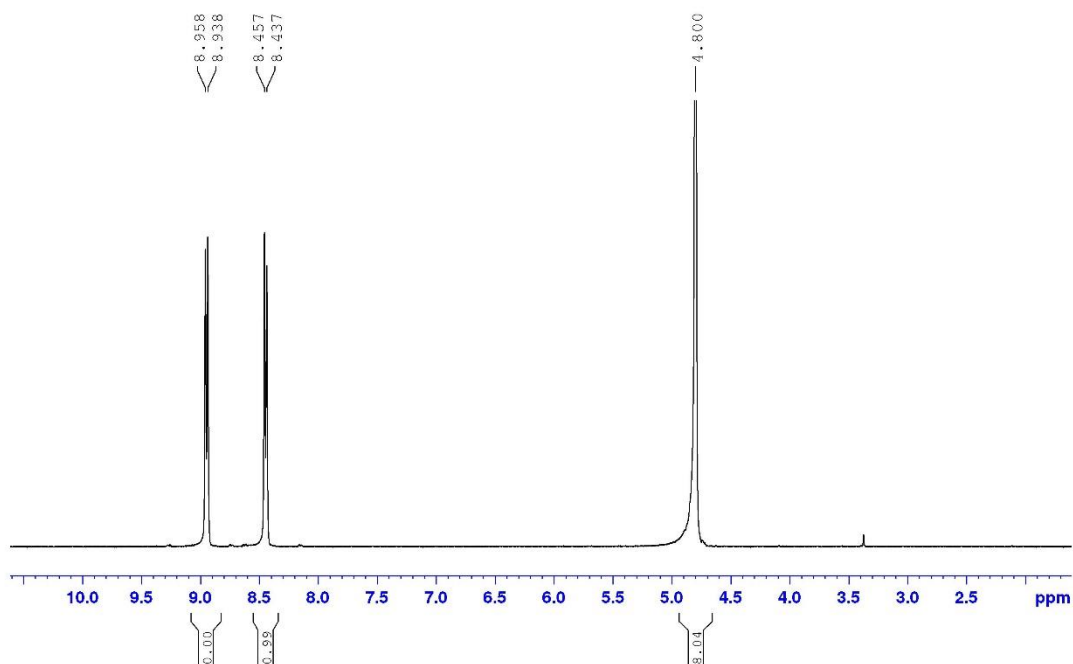
VA2618 MeOD, 4-AMINOPYRIDINE + NITRIC ACID
26.04.2018
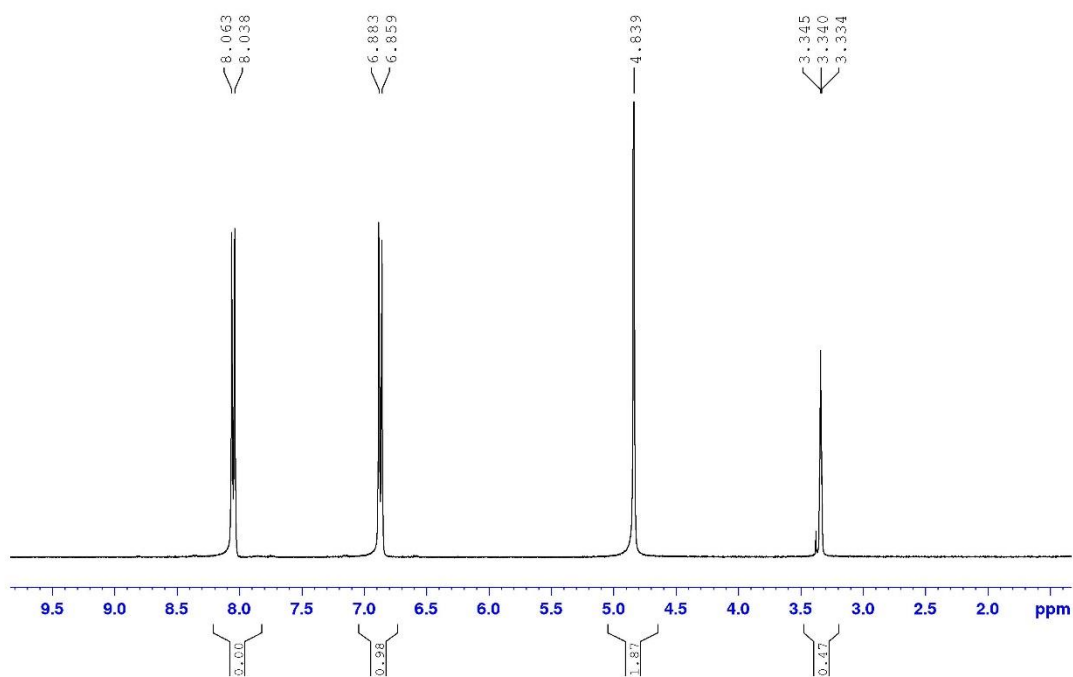
VA2718 CD3CN, 4-METHYLAMINOPYRIDINE + ACETIC ACID
26.04.2018
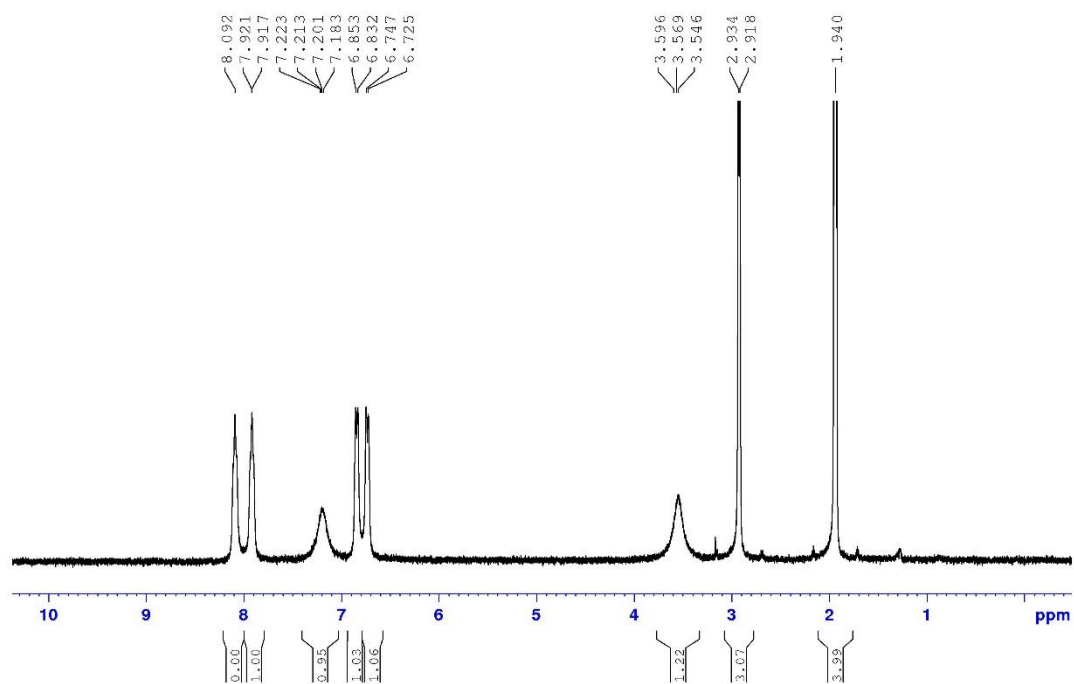
VA2818 CD3CN, 4-MERCAPTOPYRIDINE + NITRIC ACID
27.04.2018
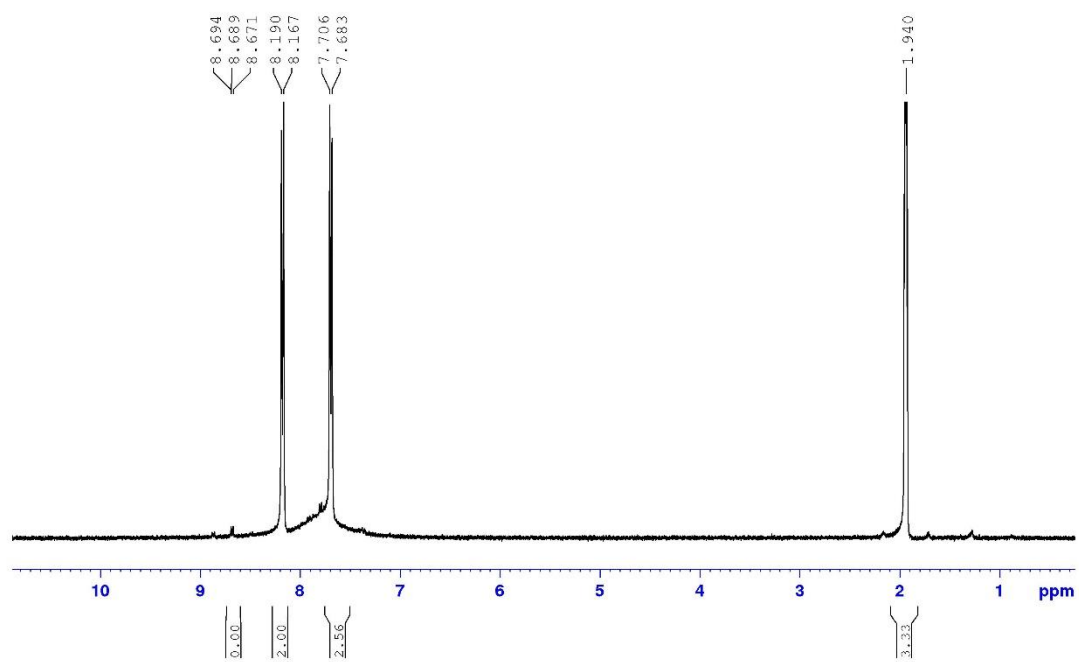
VA2918 MeOD, 4-HYDROXYPYRIDINE + NITRIC ACID
27.04.2018

8.819
8.810
8.797
8.789
8.502
8.478

7.269
7.245

4.922

3.340

10   9   8   7   6   5   4   3   2   1   ppm

0.00   1.01   1.17   0.41

VA3018 MeOD, ISONICOTINIC ACID + NITRIC ACID
09.05.2018

10.540
10.524

9.969
9.948

6.416

4.870
4.865

12.5 12.0 11.5 11.0 10.5 10.0 9.5 9.0 8.5 8.0 7.5 7.0 6.5 6.0 5.5 5.0 4.5 4.0   ppm

0.00   1.01   1.43   0.86
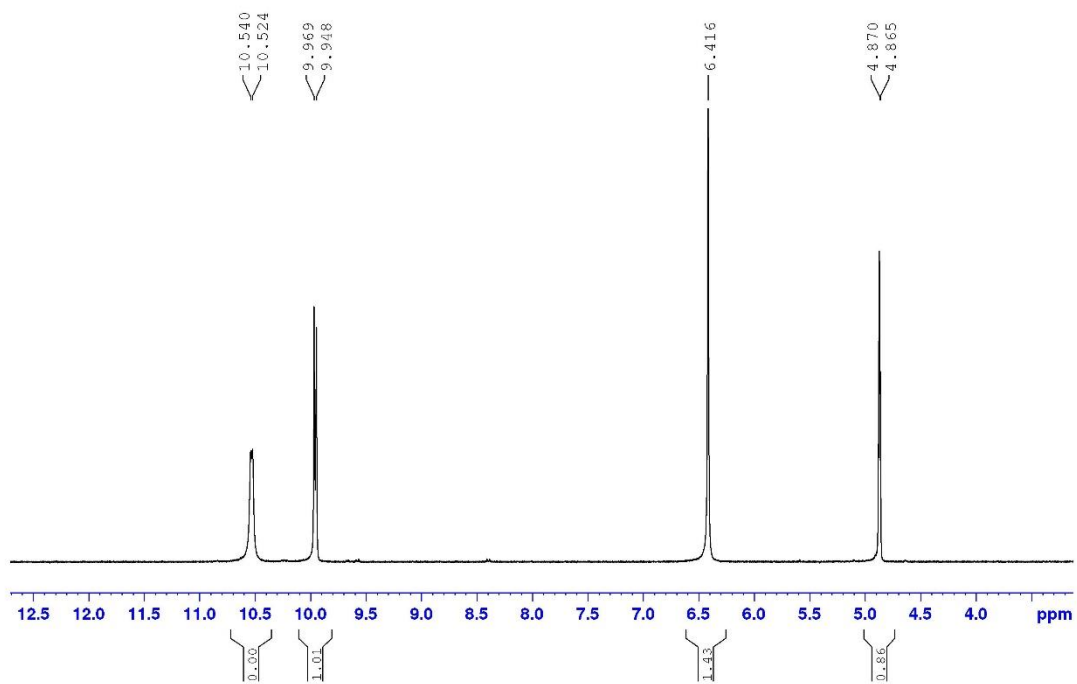
VA3118 MeOD, ISONICOTINE AMIDE + NITRIC ACID
09.05.2018
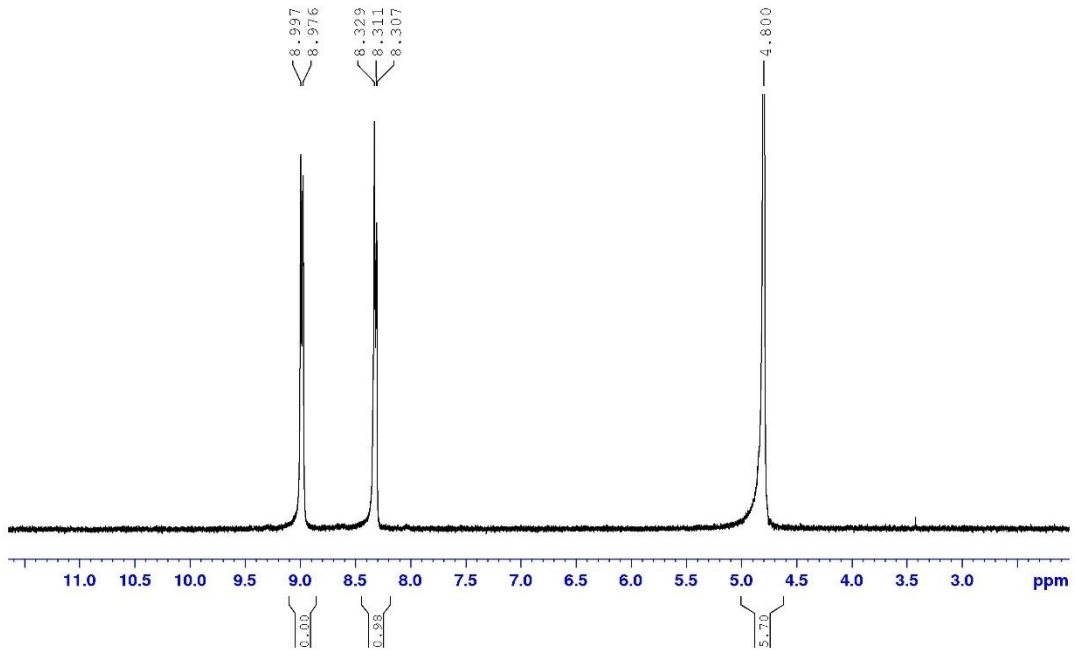
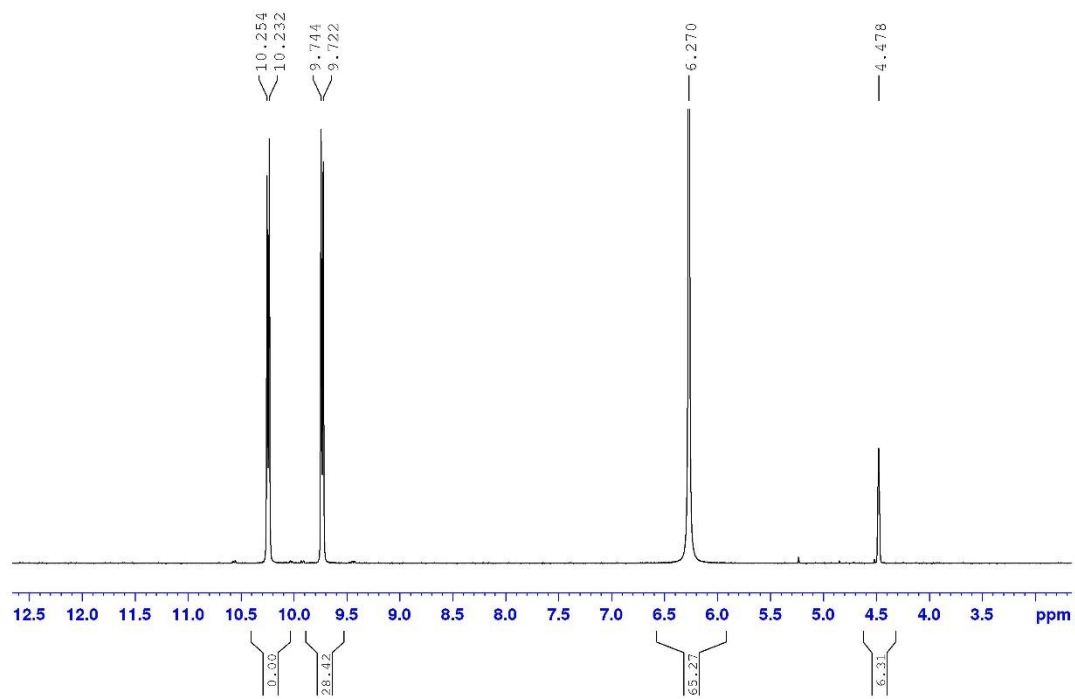VA3218 MeOD, PYRIDINETHIOAMIDE + NITRIC ACID
09.05.2018
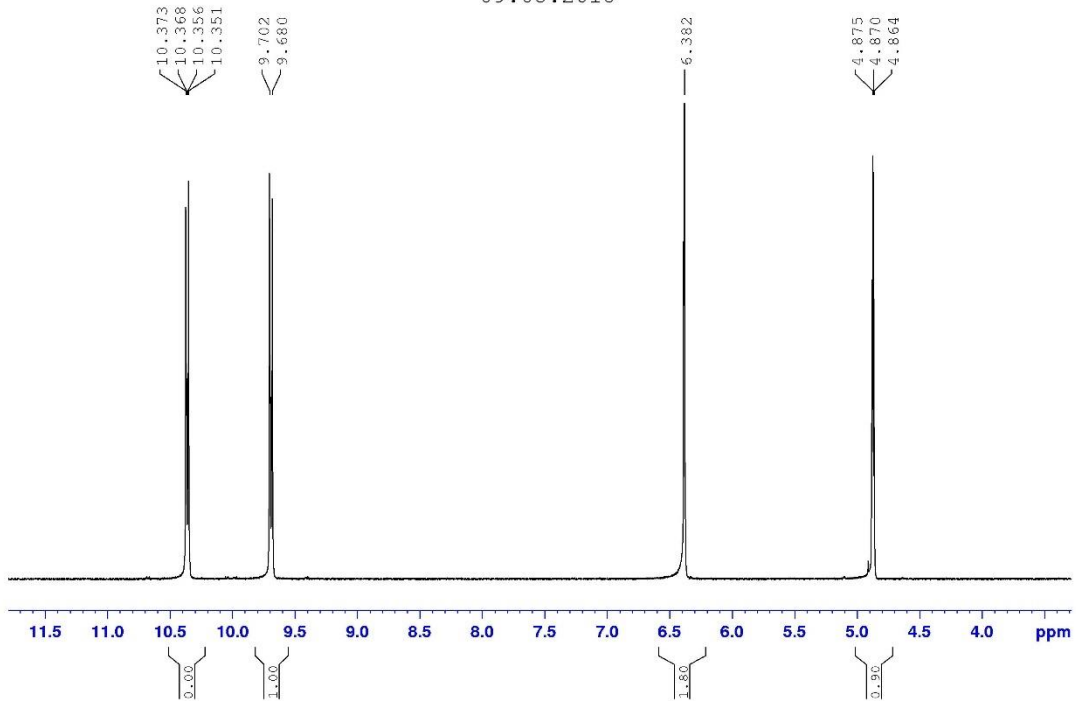
VA3318 MeOD, 4-AMINOPYRIDINE + SULPHURIC ACID
09.05.2018
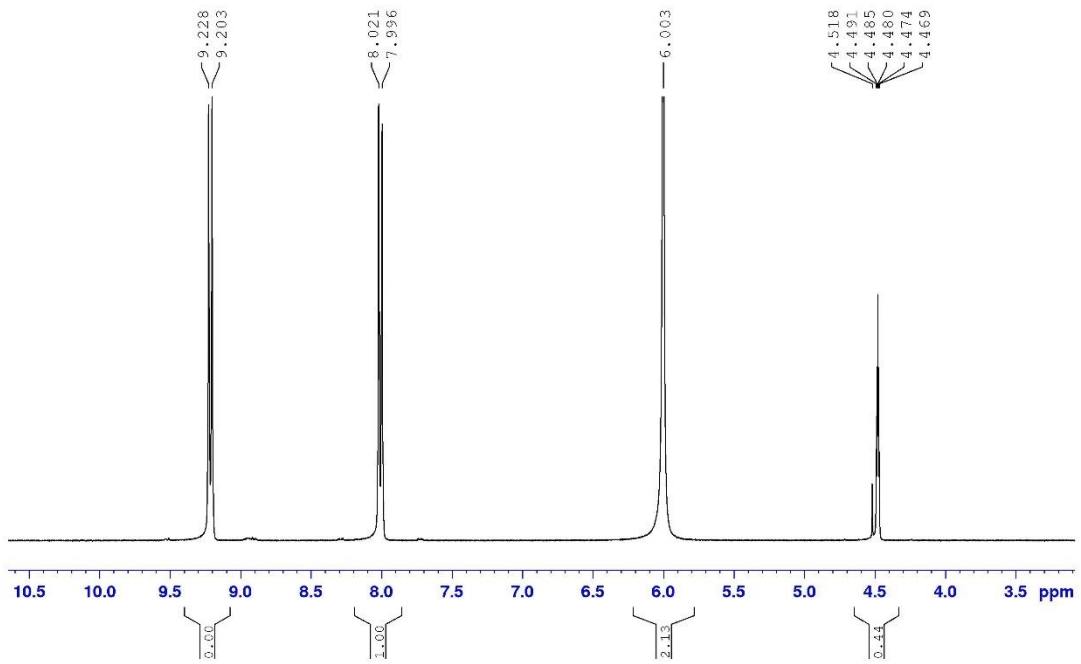
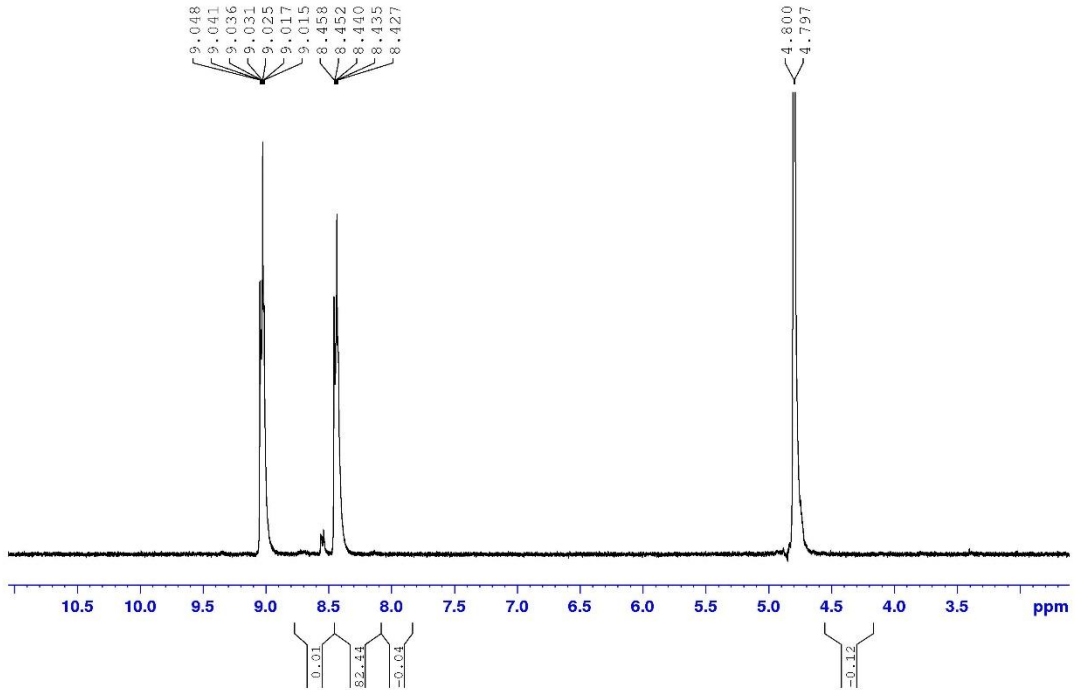VA3418 MeOD, 4-MERCAPTOPYRIDINE + SULPHURIC ACID
23.05.2018
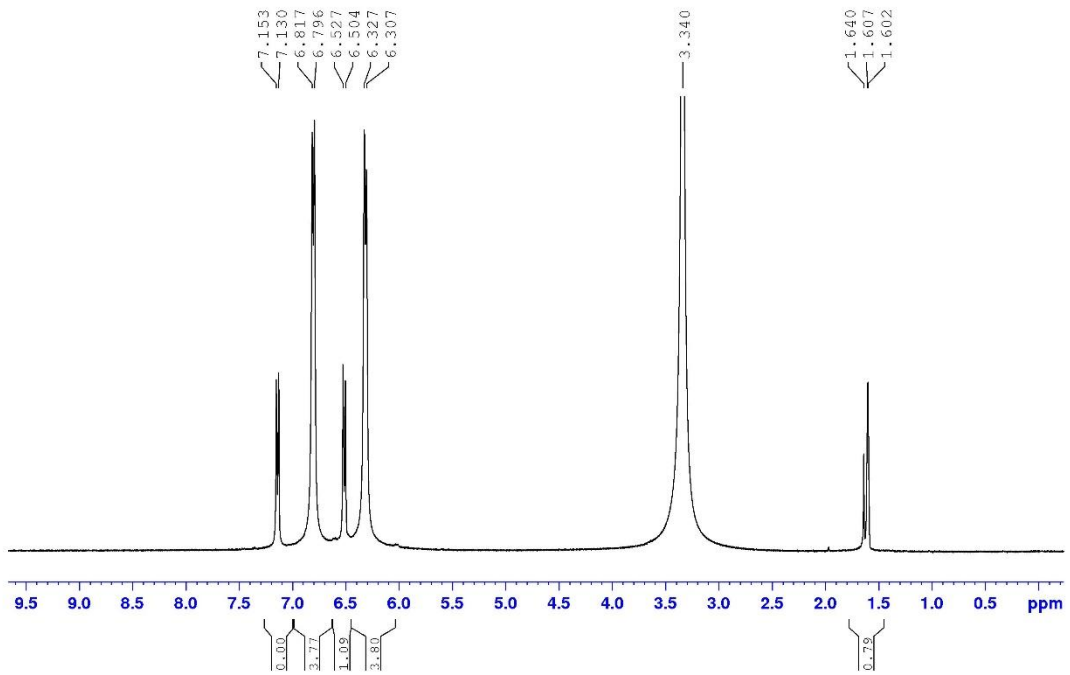
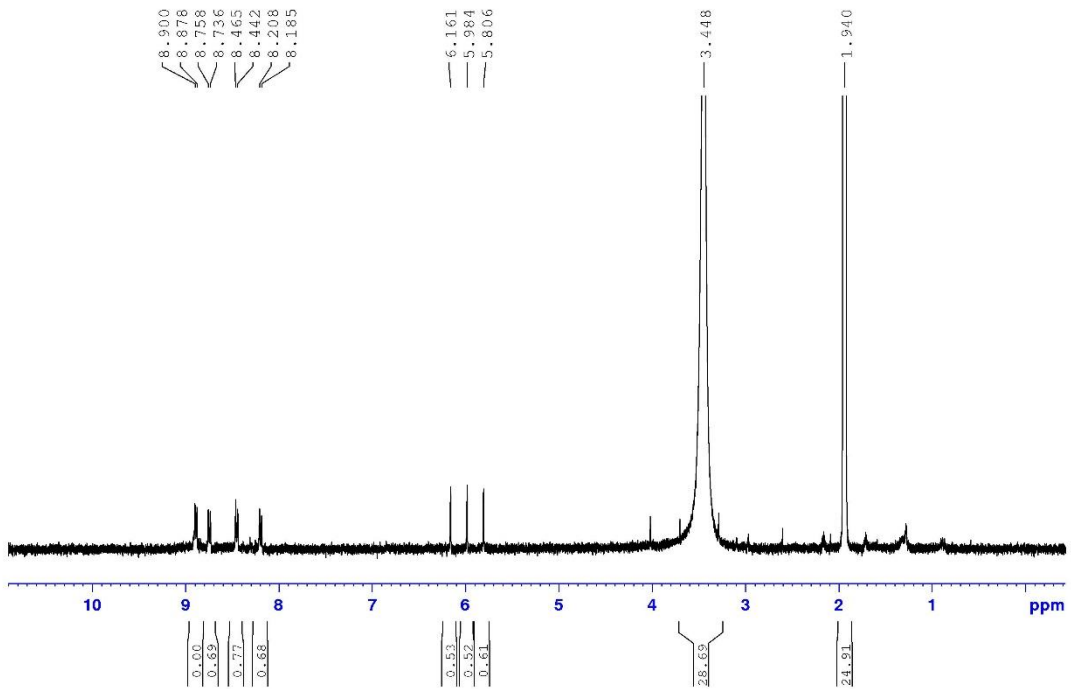VA3518 MeOD, 4-HYDROXYPYRIDINE + SULPHURIC ACID
16.05.2018
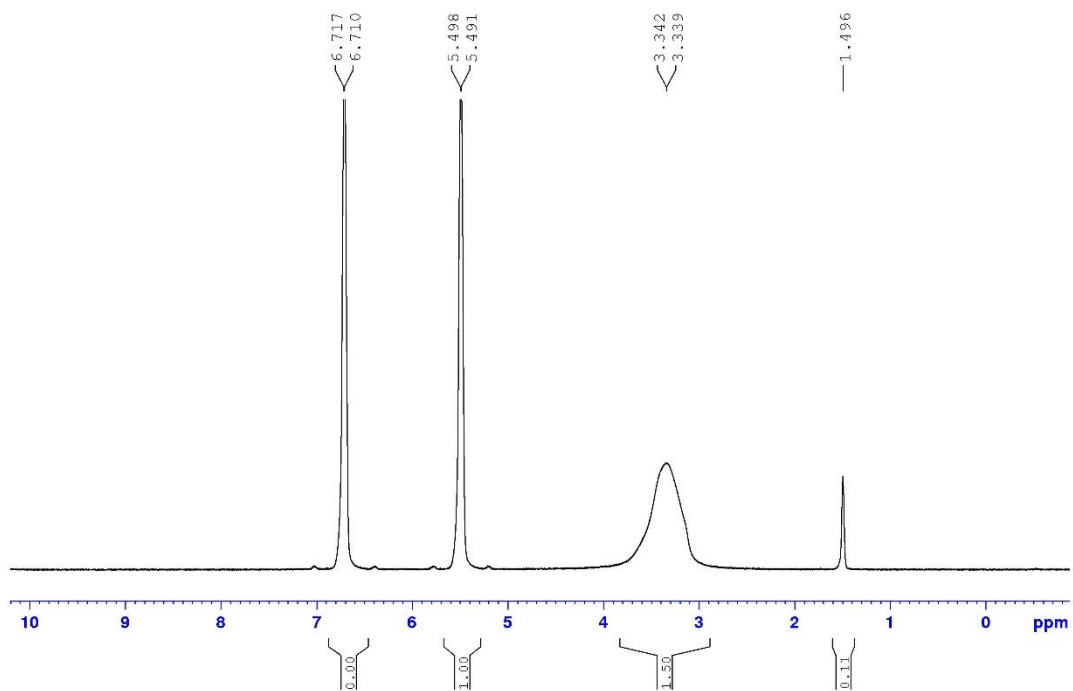
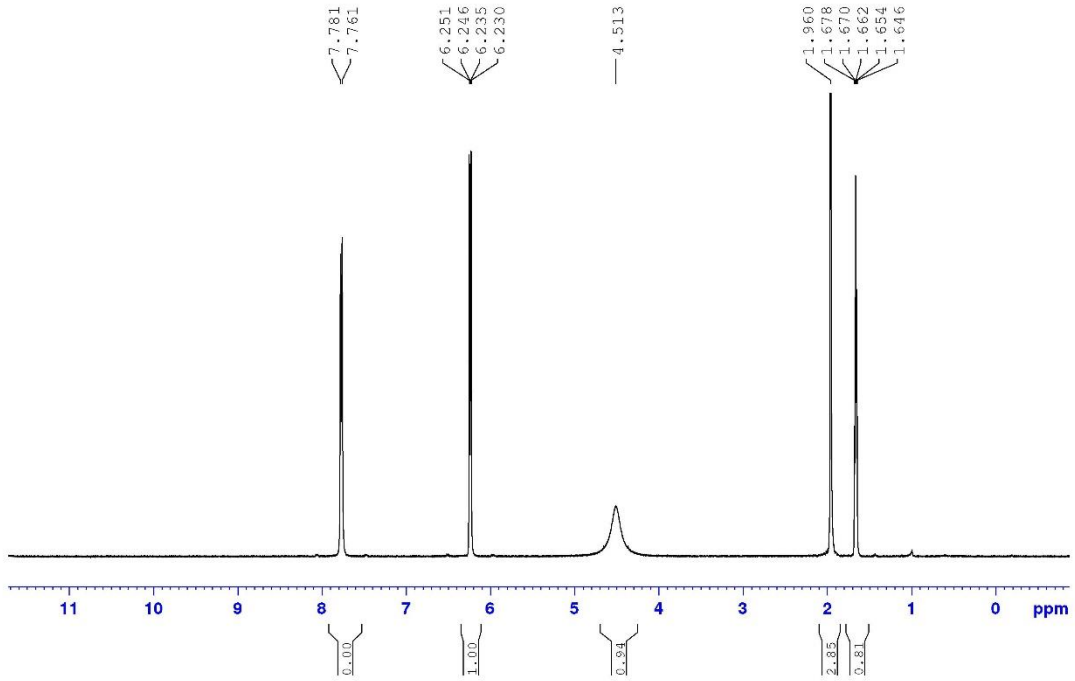VA3618 MeOD, ISONICOTINIC ACID + SULPHURIC ACID
16.05.2018

VA3718, D2O, Isonicotinamide + H2SO4
29.05.2018

9.048
9.041
9.036
9.031
9.025
9.017
9.015
8.458
8.452
8.440
8.435
8.427
4.800
4.797

10.5 10.0 9.5 9.0 8.5 8.0 7.5 7.0 6.5 6.0 5.5 5.0 4.5 4.0 3.5 ppm

0.01
82.44
-0.04
-0.12

VA3818 Me3CN, 4-pyridinethioamide + SULPHURIC ACID
29.05.2018

8.900
8.878
8.758
8.736
8.465
8.442
8.208
8.185
6.161
5.984
5.806
3.448
1.940

10 9 8 7 6 5 4 3 2 1 ppm
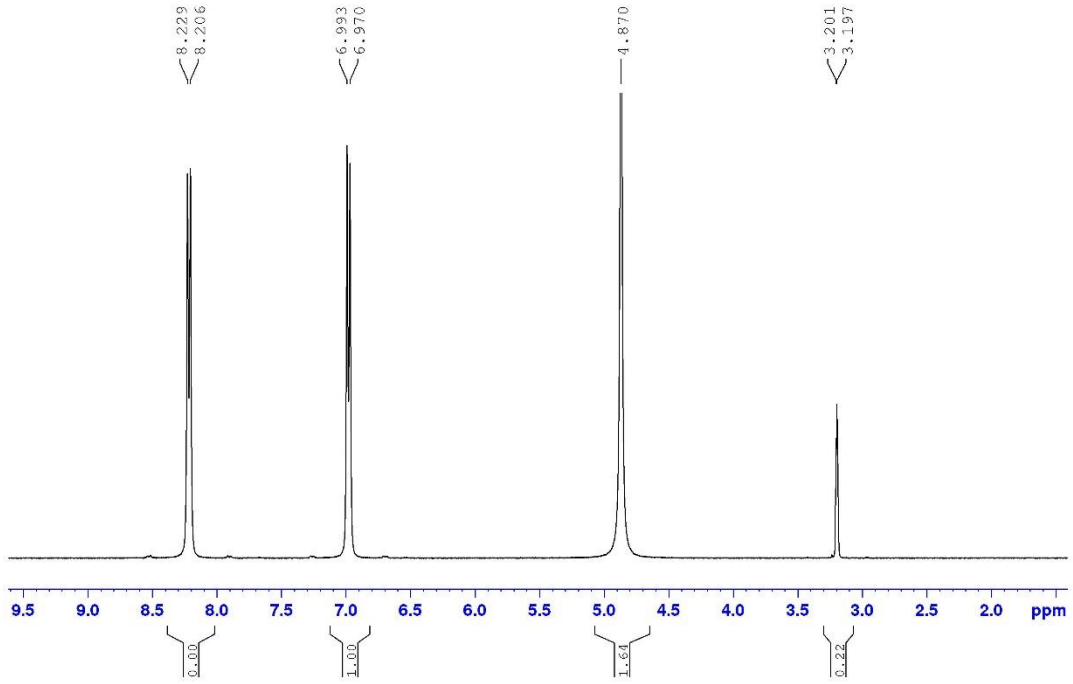
0.00
0.69
0.77
0.68
0.53
0.52
0.61
28.69
24.91

VA3918, CD3CN, 4-AMINOPYRIDINE + KH2PO4
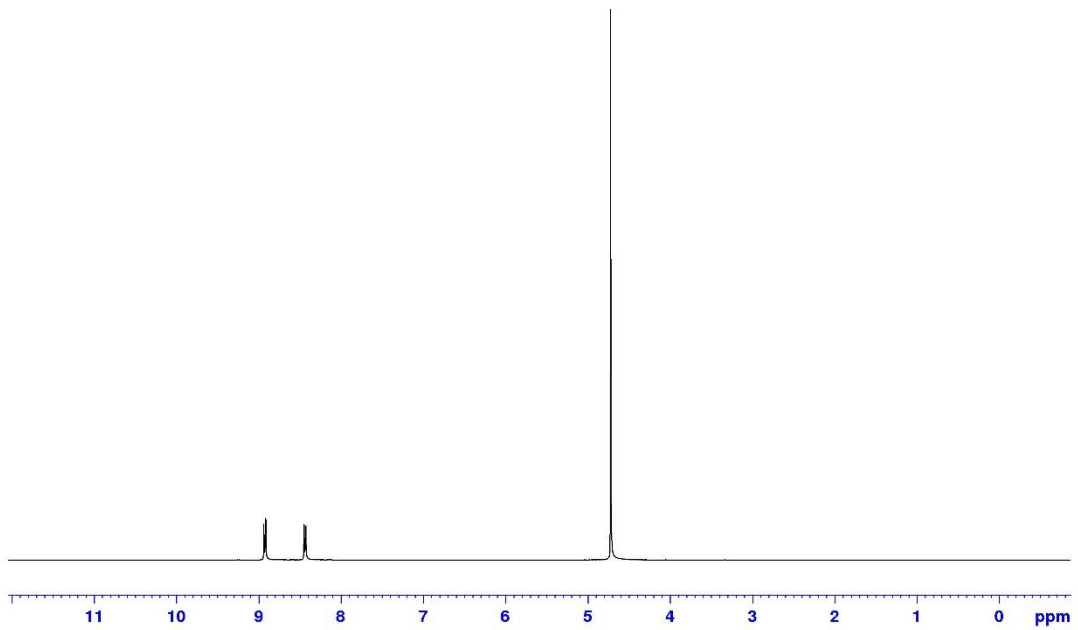23.05.2018

VA4118, CD3CN, 4-aminopyridine + SULPHURIC ACID
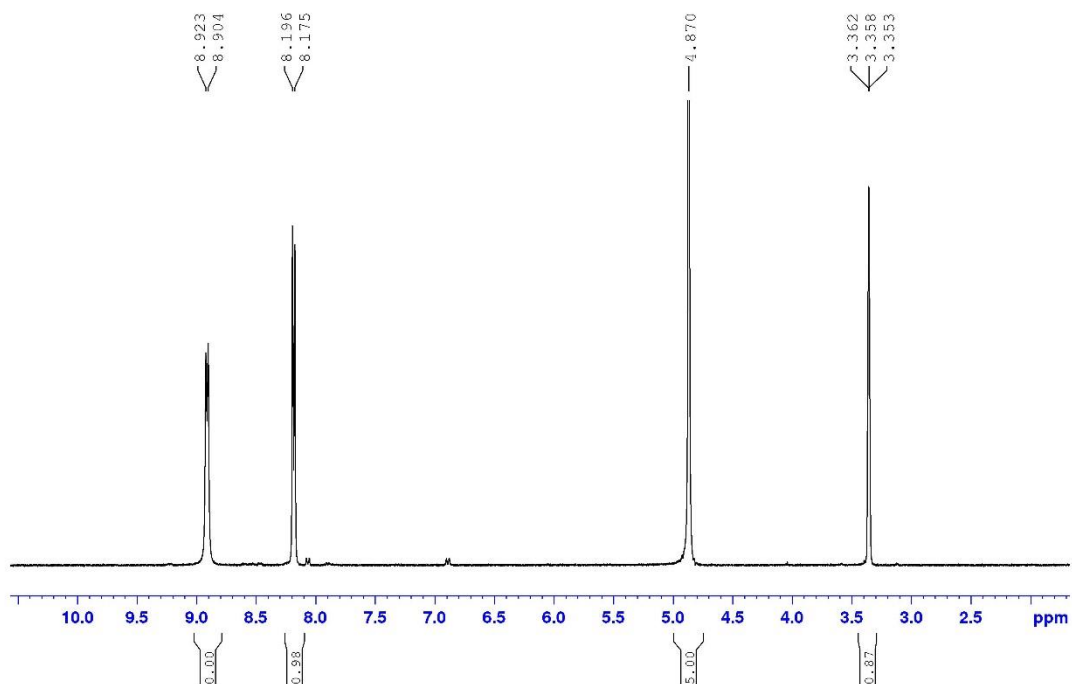01.06.2018
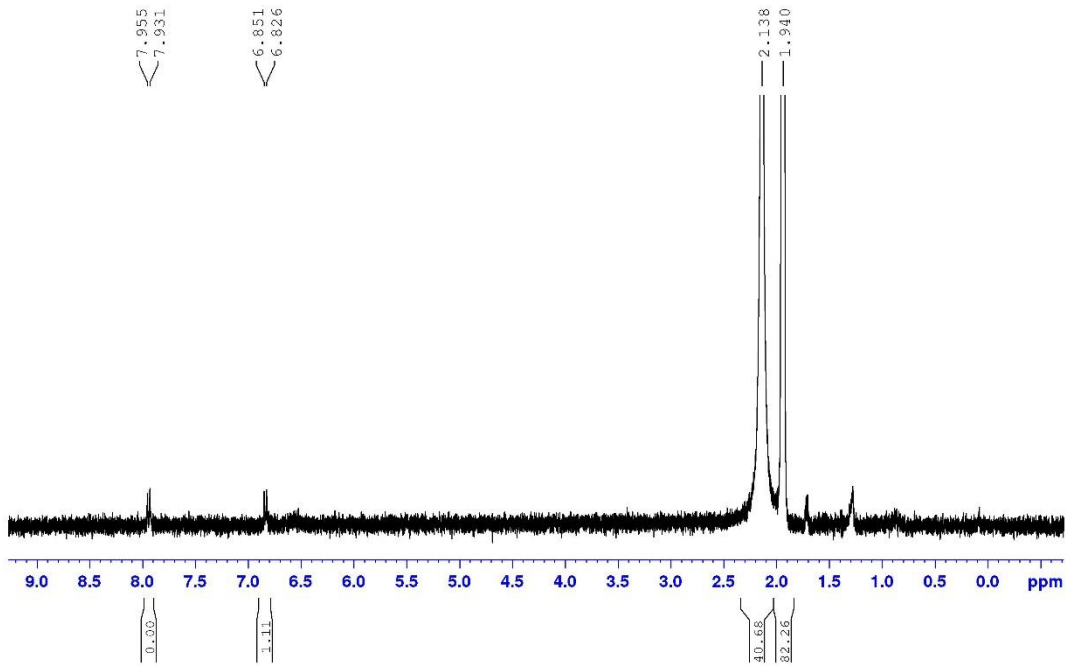
VA4318, MeOD, 4-HYDROXYPYRIDINE + SULPHURIC ACID
04.06.2018

VA4418, D2O, isonicotinic acid + SULPHURIC ACID
01.06.2018

VA4518, MeOD, 4-ISONICOTINAMIDE+ SULPHURIC ACID
04.06.2018

8.923
8.904
8.196
8.175
4.870
3.362
3.358
3.353

10.0 9.5 9.0 8.5 8.0 7.5 7.0 6.5 6.0 5.5 5.0 4.5 4.0 3.5 3.0 2.5 ppm

0.00 0.98 5.00 0.87

VA4618, MeOD, PYRIDINETHIOAMIDE + SULPHURIC ACID
04.06.2018

8.819
8.800
8.797
8.120
8.100
8.098
4.872
4.870
3.362
3.359
3.356
3.351

11 10 9 8 7 6 5 4 3 2 1 ppm

0.00 0.99 1.95 0.86